

**INTERACTION OF BASALTIC DIKES AND WET LAPILLI TUFF AT  
GLACIOVOLCANIC CENTERS: A CASE STUDY OF SVEIFLUHÁLS, ICELAND AS A  
TERRESTRIAL ANALOG FOR DIKE-CRYOSPHERE INTERACTION ON MARS**

by

**Holly Michelle Kagy**

B.A. Earth Science, University of Northern Iowa, 2007

B.A. Earth Science Teaching, University of Northern Iowa, 2007

Submitted to the Graduate Faculty of  
Geology and Planetary Science in partial fulfillment  
of the requirements for the degree of  
Master of Science

University of Pittsburgh

2011

UNIVERSITY OF PITTSBURGH  
FACULTY OF DIETRICH SCHOOL OF ARTS AND SCIENCES

This thesis was presented

by

Holly Michelle Kagy

It was defended on

November 18, 2011

and approved by

William Harbert, Associate Professor, University of Pittsburgh

Michael S. Ramsey, Associate Professor, University of Pittsburgh

Committee Chair: Ian P. Skilling, Assistant Professor, University of Pittsburgh

Copyright © by Holly Michelle Kagy

2011

**INTERACTION OF BASALTIC DIKES AND WET LAPILLI TUFF AT  
GLACIOVOLCANIC CENTERS: A CASE STUDY OF SVEIFLUHÁLS, ICELAND  
AS A TERRESTRIAL ANALOG FOR DIKE-CRYOSPHERE INTERACTION ON  
MARS**

Holly Michelle Kagy, M.S.

University of Pittsburgh, 2011

Basaltic dikes emplaced into formerly wet unconsolidated phreatomagmatic tephra deposits were investigated at a glaciovolcanic fissure-fed complex, Sveifluháls, Reykjanes Peninsula SW Iceland. Such dikes serve as excellent terrestrial analogs for high-level basaltic dike-cryosphere interactions on Mars. The dikes revealed several large and small-scale geomorphic and textural characteristics, which would aid satellite and ground-based identification of similar dikes on Mars. The dikes at Sveifluháls typically have narrow (<1.5m wide) coherent interiors of both pillowed and non-pillowed types, but they develop peperitic margins with a geomorphic expression that is often an order of magnitude larger than the coherent dike. This has important implications for recognizing dikes emplaced into the cryosphere, interpreting past climates on Mars, estimating dike widths from remote imagery, and calculating magma flux rates on Mars. Large-scale geomorphological features of the Sveifluháls dikes include local dike-bounded plateaus, adjacent and at lower elevation to phreatomagmatic tephra ridges, with surfaces of dark dike-derived talus. The dikes commonly form narrow steep-sided ridges and less frequently form eroded troughs. The dikes are associated with broad bounding areas of orange to reddish-brown host lapilli tuff (“hydrothermal reddening”), that extends for up to 20m on either side of the dikes, and contrasts with the more typical buff-colored palagonitized lapilli tuff that has not



been intruded by dikes. The reddening is likely caused by the presence of concentrically banded zones of possible hematite in vesicles and pore-spaces. Drag-folded, rotated and slumped blocks or domains of the host may extend up to 30m from dike margins. The dikes have a gross tabular morphology, but are locally pillowed or billowy along their margins, and also include finger-like or elongate pillowed projections up to 5m in length from their margins into the host lapilli tuff. Both margins also commonly display 1-3m wide peperitic zones of both blocky and fluidal (including pillow-like) types. Interestingly, the bedding or lamination in the drag folded domains is usually better developed than in the surrounding host deposits. Narrow steep conical mounds of pillow lavas resembling pillow-like haystacks, described from the submarine environment and are interpreted as areas where the dikes emerge on the substrate surface.

## TABLE OF CONTENTS

<b>PREFACE.....</b>	<b>XIX</b>
<b>1.0 MOTIVATION.....</b>	<b>1</b>
<b>2.0 QUESTIONS ADDRESSED .....</b>	<b>2</b>
<b>3.0 BACKGROUND .....</b>	<b>3</b>
<b>3.1 PUBLISHED MODELS OF DIKE EMPLACEMENT IN ROCK ON EARTH .....</b>	<b>3</b>
<b>3.2 PUBLISHED MODELS OF DIKE EMPLACEMENT INTO WET SEDIMENT AND ICE ON EARTH.....</b>	<b>4</b>
<b>4.0 FIELD STUDY OF BASALTIC DIKES EMPLACED INTO WET LAPILLI TUFF AT SVEIFLUHÁLS, ICELAND.....</b>	<b>11</b>
<b>4.1 SETTING OF THE GLACIOVOLCANIC CENTER AT SVEIFLUHÁLS, ICELAND.....</b>	<b>11</b>
<b>4.2 DESCRIPTION OF DIKES EMPLACED INTO WET LAPILLI TUFF AT SVEIFLUHÁLS, ICELAND .....</b>	<b>14</b>
<b>4.2.1 Dike Interiors .....</b>	<b>27</b>
<b>4.2.2 Dike Margins .....</b>	<b>36</b>
<b>4.2.3 Dike-Induced Deformation of Host Lapilli Tuff .....</b>	<b>43</b>
<b>4.2.4 Dike-Margin Peperite .....</b>	<b>52</b>

4.2.5	Dike-Related Hydrothermal Alteration of Host Lapilli tuff.....	58
4.3	INTERPRETATION AND MODEL OF DIKE EMPLACEMENT INTO WET LAPILLI TUFF AT SVEIFLUHÁLS, ICELAND.....	63
5.0	SUMMARY OF VOLCANO-ICE INTERACTION ON MARS.....	73
6.0	DIKE RECOGNITION ON MARS .....	81
6.1	PUBLISHED EXAMPLES OF DIKES ON MARS .....	88
7.0	RECOGNITION OF DIKES EMPLACED INTO ICE OR WET SEDIMENT ON MARS.....	93
8.0	COMPARISON OF SVEIFLUHÁLS DIKES WITH DIKES ON MARS.....	97
8.1	CAN WE USE DIKES ON MARS TO INFER PALEOCLIMATE? .....	105
9.0	CONCLUSIONS .....	106
	REFERENCES.....	110

## LIST OF TABLES

Table 1. UTM coordinates and elevations of study area stations at Sveifluháls, Iceland.....	14
Table 2. Strikes and dips of intrusions and lapilli tuff bedding near intrusions at Sveifluháls, Iceland.....	20
Table 3. Samples from intrusive areas at Sveifluháls, Iceland, including intrusion, host lapilli tuff, and hydrothermally altered lapilli tuff. ....	23

## LIST OF FIGURES

Figure 1. Model of dike-ice interaction at Hrafninnuhryggur, Iceland. Note dike mingling with wet sediment and quench fragmentation. (Tuffen and Castro, 2009).....	6
Figure 2. General overview of peperite genesis, characteristics, and morphologies (Skilling, 2002). .....	8
Figure 3. Regional view of Sveifluháls, Iceland. NASA ASTER color-infrared (15 m pixel resolution) in the background and Loftmyndir color orthophotos (0.5 m pixel resolution) in the foreground are utilized in this image. Note: annotations on field site orthophotos are described later in the thesis. ....	12
Figure 4. The main volcanic, seismic, and rift zones of Iceland. EVZ: Eastern Volcanic Zone, MAR: Mid-Atlantic Ridge, MVZ: Mid-Iceland Volcanic Zone, NVZ: Northern Volcanic Zone, ÖVZ: Öräfajökull Volcanic Zone, SISZ: South Iceland Seismic Zone, SVZ: Snæfellsnes Volcanic Zone, TFZ: Tjörnes Fracture Zone, WVZ: Western Volcanic Zone, A: Northwest rift axis, B: Snæfellsnes-Húnaflói rift axis, C: Skagafjörður rift axis, the circle shows the location of the Icelandic plume. (Harðarson et al., 2008).....	13
Figure 5. A) and b) shoe locations of basaltic dike intrusions at Sveifluháls, Iceland. Loftmyndir color orthophotos (0.5 m pixel resolution) are utilized in this image. Note dike outcrops and extensions. Note plateau areas in purple shading. ....	18

Figure 6. Inset of Sveifluháls, Iceland field area. Confirmed and inferred dike outcrops, hydrothermal and plateau areas, and inferred faults and troughs are outlined. Note plateau areas shaded in purple. ....	19
Figure 7. a) Annotated photomosaic of illustrating the margins of intrusive domains (red) with distinctive cavities (potential “cryoliths”) (blue) at Station 1, Sveifluháls, Iceland. Note the distinctive geomorphic expression of the dikes. b) Extracted annotated overlay of Station 1. ....	22
Figure 8. Generalized sketch of intrusions emplaced into wet lapilli tuff at Sveifluháls, Iceland. Intrusion, hydrothermal alteration area and disturbed host lapilli tuff width ranges are shown. Note that in some areas one or more of these zones were not exposed. ....	24
Figure 9. a) An area of fingering intrusions at Sveifluháls, Iceland. This view was obtained at Station 2L. Intrusion/matrix contacts are shown in red, pillow forms in light blue (pillow lavas, pillow tubes, and possible subaqueous pillow “haystacks”), jointing/bedding in medium blue, plateau area, and peperitic zones. b) Annotated overlay of a). ....	25
Figure 10. Plateau region at Sveifluháls, Iceland which develops along the intrusion zone at Station 2j. Note mixing of intrusion (grey) and hydrothermally altered lapilli tuff (dark red) and general strike of intrusions along the mid-slope on the ridge. Note plateau areas highlighted in purple. ....	26
Figure 11. Interior of a basaltic dike at Sveifluháls, Iceland, displaying a knobby pillow-like structure with blocky jointing at Station 6c. Pillow forms are outlined in green. Note mixing of lapilli tuff (orange) and intrusion (grey). ....	28
Figure 12. Dike with compressed pillow margins and non-pillowed blocky-jointed interior at Station 8b at Sveifluháls, Iceland. ....	29

Figure 13. A blocky parallel jointed non-pillowed dike interior with a pillowy margin at Sveifluháls, Iceland. Notice the minimal or absence of peperite development. Contact of intrusion and host lapilli tuff is outlined in red. This area is located at Station 7b.....	30
Figure 14. Curvicolumnar jointing of multiple pillowy dikes at Station 7b at Sveifluháls, Iceland. Discrete dike domains of several pulses or fingers may be seen. Note unmingled contact with host lapilli tuff in orange, dike pulses in red, and joints in yellow. ....	31
Figure 15. Pillow tubes and a potential pillow haystack within a dike interior at Station 7a at Sveifluháls, Iceland. Note jointing within pillow tube structures. Jointing is delineated in yellow and pillow forms are outlined in green. ....	32
Figure 16. Distinctive cavity of unknown origin within a dike interior at Station 4a at Sveifluháls, Iceland. Such a cavity may indicate the former presence of a “cryolith”.....	33
Figure 17. Gaps between pillows within a dike interior at Station 8a at Sveifluháls, Iceland. Note the apparently compressed nature of the pillows. Pillow gaps are outlined in light blue and pillow forms in green. ....	34
Figure 18. Pillows from dikes at Sveifluháls, Iceland with multiple rinds and concentric vesicle banding. Vesicle bands representing separate pulses of magma injection are outlined in light blue. a) was taken at Station 1a. b) was obtained at Station 1d. ....	35
Figure 19. Microscopic view of a basaltic intrusion at Sveifluháls, Iceland displaying vesicles, plagioclase, and clinopyroxene. Thin section extracted from Sample 6, which was obtained at Station 5c. ....	36
Figure 20. Fluidal pillowy margin of an dike at Station 1b at Sveifluháls, Iceland with peperite, a product of wet lapilli tuff-intrusion mixing. Note joints in yellow and approximate dike-host contact in red.....	37

Figure 21. Peperitic dike margin with pillowy lobes at Station 1b at Sveifluháls, Iceland. Note hydrothermal alteration of host lapilli tuff. Note joints in yellow. ....	38
Figure 22. Exposed intrusion at Sveifluháls, Iceland, showing a pillowed dike margin and compressed pillow tubes at Station 8a. Note pillow forms outlined in green and fractures in orange.....	39
Figure 23. Possible pillow haystack at Station 6c at Sveifluháls, Iceland. Such a structure may be analogous to subaqueous pillow haystacks (steep cone-like feature similar to subaerial hornitos) observed on the seafloor in other studies. Note pillow forms outlined in green. ....	40
Figure 24. Intrusion (red) and subaqueous lava flow (light blue) at Station 1d at Sveifluháls, Iceland. Note hydrothermal alteration and the high-level nature of the intrusion in reference to the paleoslope.....	41
Figure 25. “Ooze-outs” along polygonal cooling joints, developed along compressed dike-margin pillows, located at Station 8a at Sveifluháls, Iceland. Such structures indicate characteristics of this intrusion’s cooling process where magma was later squeezed through fractures in the previously chilled margin. ....	42
Figure 26. Drag-folded overturned lapilli tuff adjacent to dike at Station 2j at Sveifluháls, Iceland. Note the deformed and nearly overturned nature of the host lapilli tuff.....	44
Figure 27. Drag-folded lapilli tuff domains adjacent to a dike at Station 1c at Sveifluháls, Iceland. Note area of cross-lamination, scours, and overturned beds. A possible synsedimentary fault is outlined in orange. ....	45
Figure 28. Synsedimentary deformation observed within host lapilli tuff near a dike at Station 2k at Sveifluháls, Iceland.....	46



Figure 29. Drag-folded and overturned bedding in lapilli tuff adjacent to a dike at Station 1c at Sveifluháls, Iceland.....	47
Figure 30. Deformation of lapilli tuff adjacent to dike at Station 1c at Sveifluháls, Iceland. The lapilli tuff here displays scours and horizons of well-developed parallel laminae.....	48
Figure 31. Laminae within drag-folded domains of lapilli tuff adjacent to a dike at at Station 2j at Sveifluháls, Iceland. Note the fan-like and arch-like patterns of the laminae. An approximate axis of the fold is outlined in orange. ....	49
Figure 32. Distal rotation of host lapilli tuff at Sveifluháls, Iceland. The intrusion in this area is less than 200m to the left of this image. (Mercurio, shared data).....	50
Figure 33. Tephra may post-date the intrusions for this site at Station 5g at Sveifluháls, Iceland. Suspected post-intrusive tephra (orange) and intrusive mixing with lapilli tuff (peperite) (red) are shown. Note fractures (blue) and bedding (green).....	51
Figure 34. Fluidal and blocky peperite domains along the margin of an intrusion at Sveifluháls, Iceland. (Skilling, unpublished).....	52
Figure 35. Blocky dike-margin peperite at Station 9b at Sveifluháls, Iceland, that displays several clasts clearly derived from pillow rinds. Note pillow joint blocks and cubes breaking off from the dike.....	54
Figure 36. Blocky peperite associated with drag-folded host lapilli tuff at Station 9a at Sveifluháls, Iceland. Note adjacent host lapilli tuff deformation. ....	55
Figure 37. Dike emplaced into lapilli tuff featuring fractured angular blocks, pillow forms, and marginal blocky peperite at Station 2a at Sveifluháls, Iceland. ....	56
Figure 38. A blocky-jointed dike interior with peperite at Sveifluháls, Iceland, located at Station 5d.....	57

Figure 39. Blocky to ragged juvenile vesicular clasts (black/grey) in dike-margin peperite at Station 2c at Sveifluháls, Iceland surrounded by host lapilli tuff (orange). Moss patch (bottom right) is about 10 cm. Note the scoriaceous/highly vesicular nature of these juvenile clasts.....	58
Figure 40. Hydrothermal reddening of tephra adjacent to dike margin at Station 2j at Sveifluháls, Iceland with deformed lapilli tuff. Note the deep shade of red to the hydrothermal alteration, indicating a possible higher temperature of the hydrothermal fluids in this area.....	59
Figure 41. Dike-like intrusion into hydrothermally reddened lapilli tuff at Station 2i at Sveifluháls, Iceland. The lapilli tuff displays a reddening that is distinct from the “background” buff palagonitization. ....	60
Figure 42. Microscopic view of possible hematite lining vesicles within a dike at Sveifluháls, Iceland. The thin section was taken from Sample 5 at Station 2d. ....	61
Figure 43. Possible hematite spherules infilling a vesicle at Sveifluháls, Iceland. (Mercurio, shared data) .....	61
Figure 44. Red soils developed near areas of hydrothermal reddening of lapilli tuff along dike margins at Station 2a at Sveifluháls, Iceland. Note the plateau region along the strike of the dike. ....	62
Figure 45. Fracture trends of the Reykjanes Peninsula, SW Iceland. The rose diagram indicates an overall NE trend among the fractures. Strike trends are denoted by color: 000°- 20° (red), 021° - 040° (yellow), 041° - 060° (green), 061° - 080° (blue), 081° - 180° (purple). (Clifton and Kattenhorn, 2006) .....	64
Figure 46. Strike-slip faults (white) and fractures (black) at Sveifluháls, Iceland were interpreted from photographic and field data (fault 1). Faults 1 - 4 were identified with the aid of seismic data. (Clifton and Kattenhorn, 2006) .....	65

Figure 47. “Ice-block meltout cavities” at Höðufell, Iceland. (Skilling, 2009).....	66
Figure 48. Model of the evolution of “ice-block meltout cavities” at Höðufell, Iceland. (Skilling, 2009) .....	67
Figure 49. Submarine pillow haystack on the Juan de Fuca Ridge. (Stakes et al., 2006) .....	68
Figure 50. Submarine pillow haystack on the Juan de Fuca Ridge. (Stakes et al., 2006) .....	69
Figure 51. Subaqueous pillow haystack found in a dive on the Juan de Fuca Ridge. (Stakes et al., 2006) .....	69
Figure 52. Evolution and morphologies of the dike-wet lapilli tuff system at Sveifluháls, Iceland. (Skilling, unpublished).....	71
Figure 53. a) Viking image of ridges at Pavonis Mons. b) THEMIS VIS image of potential drop moraines. c) MOC narrow-angle image of ridges at Pavonis Mons. d) Viking image of knobby features at Pavonis Mons. e) THEMIS VIS image of ridges thought to be lobate flow features, and knobby features over flow-like features. f) MOC narrow-angle image of the knobby features and dune fields. g) Viking image of the main smooth facies deposit at Pavonis Mons. h) THEMIS VIS image of the main smooth facies deposit at Pavonis Mons. Circular depressions may be softened impact craters. i) MOC narrow-angle image of smooth facies and dune fields at Pavonis Mons. (Shean et al., 2005).....	76
Figure 54. a) THEMIS daytime IR image of the Pavonis fan-shaped deposit. Some knobs in the upper portion on this image may be drumlins (Scott et al., 1998). b) Sketch of the image in a) showing smooth facies (SF, dark gray), knobby facies (KF, light gray), primary ridges (solid lines), and secondary ridges (dashed lines). The thick solid line with triangles shows possible meltwater channel. (Shean et al., 2005).....	77

Figure 55. MOLA profiles of ridges at Pavonis Mons. DR1 and DR2 show clustered central ridges. The smooth facies (SF) is present in some profiles. Vertical exaggeration is approximately 158X. (Shean et al., 2005) .....	78
Figure 56. (a) THEMIS daytime IR and Viking data with MOLA overlay of radial ridges. b) Sketch of flow features (arrows) that may be subglacial flows. Thick solid lines show radial ridges that are interpreted as dikes that once interacted with ice. One radial ridge transitions into a pancake-like feature and was interpreted as a potential subglacial sill. (Shean et al., 2005).....	79
Figure 57. THEMIS daytime IR image showing possible meltwater outflow features northeast of the Pavonis fan-shaped deposit. These features may originate from eruptions beneath a glacier at Pavonis Mons. (Shean et al., 2005).....	80
Figure 58. HiRISE images (NASA/JPL/University of Arizona) of a) graben within Memnonia Fossae, Mars, that may be due to an underlying dike. White scale bar (top right) = 1,000m. (PSP_005376_1575) b) graben and collapse pits at Cyane Fossae, Mars. White scale bar (top right) = 500m. (PSP_010345_2150) .....	83
Figure 59. HiRISE images (NASA/JPL/University of Arizona) of a) pit crater chains near the summit of Tyrrhena Patera, Mars. White scale bar (top right) = 500m. (PSP_006487_1580) b) pit crater chains at Elysium Mons Caldera, Mars. White scale bar (top right) = 1,000m. (PSP_004903_2050) c) a collapse pit and possible dikes in Tractus Fossae, Mars. White scale bar (top right) = 500m. (ESP_011386_2065) .....	85
Figure 60. Model of dike emplacement on Mars. a) Fracturing via propagation of the dike. b) Graben formation. c) Pit crater chain formation as volatiles escape. d) Fissure eruption related to a dike. e) Erosion of country rock. f) Model of a partially eroded surface. (Korteniemi et al., 2009) .....	86

Figure 61. HiRISE images (NASA/JPL/University of Arizona) of a a) possible dike splay in the Coloe Fossae Region of Mars. White scale bar (top right) = 500m. (PSP_004181_2170) b) possible dike in Hrad Vallis, Mars. White scale bar (top right) = 500m. (PSP_007527_2135)...	87
Figure 62. Shaded relief map of Tharsis-radial graben in the Memnonia region. (Schultz et al., 2004). .....	89
Figure 63. Mars Orbiter Laser Altimeter (MOLA) topographic profiles of graben. (Schultz et al, 2004) .....	89
Figure 64. MOC narrow-angle images of radial ridges: a) A curvilinear radial ridge possibly formed via volcano-ice interaction. b) A radial ridge with collapse pits along the ridge axis. (Shean et al, 2005) .....	95
Figure 65. THEMIS IR images of dike swarms in the Elysium Rise and Utopia Basin regions of Mars. Red boxes show locations for B, C, D, and E. Black arrows show “stubby flows” and white arrows show symmetric fractures atop ridges. (Pedersen et al., 2010).....	98
Figure 66. THEMIS IR imagery of single dikes in the Elysium Rise and Utopia Basin of Mars. Red boxes show locations for B, C, D, and E. (Pedersen et. al, 2010).....	100
Figure 67. Comparison at the same scale of THEMIS IR imagery of dike swarms in the Elysium Rise and Utopia Basin regions of Mars in a) by Pedersen et al. (2010) to the tinar b) comprised of phreatomagmatic tephra ridges and dikes at Sveifluháls, Iceland, seen in Loftmyndir color orthophotos. Black arrows show “stubby flows” and white arrows show symmetric fractures atop ridges. (Pedersen et al., 2010).....	102
Figure 68. Comparison at nearly the same scale of a Martian curvilinear radial ridge of potential volcano-ice interaction origin in a) from Shean et al. (2005) to tephra ridges and dikes at Sveifluháls, Iceland, seen in Loftmyndir color orthophotos.....	103

Figure 69. Comparison at the same scale of a color HiRISE image (ESP_013903_1650) of a CRISM-confirmed olivine dike in the Coprates Chasma central horst of Valles Marineris on Mars (Flahaut et al., 2011) in a) to dikes at Sveifluháls, Iceland seen in Loftmyndir color orthophotos in b) and c).....	104
---	-----

## **PREFACE**

I would like to thank my advisor Dr. Ian Skilling and my committee, Dr. Bill Harbert and Dr. Michael Ramsey, for their advice, patience, and willingness to aid in my research and growth as a professional. I would also like to thank my family, my friends scattered throughout the world, and my colleagues and friends in the University of Pittsburgh Geology and Planetary Science and Physics and Astronomy departments. Funding for this research was made possible through grants from GSA and NSF as well as teaching assistantships.

## **1.0 MOTIVATION**

The interaction of basaltic dikes with water ice or water ice-cemented clastic rocks should be very common on Mars; with the prevalence of volcanism, water ice within the cryosphere, and erosion; but no clear examples have been described in the literature. The principal motivation for this project was to study examples of the interaction of dikes with formerly wet clastic rocks at a glaciovolcanic center in Iceland, on the assumption that this would provide the best accessible analogs to dike-cryosphere interactions on Mars. The interaction of dikes with the cryosphere on Mars is important for several reasons. The recognition of areas on Mars where this interaction may have taken place, provides a useful paleoenvironmental or paleoclimatic fingerprint in areas where evidence of ice at present or in the past may not be obvious at the surface. Dike-cryosphere interaction could also have provided suitable habitats for life on Mars. The interaction of basaltic dikes with ice-cemented clastic rocks may have induced the formation of features wider than the dikes themselves, lending to important implication for estimates of magma flux within Martian dikes. The recognition of dikes emplaced into any sort of material on Mars is not easy, because similar linear features may be produced by a wide variety of processes. As interaction with the cryosphere is likely to be one of the commonest styles of interaction on Mars, then studying such dikes will aid in the recognition of all dikes on Mars.



## **2.0 QUESTIONS ADDRESSED**

This study focused on a detailed description of basaltic dikes emplaced into formerly wet volcanoclastic sediments at a glaciovolcanic center in Iceland. Description and interpretation of these dikes were then compared and contrasted with putative dikes on Mars, and conclusions drawn about the recognition and significance of dike-cryosphere interaction on Mars. The principal questions addressed included: (1) What are the processes and products of the interaction of basaltic dikes and wet sediments on Earth? (2) How do we recognize dikes on Mars? (3) How do we recognize dike-cryosphere interaction on Mars? (4) How do the putative dikes on Mars compare with the examples studied in Iceland? (5) What conclusions can be drawn about dike-cryosphere interactions on Mars from this study?

### **3.0 BACKGROUND**

Dike emplacement into rock versus emplacement into wet sediment and ice are fundamentally different. This chapter will describe models of dike emplacement into rock on Earth and dike emplacement into wet sediment and ice as an analog for dike-cryosphere interaction on Mars.

#### **3.1 PUBLISHED MODELS OF DIKE EMPLACEMENT IN ROCK ON EARTH**

Rising magma diapirs are the most commonly accepted model for the initial upward movement of basaltic magma at depth (Winter, 2001). These inverse-teardrop-shaped bodies rise buoyantly (Francis and Oppenheimer, 2004; Winter, 2001). Upward movement ceases when the density of the intrusion equals or exceeds the density of the surrounding rock (Winter, 2001). When such a situation occurs, the diapir stops rising and begins to flatten out and form sills (Winter, 2001). Dikes and some sills form when a magma reservoir is over-pressurized such that the pressure within the reservoir (largely due to volatiles within the melt) surpasses the confining pressure of surrounding rocks by several megapascals (Francis and Oppenheimer, 2004). Magma is then forced into the country rock as dikes and sills through preexisting cracks in the host rock or when the intrusion itself fractures the host rock, providing a thoroughfare for the magma (Francis and Oppenheimer, 2004). Steam explosions may occur at the dike tip, which can further perpetrate the fracturing of country rock (Francis and Oppenheimer, 2004).

Models of igneous intrusion evolution and dynamics may be demonstrated through the use of laboratory experiments (Acocella et al., 2002; Benn et al., 1998). Dike intrusion laboratory experiments incorporate a variety of methods, such as the use of metal plates emplaced into sand (Acocella et al., 2002), and Newtonian silicone putty placed in dry (Acocella et al., 2002; Benn et al., 1998) or pre-fractured wet sand (Acocella et al., 2002).

### **3.2 PUBLISHED MODELS OF DIKE EMPLACEMENT INTO WET SEDIMENT AND ICE ON EARTH**

Volcanic edifices generated by basaltic magma-ice interaction have been studied at several locations on Earth, including Iceland (Allen et al., 1982; Gudmundsson et al., 2004; Schopka et al., 2006; Skilling, 2009), Antarctica (Smellie et al., 1993; Smellie and Hole, 1997; Smellie and Skilling, 1994; Skilling 1994; Wörner and Viereck, 1987), British Columbia (Allen et al., 1982; Edwards et al., 2009), and Siberia (Komatsu et al., 2004). A fundamental aspect of such interactions is the intrusion of magma into ice, ice-cemented tephra and wet tephra. Theoretical models of dike emplacement into ice on Earth have been described by Wilson and Head (2002). Tuffen and Castro (2009) studied the intrusion of a rhyolitic dike into ice. However, at present there are no published field studies of basaltic intrusion interactions with ice, ice-cemented tephra, or wet tephra at glaciovolcanic centers.

Hlöðufell, a basaltic sub-ice to emergent volcano in south-western Iceland displays subaqueously emplaced basaltic lava mounds derived from eruptions beneath ice and/or into wet tephra beneath ice (Skilling, 2009). Skilling described ice contact lava confinement surfaces,

pillows with mini-pillow breakouts, dikes, cavities within lava mounds, and intrusion into wet ice-confined volcanoclastic sediments at Hlöðufell (Skilling, 2009).

Wilson and Head (2002) presented the first theoretical model of basaltic dike intrusion into ice, which they suggested would result in rubble piles derived from collapsed dikes, as the adjacent ice melted. No such deposits have been recognized to date, but such features would be difficult to confidently identify. It is important to note that the model by Wilson and Head (2002) does not include basaltic dike emplacement into wet sediment or ice-cemented sediment, which after the initial dike emplacement into ice, would be the common process.

Wilson and Head (2002) state that dikes initially interact with ice in a manner similar to intrusion/rock environments, resulting from a high strain rate at the dike tip. They suggested that dikes can overshoot the rock-ice interface to intrude through 20-30% of the thickness of the overlying ice (Wilson and Head, 2002). They also contend that such basaltic intrusions could evolve into a sub-ice sill with sideways spreading actions enhanced by the overlying ice (Wilson and Head 2002). Wilson and Head state that the heat of the lava would quickly melt the surrounding ice, creating a vault of hot meltwater which may transfer heat to neighboring ice through convection (Wilson and Head 2002). Drainage of meltwater and/or contact with the atmosphere (vastly decreasing the overlying pressure), aids in reducing the explosive potential of sub-ice lava flows (Wilson and Head 2002). When the meltwater is trapped and pressure remains dependent upon surrounding ice, carbon dioxide and water exsolution may cause explosive magma fragmentation (Wilson and Head, 2002).

Tuffen and Castro (2009) is the only paper to date to focus specifically on dike-ice interaction on Earth with the aid of field evidence. Although the dike Tuffen and Castro (2009) studied was rhyolitic in composition, their model has some bearing on the current study. They

described and interpreted emplacement of a rhyolitic obsidian dike through thin ice at Hrafninnuhryggur, Krafla Volcano, Iceland (Figure 1) (Tuffen and Castro, 2009).

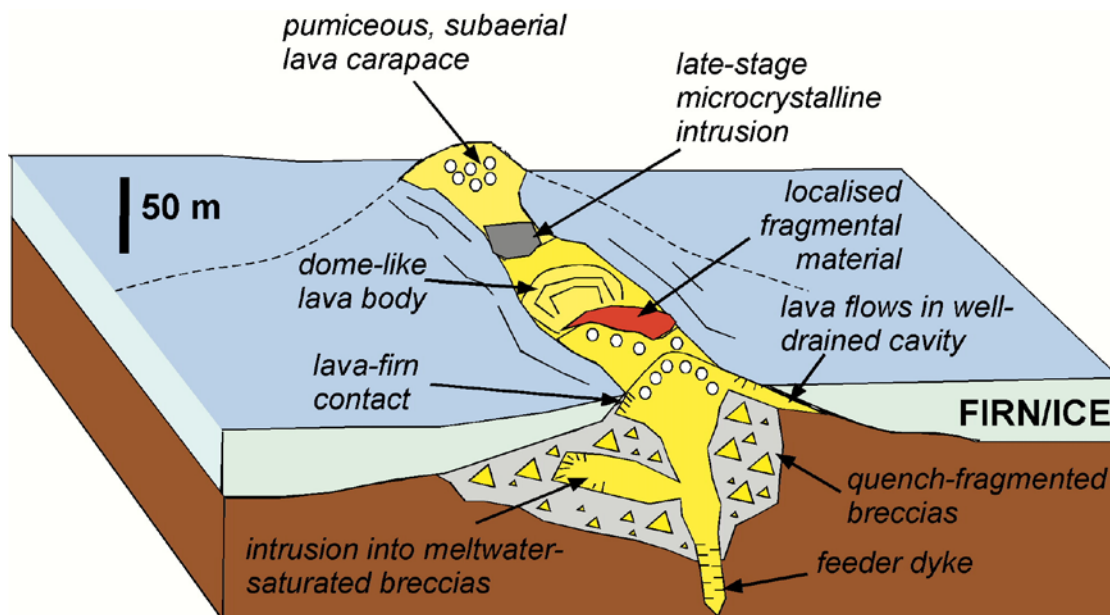


**Figure 1. Model of dike-ice interaction at Hrafninnuhryggur, Iceland. Note dike mingling with wet sediment and quench fragmentation. (Tuffen and Castro, 2009)**

Hrafninnuhryggur is interpreted as the product of a fissure eruption into ice which created dike margin hyaloclastite, and a distinctive pattern of cooling joints within the dike interior (Tuffen and Castro, 2009). The eruption initially developed in a sub-ice environment, but later melted through a thin ice cover (35-55m) to become a subaerial eruption (Tuffen and Castro, 2009). Meltwater accumulation evidence is limited, suggesting an efficient escape route (Tuffen and Castro, 2009).

Basaltic intrusion into wet sediment is very common on Earth in a wide variety of settings (Befus et al., 2009; Busby-Spera and White, 1987; Squire and McPhie, 2002; White and Busby-Spera, 1987), including glaciovolcanic settings, though rarely described in detail. Such

interaction typically results in distinctive gross and surface morphologies, jointing, and the development of peperite. A definition by White et al. (2000), defines peperite as “rock formed essentially in situ by disintegration of magma intruding and mingling with unconsolidated or poorly consolidated, typically wet sediments”. Skilling et al (2002) described peperite genesis in detail (Figure 2).

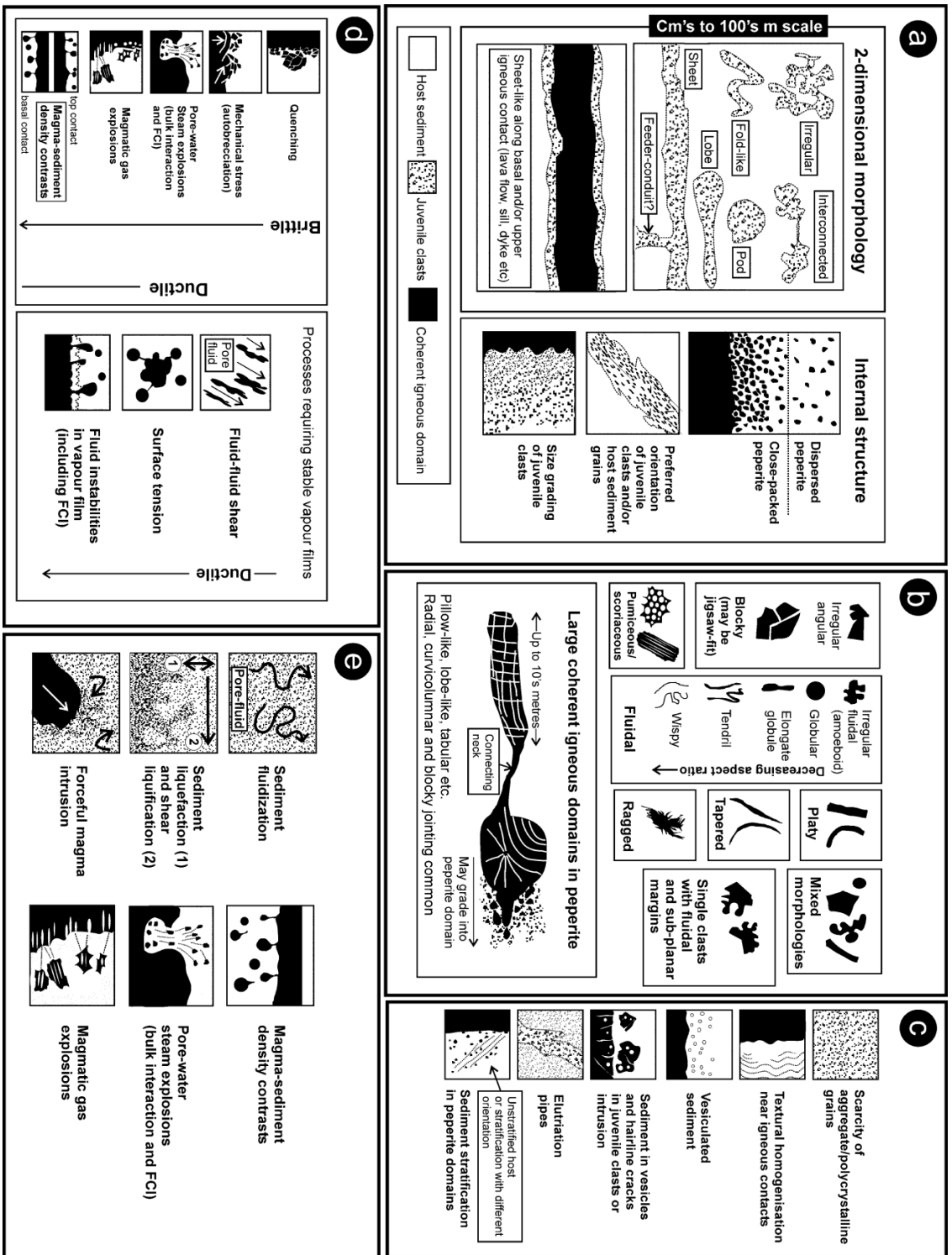


Figure 2. General overview of peperite genesis, characteristics, and morphologies (Sking, 2002).

Peperite forms when magma or lava interacts non-explosively with wet sediment and can result in several different juvenile morphologies and deformation of the clastic host (Skilling et al., 2002). Juvenile clasts in peperite can form several shapes, but are generally described as either blocky or fluidal (Busby-Spera and White, 1987; Skilling et al., 2002).

Several conditions affect the processes and products of basaltic wet sediment-ice interactions, such as the nature of the host sediment, magma injection velocity, the amount of volatiles in the melt, ratio of magma to wet sediment, the occurrence of shock waves, and the amount of confining pressure (Skilling et al., 2002). But, the intermingling of juvenile magma and host sediment is maximized when both have similar densities and viscosities (Skilling et al., 2002). Skilling et al. (2002) describe several possible mechanisms of magma-sediment mingling including force of magma injection, explosive magmatic vesiculation, pore-water steam explosions, surface tension, density ratios of the magma and wet sediment, and vapor film fluid instabilities. Peperite volumes range from a few cubic meters to several cubic kilometers on Earth (Skilling et al., 2002). Domains of peperite are usually parallel to igneous intrusions when they can be described as closely-packed, but can have irregular shapes when more dispersed (Skilling et al., 2002). Juvenile clasts can have several different shapes, for example, blocky clasts are sub-equant, polyhedral to tabular, with curvilinear to planar surfaces (Skilling et al., 2002). Such blocky clasts generally retain a jigsaw-like quality in their fit with each other (Skilling et al., 2002). Fluidal glassy clasts in peperite are more globular and irregular in shape, may have laminae or tendrils, and have clearly been fragmented in a ductile manner (Skilling et al., 2002). Other shapes of juvenile clasts in peperite are platy, tapered, or ragged clasts, which described by Skilling et al. (2002), are elongate with margins varying from curvilinear to



subplanar and planar. Margins of ragged clasts are irregular and spinose whereas tapered clasts have thinner ends and are elongate (Skilling et al., 2002).

Phreatomagmatic explosions may occur during peperite genesis, with explosions more common along intrusive margins than during the mixing process (Skilling et al., 2002). Heat transfer and maximized volatile-release rates are more likely to create an unstable situation closer to the intrusion (Skilling et al., 2002). Explosions during mingling could theoretically set off further explosions in a domino effect (Skilling et al., 2002). Volumes of peperite domains could be expanded through such explosions, as they can aid in additional fragmentation and mingling of magma with wet sediment (Skilling et al., 2002).

## **4.0 FIELD STUDY OF BASALTIC DIKES EMPLACED INTO WET LAPILLI TUFF AT SVEIFLUHÁLS, ICELAND**

A detailed study of dikes emplaced into wet lapilli tuff at Sveifluháls, Iceland was conducted as a terrestrial analog for Martian dike-cryosphere interactions. This chapter will describe the overall morphologies, internal textures, and effects of the dikes on the surrounding host tephra.

### **4.1 SETTING OF THE GLACIOVOLCANIC CENTER AT SVEIFLUHÁLS, ICELAND**

Sveifluháls is a 21 km long and 2.5 km wide glaciovolcanic ridge complex (tindar) produced by ice-confined basaltic fissure eruptions (Mercurio, 2011). Thicknesses of 450-600m of ice overburden are estimated during the formation of Sveifluháls, Iceland (Mercurio, 2011). Sveifluháls is located on the Reykjanes Peninsula in south-western Iceland adjacent to lake Kleifarvatn (Figure 3).

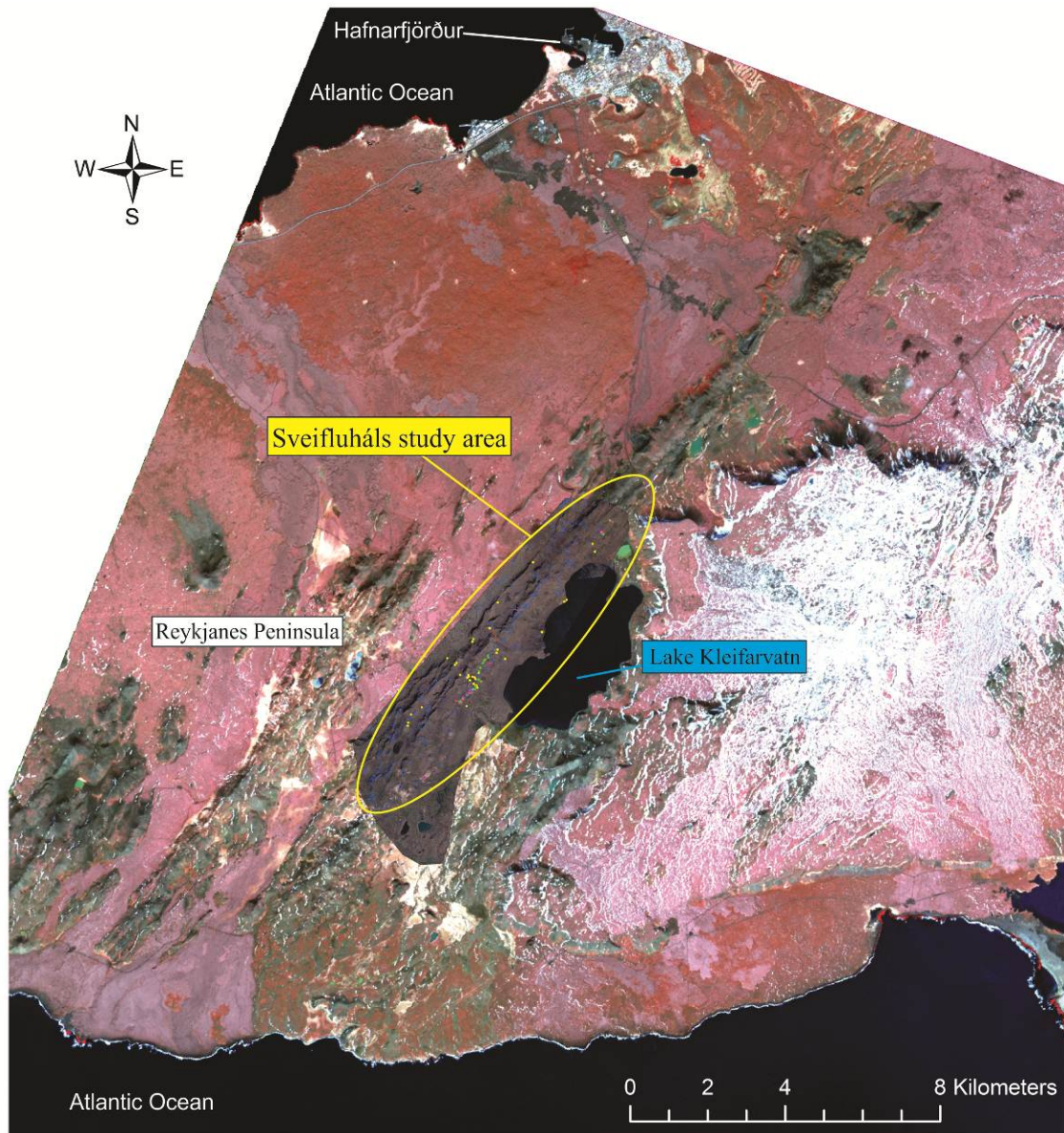


**Figure 3. Regional view of Sveifluháls, Iceland. NASA ASTER color-infrared (15 m pixel resolution) in the background and Loftmyndir color orthophotos (0.5 m pixel resolution) in the foreground are utilized in this image. Note: annotations on field site orthophotos are described later in the thesis.**

Sveifluháls is thought to have formed between 43,000-12,400 years ago (Mercurio, 2011). Sveifluháls is an onland expression of the Mid-Atlantic Ridge in Iceland and trends from SW to NE, consistent with the Mid-Atlantic Ridge trend about 3km offshore from the south-

western end of Sveifluháls. Sveifluháls lies within the Reykjanes Peninsula Volcanic Zone (RPVZ) (Clifton et al., 2003), located between the Mid-Atlantic Ridge (MAR) and the Western Volcanic Zone (WVZ) (Harðarson et al., 2008) (Figure 4).

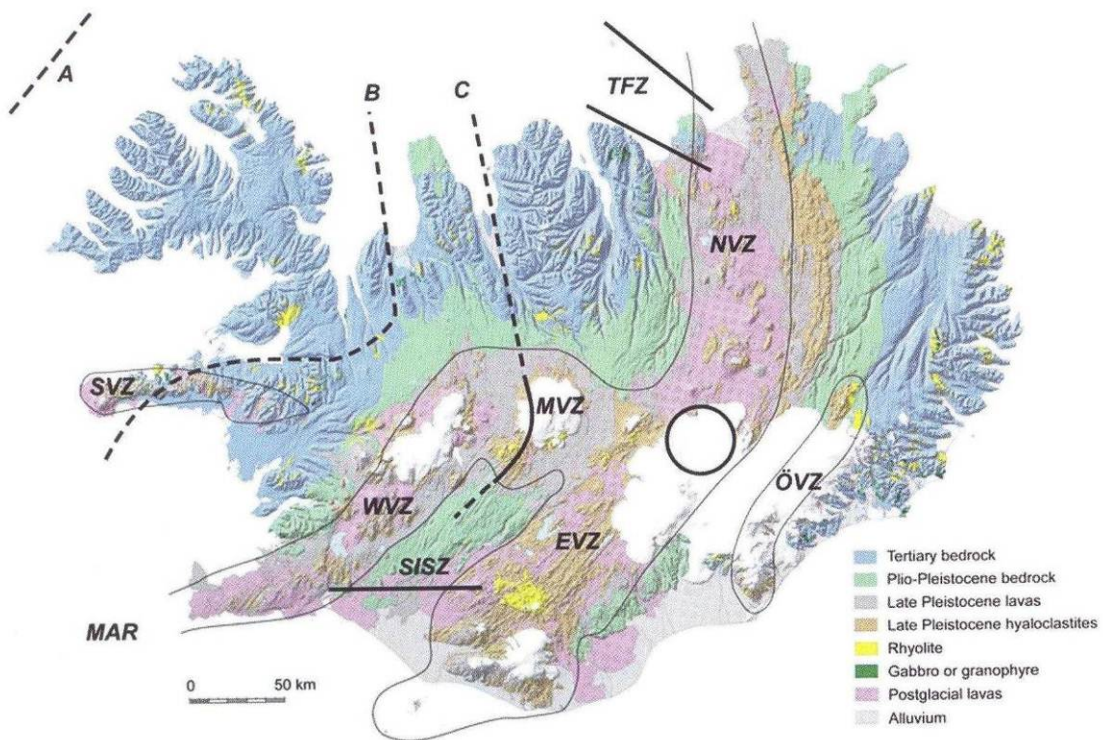


**Figure 4. The main volcanic, seismic, and rift zones of Iceland. EVZ: Eastern Volcanic Zone, MAR: Mid-Atlantic Ridge, MVZ: Mid-Iceland Volcanic Zone, NVZ: Northern Volcanic Zone, ÖVZ: Örfajökull Volcanic Zone, SISZ: South Iceland Seismic Zone, SVZ: Snæfellsnes Volcanic Zone, TFZ: Tjörnes Fracture Zone, WVZ: Western Volcanic Zone, A: Northwest rift axis, B: Snæfellsnes-Húnaflói rift axis, C: Skagafjörður rift axis, the circle shows the location of the Icelandic plume. (Harðarson et al., 2008)**

## 4.2 DESCRIPTION OF DIKES EMPLACED INTO WET LAPILLI TUFF AT SVEIFLUHÁLS, ICELAND

Basaltic dike intrusion into phreatomagmatic tephra deposits were investigated in detail at Sveifluháls. The following aspects of the intrusive domains were described in detail: dike orientation, mineralogy, gross morphology and dimensions of the dikes, dike interior characteristics, intrusive margin morphology and textures, peperite characteristics, proximal and distal host lapilli tuff deformation, and hydrothermal alteration of lapilli tuff adjacent to the intrusions.

Locations of studied intrusive areas at Sveifluháls, Iceland, were recorded with handheld global positioning satellite (GPS) units in Universal Transverse Mercator (UTM) coordinates and elevation in meters above sea level (ASL) in Table 1. The Earth shape model utilized was WGS 84 and the UTM zone was 27N.

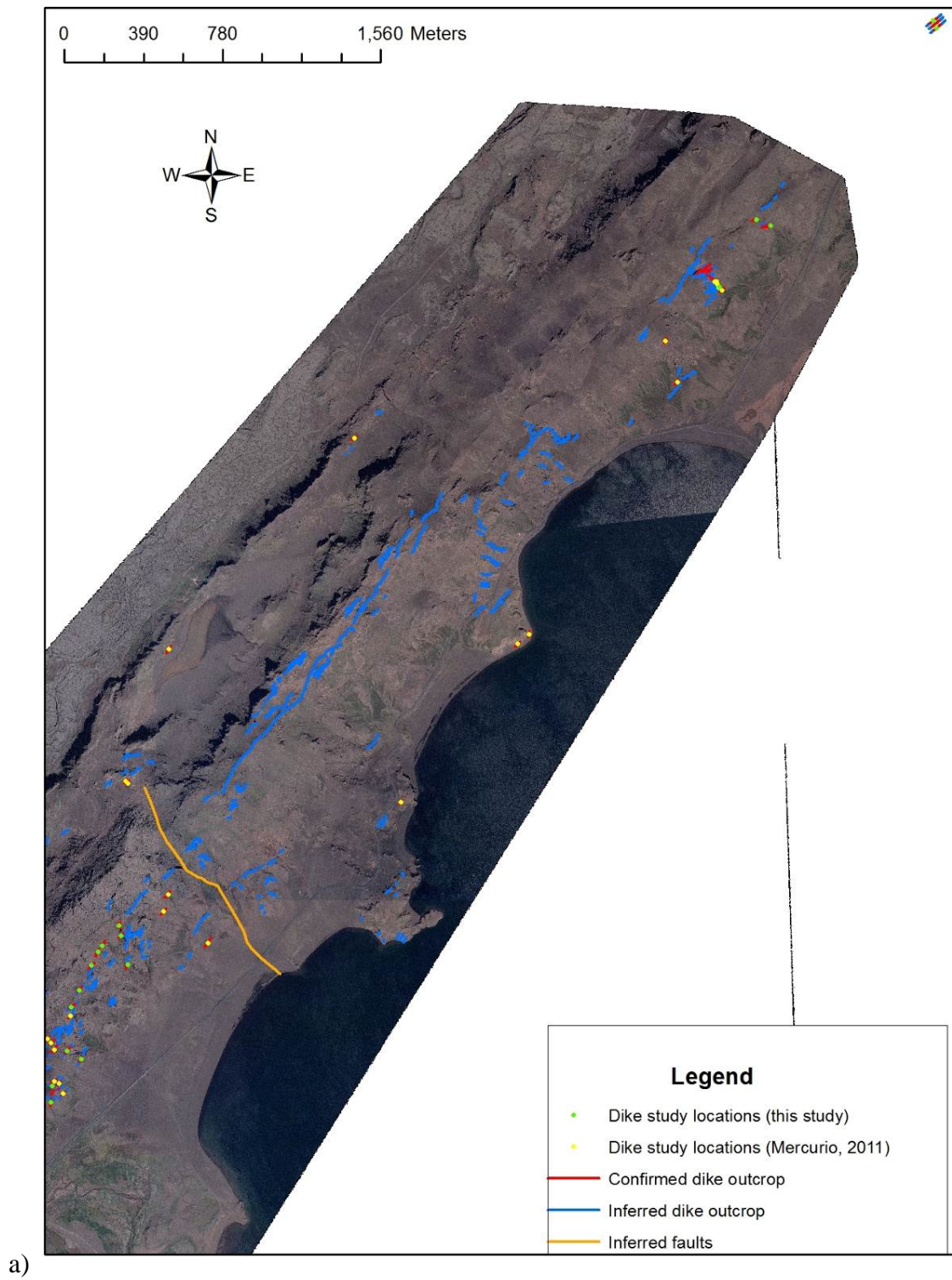
**Table 1. UTM coordinates and elevations of study area stations at Sveifluháls, Iceland.**

Station	UTM Coordinates	Elevation ASL (m)
1	0449629, 7087904	152
1a	0449439, 7088017	198
1b	0449426, 7088041	210
1c	0449409, 7088056	211
1d	0449484, 7088099	218
1e	0449532, 7088171	223
2a	0449124, 7087737	185
2b	0449162, 7087775	182
2c	0449183, 7087802	181
2d	0449033, 7087798	184
2e	0448996, 7087751	190
2f	0448880, 7087636	212
2g	0448775, 7087581	239
2h	0449114, 7087776	180
2i	0449216, 7087892	192

2j	0449336, 7087964	186
2k	0449359, 7087996	202
2L	0449399, 7088022	203
3a	0449523, 7088093	203
4a	0449415, 7088032	201
4b	0449461, 7088082	207
5a	0450316, 7089075	248
5b	0450070, 7088701	243
5c	0449905, 7088771	268
5d	0449870, 7088914	309
5e	0449859, 7088965	309
5f	0449779, 7088864	305
5g	0449756, 7088834	300
5h	0449725, 7088768	305
6a	0449663, 7088645	286
6b	0449624, 7058562	298
6c	0449605, 7088344	193
6d	0449674, 7088305	192
7a	0452880, 7092031	242
7b	0452822, 7092113	247
7c	0452859, 7091989	200
7d	0452753, 7091980	262
7e	0452750, 7091943	264
8a	0453892, 7093393	216
8b	0453877, 7093429	216
9a	0453075, 7092417	251
9b	0453004, 7092447	267

Commercially available color orthophotos (0.5m pixel resolution) from Loftmyndir were projected with GPS data in ESRI ArcMap, a geographic information system (GIS) program (Figure 5). The Earth shape model utilized was WGS 84 and the UTM zone was 27N.







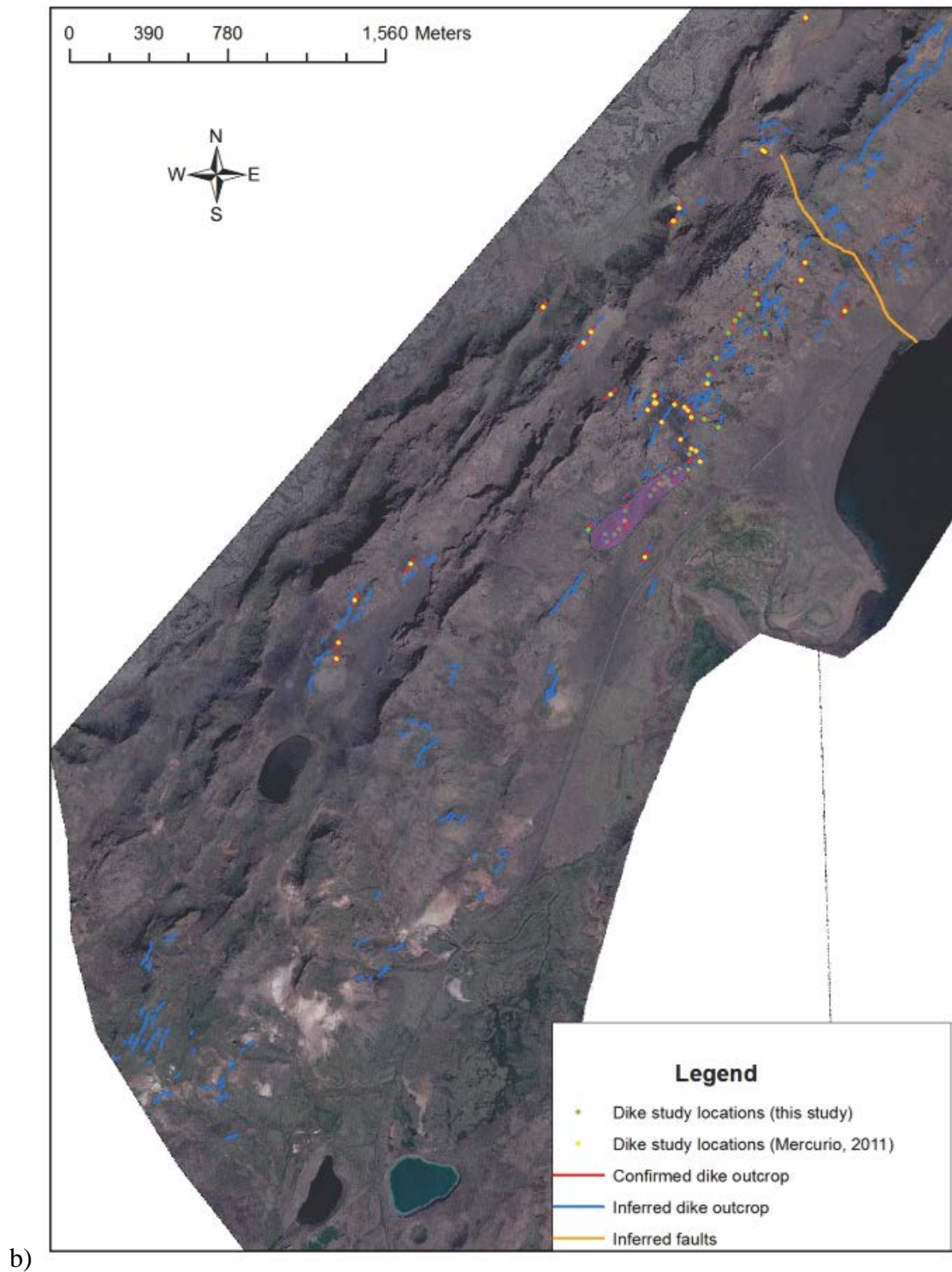
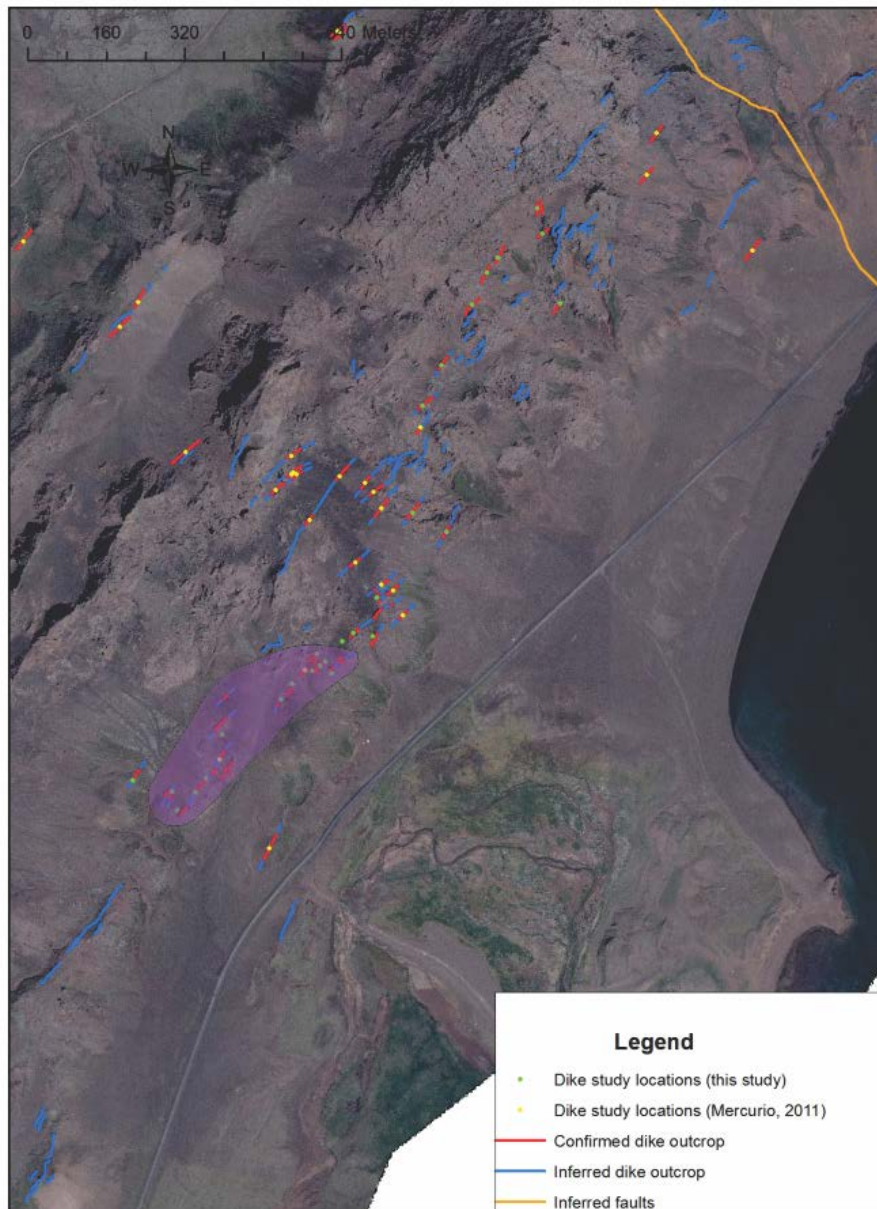


Figure 5. A) and b) show locations of basaltic dike intrusions at Sveifluháls, Iceland. Loftmyndir color orthophotos (0.5 m pixel resolution) are utilized in this image. Note dike outcrops and extensions. Note plateau areas in purple shading.

Figure 6 shows a close-up view of the intrusion-related features observed or inferred at Sveifluháls, Iceland.



**Figure 6. Inset of Sveifluháls, Iceland field area. Confirmed and inferred dike outcrops, hydrothermal and plateau areas, and inferred faults and troughs are outlined. Note plateau areas shaded in purple.**

Intrusions generally ran parallel to lake Kleifarvatn in a SW to NE trend. Strikes and dips were taken at various stations in the field area of intrusions and lapilli tuff bedding adjacent to intrusions (Table 2).

**Table 2. Strikes and dips of intrusions and lapilli tuff bedding near intrusions at Sveifluháls, Iceland.**

<b>Station</b>	<b>Medium</b>	<b>Strike</b>	<b>Dip</b>
1c	lapilli tuff bedding	060°	90°
2a	lapilli tuff bedding	107°	38°
2c	lapilli tuff bedding	014°	85°
2g	lapilli tuff bedding	118°	3°
2h	lapilli tuff bedding	067°	82°
2i	lapilli tuff bedding	092°	15°
2j	lapilli tuff bedding	040°	45°
2j	lapilli tuff bedding	065°	63°
5c	lapilli tuff bedding	150°	30°
5e	lapilli tuff bedding	031°	30°
5g	lapilli tuff bedding	065°	6°
5h	lapilli tuff bedding	063°	74°
6a	lapilli tuff bedding	077°	36°
6a	lapilli tuff bedding	099°	73°
6a	lapilli tuff bedding	235°	49°
6a	lapilli tuff bedding	095°	68°
6b	lapilli tuff bedding	038°	66°
7b	lapilli tuff bedding	265°	10°
7b	intrusion	235°	near 90°
7b	intrusion	350°	unknown
7b	lapilli tuff bedding	105°	46°
7c	intrusion	230°	85°
8a	intrusion	050°	sub-vertical
9a	lapilli tuff bedding	115°	25°
9a	intrusion	077°	sub-vertical
9a	intrusion	047°	sub-vertical
9b	intrusion	054°	sub-vertical

Photomosaics of all locations were created, and interpreted in the field and later. It is clear that the dikes most commonly form steep-sided ridges with irregular knobbly upper surfaces, and develop a distinctive talus of joint blocks. Gaps in the ridges are common, as are large variations in ridge widths, which may reflect the variations in the number of sub-parallel dikes (“dike swarms”) or changes in individual dike widths. Figure 7 outlines intrusive domains with distinctive cavities (potential “cryoliths”) at Station 1 and clearly shows the typical gross morphology of the dikes.

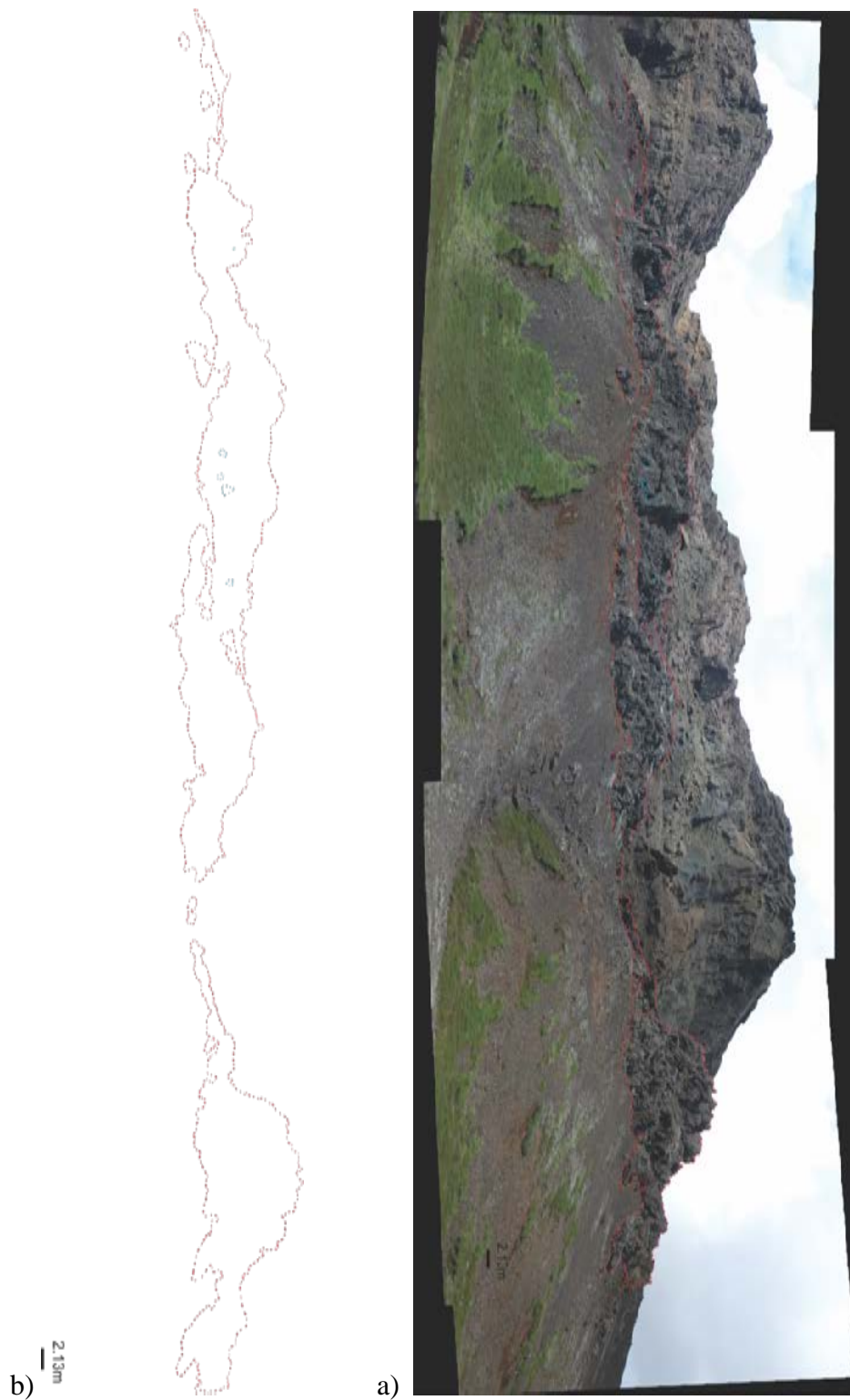


**Figure 7. a) Annotated photomosaic of illustrating the margins of intrusive domains (red) with distinctive cavities (potential “cryoliths”) (blue) at Station 1, Sveifluháls, Iceland. Note the distinctive geomorphic expression of the dikes. b) Extracted annotated overlay of Station 1.**

Samples of the intrusions, immediately adjacent host lapilli tuff and more distal lapilli tuff were collected at locations with GPS UTM coordinates, elevations, and a basic description of each sample (Table 3). The Earth shape model utilized was WGS 84 and the UTM zone was 27N.

**Table 3. Samples from intrusive areas at Sveifluháls, Iceland, including intrusion, host lapilli tuff, and hydrothermally altered lapilli tuff.**

Sample #	Details	GPS points (UTM)	Elevation (m)
hk1	basaltic intrusion	0449426, 7088041	210
hk2	lapilli tuff near intrusion	0449426, 7088041	210
hk3a	pillow breccia	0449124, 7087737	185
hk3b	lapilli tuff near intrusion	0449124, 7087737	185
hk4	lapilli tuff with bedding near intrusion	0449124, 7087737	185
hk5	basaltic intrusion	0449033, 7087798	195
hk6	pillowed intrusion	0449905, 7088771	268
hk7	lapilli tuff at contact with intrusion	0449859, 7088965	309
hk8	basaltic intrusion	0453892, 7093393	216

A generalized sketch of intrusion, disturbed lapilli tuff, and hydrothermal alteration zone widths are illustrated in Figure 8.

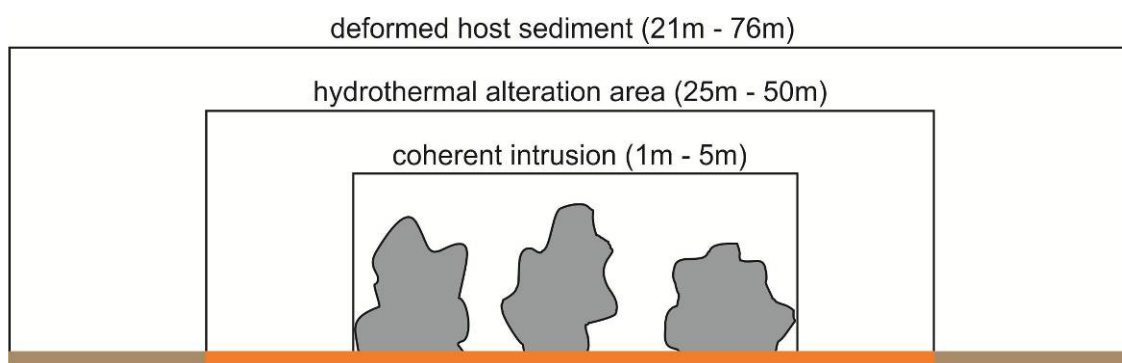


**Figure 8. Generalized sketch of intrusions emplaced into wet lapilli tuff at Sveifluháls, Iceland. Intrusion, hydrothermal alteration area and disturbed host lapilli tuff width ranges are shown. Note that in some areas one or more of these zones were not exposed.**

The coherent part of the intrusions have widths that varied from >1m - 5m with the majority of intrusions of widths between 3m and 5m. Some of these wider “dikes” represent multiple dikes. The host lapilli tuff along the margins of the dikes are commonly drag folded, and more distal rotated and slumped domains of host lapilli tuff area are also common. Width estimates for the distal disturbance zones varied from 21m - 76m. Width estimates of hydrothermal alteration areas varied from 25m - 50m. The various dike-related “zones” at Sveifluháls are described thoroughly in later sections of the thesis.

Figure 9 highlights intrusion/matrix contacts, pillow forms (pillow lavas, pillow tubes, and possible subaqueous pillow “haystacks”), jointing/bedding in blue, plateau area, and peperitic zones. Circular structures with radiating pillow forms were observed (Figure 9), which may be subaqueous pillow “haystacks”, ie (areas that represent locations of dike emergence on the subaqueous substrate surface).



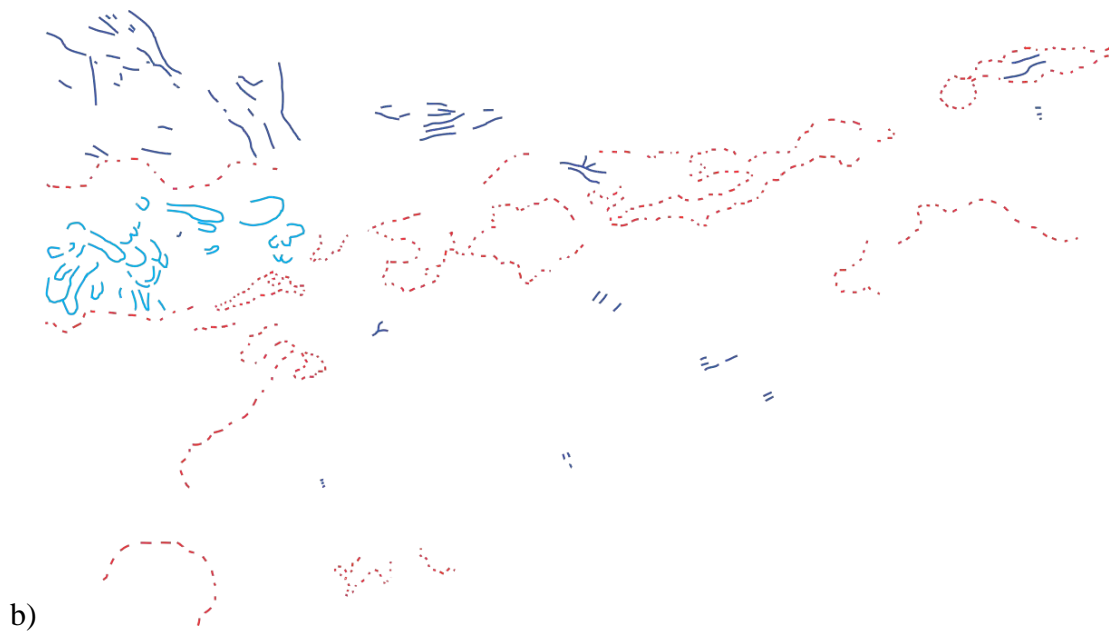


**Figure 9. a) An area of fingering intrusions at Sveifluháls, Iceland. This view was obtained at Station 2L. Intrusion/matrix contacts are shown in red, pillow forms in light blue (pillow lavas, pillow tubes, and possible subaqueous pillow “haystacks”), jointing/bedding in medium blue, plateau area, and peperitic zones. b) Annotated overlay of a).**



A plateau region related to dike emplacement is illustrated in Figure 10 along the strike of a dike at Sveifluháls.



**Figure 10. Plateau region at Sveifluháls, Iceland which develops along the intrusion zone at Station 2j. Note mixing of intrusion (grey) and hydrothermally altered lapilli tuff (dark red) and general strike of intrusions along the mid-slope on the ridge. Note plateau areas highlighted in purple.**

Such plateau-like regions were observed parallel to the mean dike trend along the ridge at Sveifluháls, Iceland. In general, slopes at Sveifluháls are steep, near the angle of repose. The plateau regions on the middle-upper slopes of Sveifluháls appear to be associated with the

emplacement of multiple dikes. The dikes, which are more resistant to erosion, have acted as a barrier to which talus was dammed.

#### **4.2.1 Dike Interiors**

Studied dike interiors at Sveifluháls, Iceland displayed a range of structures and characteristics that varied with location. A combination of several of the following were observed within the studied dike interiors: knobby pillow-like structures, blocky jointing, pillow forms, a non-pillowed nature, parallel jointing, potential pillow haystacks, distinctive cavities thought to be indicative of prior cryolith presence, and gaps between pillows.

Figure 11 shows the interior of a basaltic dike displaying a knobby pillow-like bodies with blocky jointing.



**Figure 11. Interior of a basaltic dike at Sveifluháls, Iceland, displaying a knobby pillow-like structure with blocky jointing at Station 6c. Pillow forms are outlined in green. Note mixing of lapilli tuff (orange) and intrusion (grey).**

Figure 12 shows a dike with compressed pillow margins and a non-pillowed blocky-jointed interior at Sveifluháls.





**Figure 12. Dike with compressed pillow margins and non-pillowed blocky-jointed interior at Station 8b at Sveifluháls, Iceland.**

A margin of fine-grained tephra and blocky-jointed intrusion is observed in Figure 13.



**Figure 13. A blocky parallel jointed non-pillowed dike interior with a pillowy margin at Sveifluháls, Iceland. Notice the minimal or absence of peperite development. Contact of intrusion and host lapilli tuff is outlined in red. This area is located at Station 7b.**

Curvicolumnar margin parallel jointing and blocky jointing of what appear to be of multiple dike interiors is seen in Figure 14.



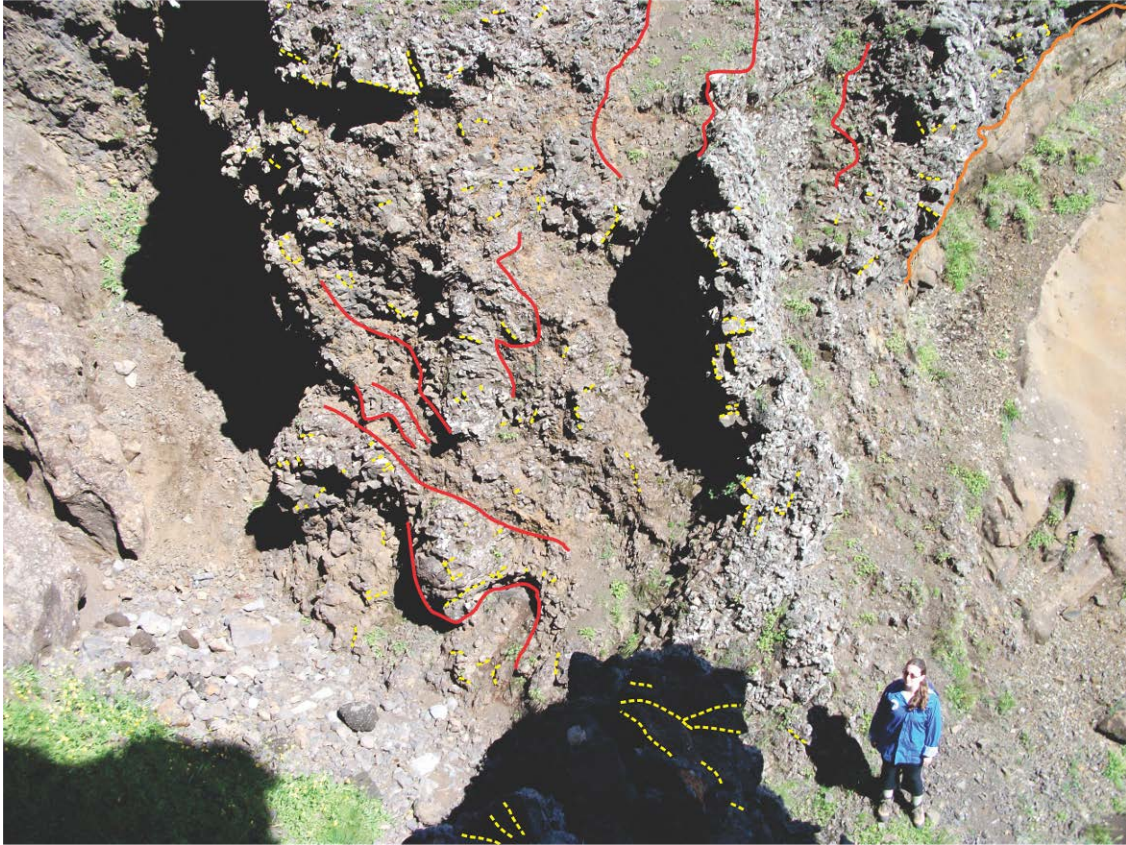


**Figure 14. Curvilinear jointing of multiple pillow dikes at Station 7b at Sveifluháls, Iceland. Discrete dike domains of several pulses or fingers may be seen. Note unmingled contact with host lapilli tuff in orange, dike pulses in red, and joints in yellow.**

The intrusive cooling domains in Figure 14 appear to have been initially restricted to within fissures. Upon reaching the paleosurface, the intrusions in Figure 14 may have generated pillow lava piles adjacent to the fissures.

Figure 15 shows a pillow haystack-like dike interior at Sveifluháls, which may be analogous to subaqueous pillow haystacks (similar to subaerial hornitos).

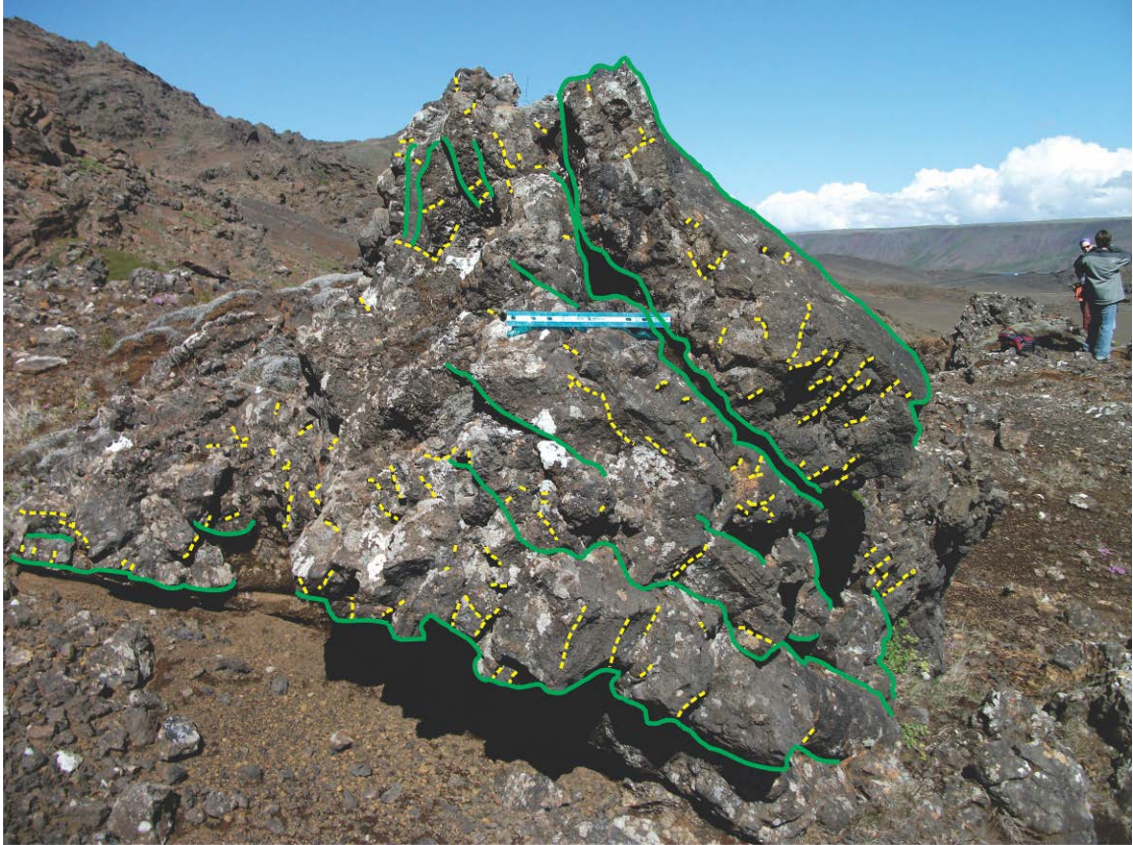


**Figure 15. Pillow tubes and a potential pillow haystack within a dike interior at Station 7a at Sveifluháls, Iceland. Note jointing within pillow tube structures. Jointing is delineated in yellow and pillow forms are outlined in green.**

Figure 16 displays an example of a distinctive cavity (a potential “cryolith”) within a dike interior at Sveifluháls. The interpretation of such cavities is described later in the thesis.





**Figure 16. Distinctive cavity of unknown origin within a dike interior at Station 4a at Sveifluháls, Iceland. Such a cavity may indicate the former presence of a “cryolith”.**

Figure 17 shows smaller cavities, interpreted as gaps between pillows within a dike interior at Sveifluháls with apparent compression of some pillows along the margin of the dike. Such compression may indicate a former ice or ice-cemented sediment contact (Skilling, 2009).



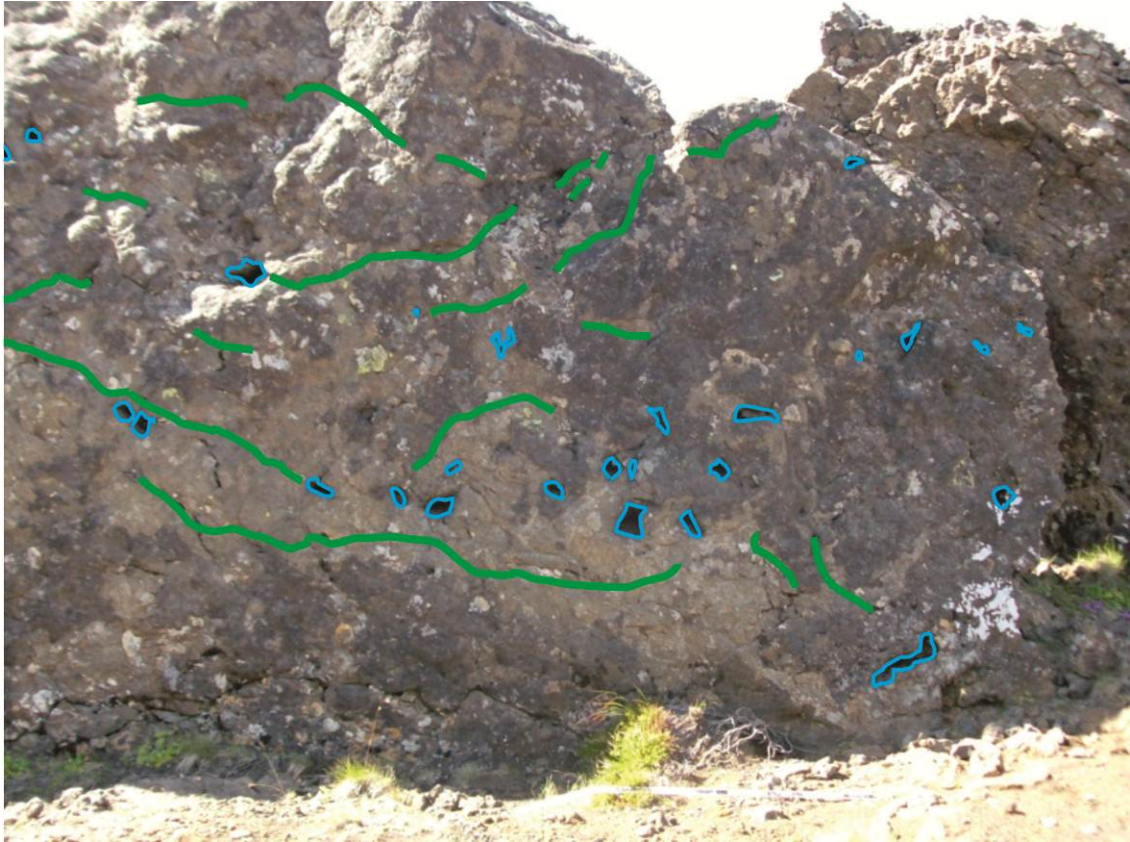


**Figure 17. Gaps between pillows within a dike interior at Station 8a at Sveifluháls, Iceland. Note the apparently compressed nature of the pillows. Pillow gaps are outlined in light blue and pillow forms in green.**

Figure 18 shows dike interiors displaying pillows with concentric vesicle banding produced by multiple magma pulses within the dike.

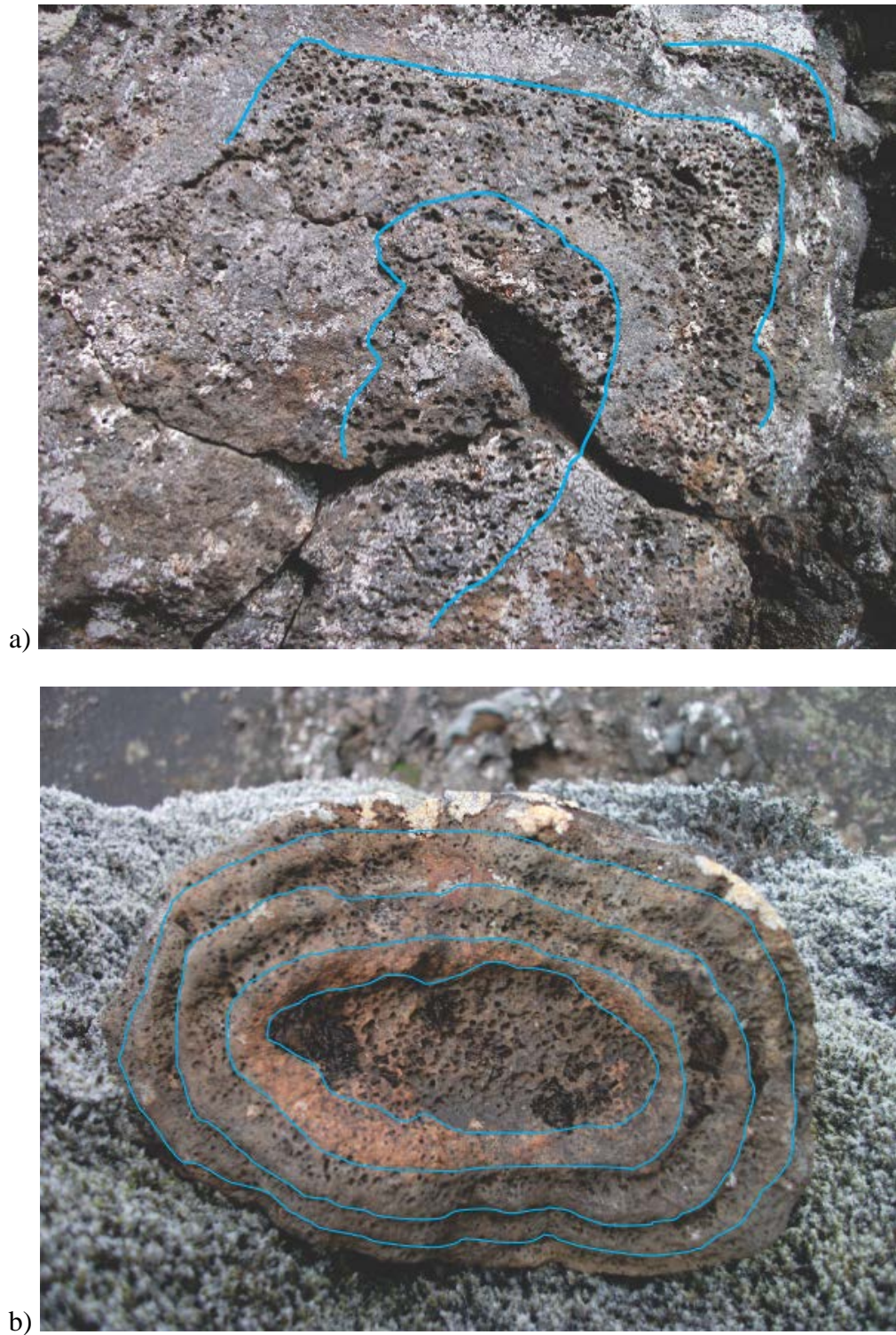


**Figure 18. Pillows from dikes at Sveifluháls, Iceland with multiple rinds and concentric vesicle banding. Vesicle bands representing separate pulses of magma injection are outlined in light blue. a) was taken at Station 1a. b) was obtained at Station 1d.**



Figure 19 shows a microscopic view of an interior of a basaltic dike at Sveifluháls with plagioclase crystals, pyroxene crystals, and vesicles.

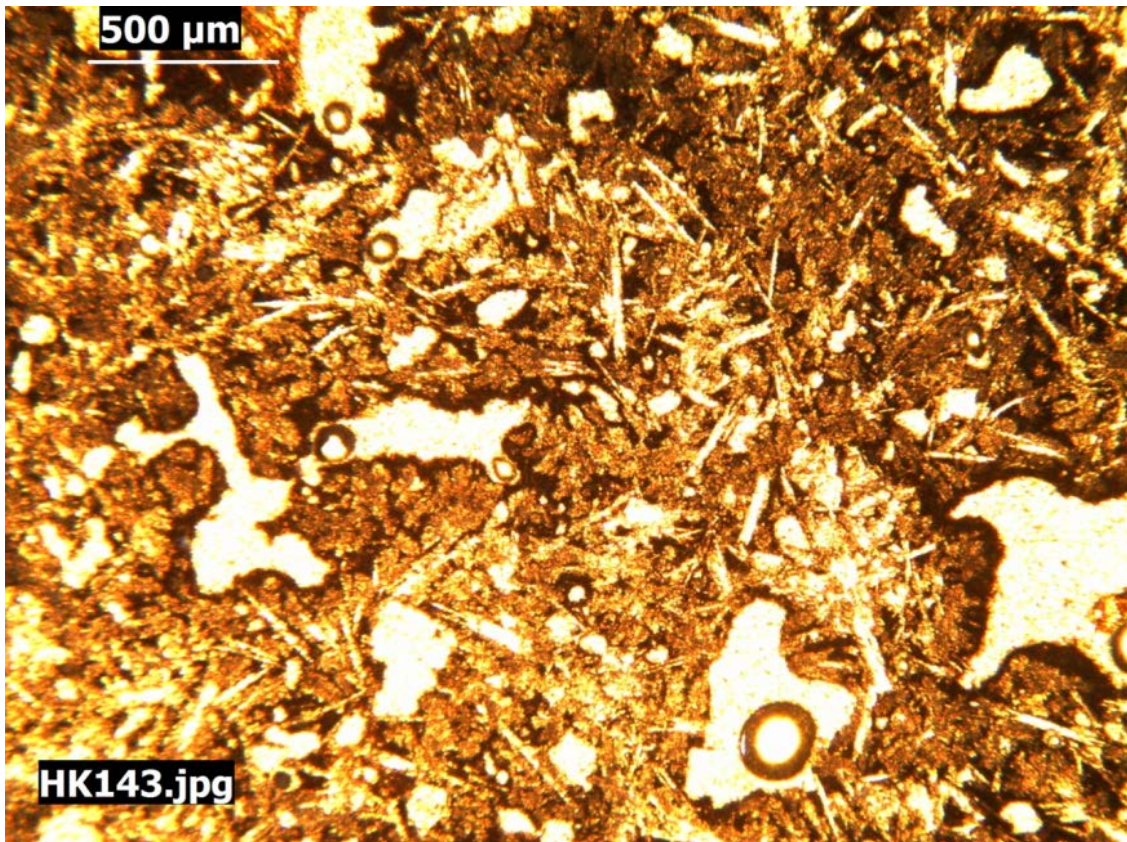


**Figure 19. Microscopic view of a basaltic intrusion at Sveifluháls, Iceland displaying vesicles, plagioclase, and clinopyroxene. Thin section extracted from Sample 6, which was obtained at Station 5c.**

#### **4.2.2 Dike Margins**

The dike margins at Sveifluháls are varied, but include examples without peperite development that are linear, resembling dikes emplaced into rock, margins that are “billowy”, clearly



pillowed, and examples with significant development of both fluidal and blocky peperite. Figure 20 illustrates a pillowed/lobate dike margin with development of peperite.

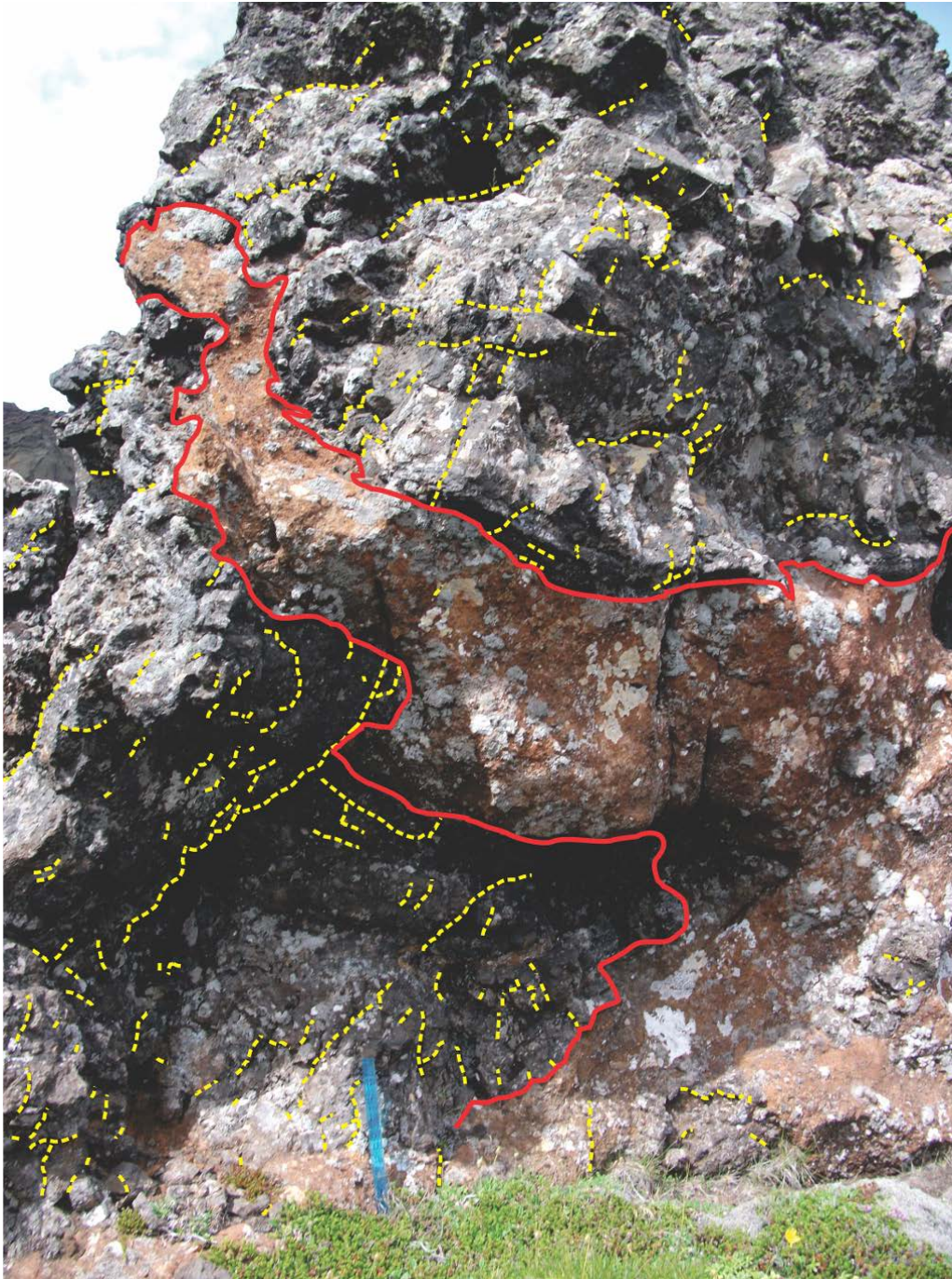


**Figure 20. Fluidal pillowy margin of an dike at Station 1b at Sveifluháls, Iceland with peperite, a product of wet lapilli tuff-intrusion mixing. Note joints in yellow and approximate dike-host contact in red.**

A pillowed dike margin with peperite and a reddish hydrothermally altered host lapilli tuff may be seen in Figure 21.



**Figure 21. Peperitic dike margin with pillowy lobes at Station 1b at Sveifluháls, Iceland. Note hydrothermal alteration of host lapilli tuff. Note joints in yellow.**



A pillowed dike margin with numerous pillow tubes, some compressed, is shown in Figure 22.

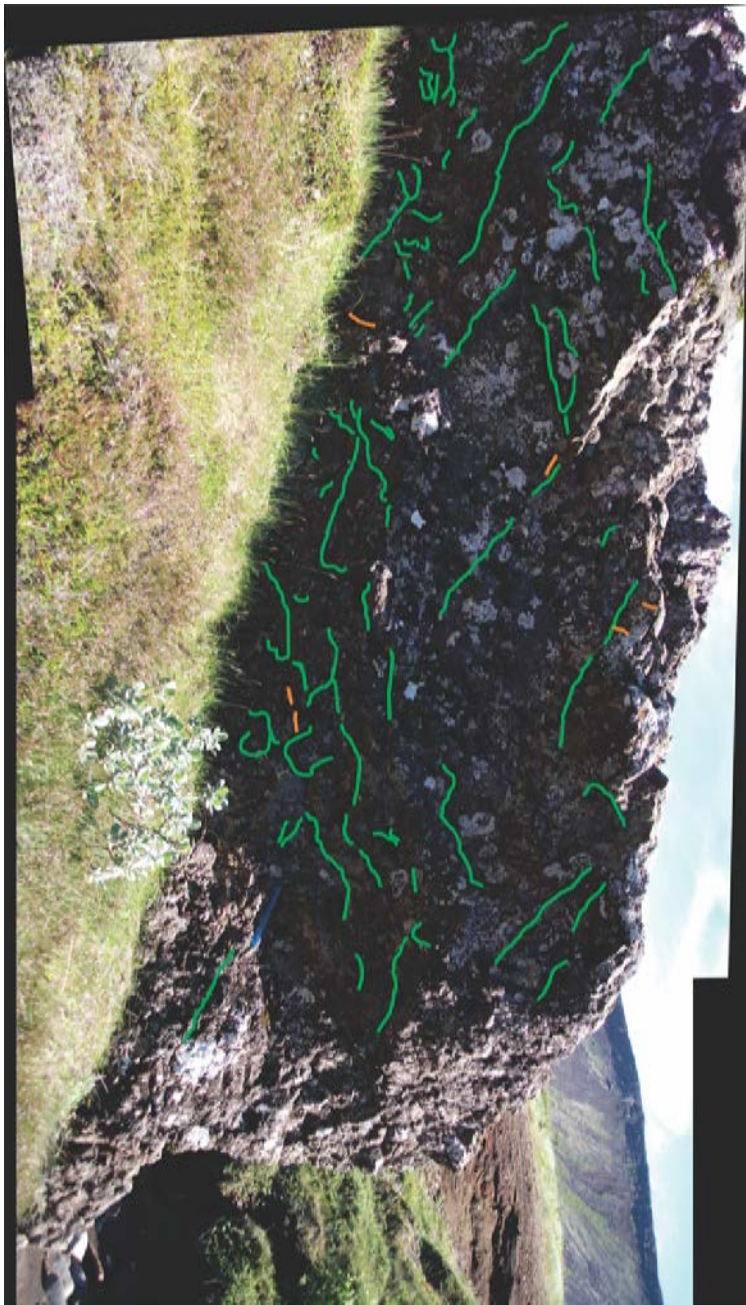


**Figure 22. Exposed intrusion at Sveifluháls, Iceland, showing a pillowed dike margin and compressed pillow tubes at Station 8a. Note pillow forms outlined in green and fractures in orange.**

Figure 23 shows a possible subaqueous pillow haystack (steep cone-like feature similar to subaerial hornitos) at Sveifluháls.

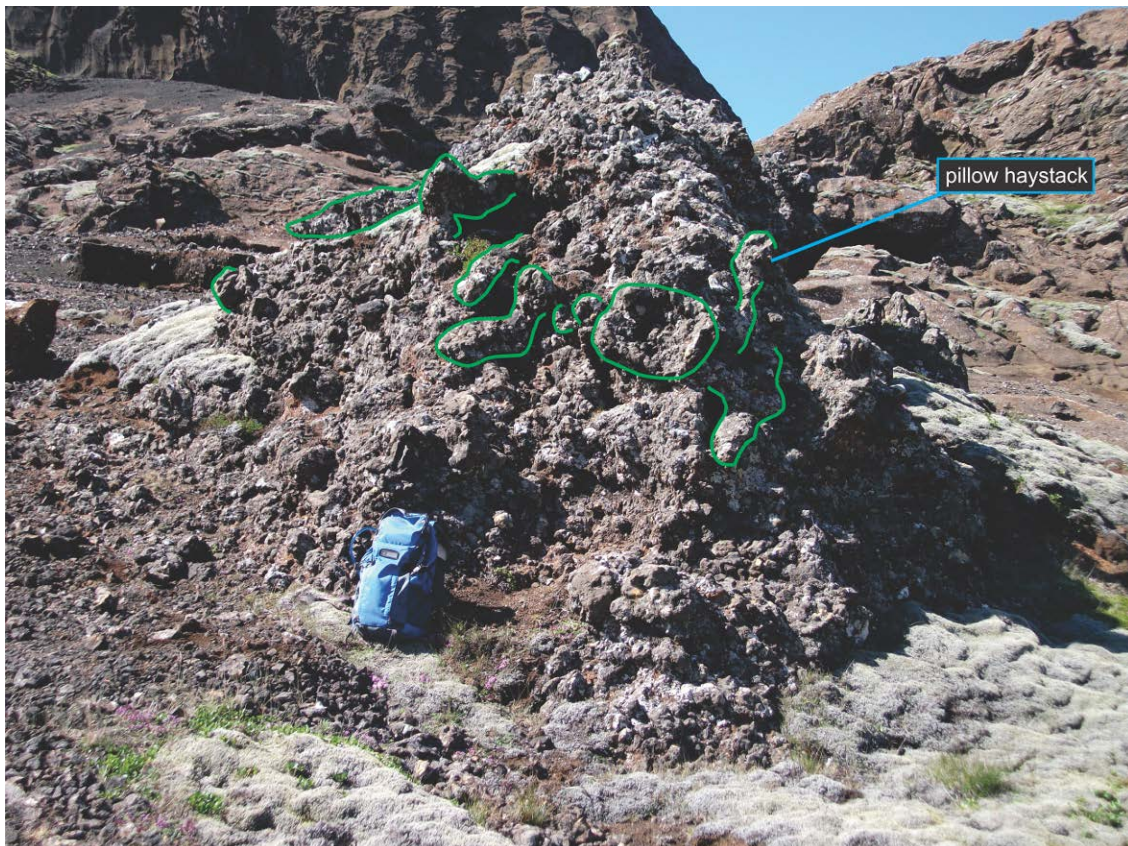


**Figure 23. Possible pillow haystack at Station 6c at Sveifluháls, Iceland. Such a structure may be analogous to subaqueous pillow haystacks (steep cone-like feature similar to subaerial hornitos) observed on the seafloor in other studies. Note pillow forms outlined in green.**

Such structures exhibit similarities to subaqueous pillow lava haystacks, described by Stakes et al. (2006). At one station a dike-like body clearly fed a subaqueous lava flow down the steep slope of lapilli tuff deposits (Figure 24).



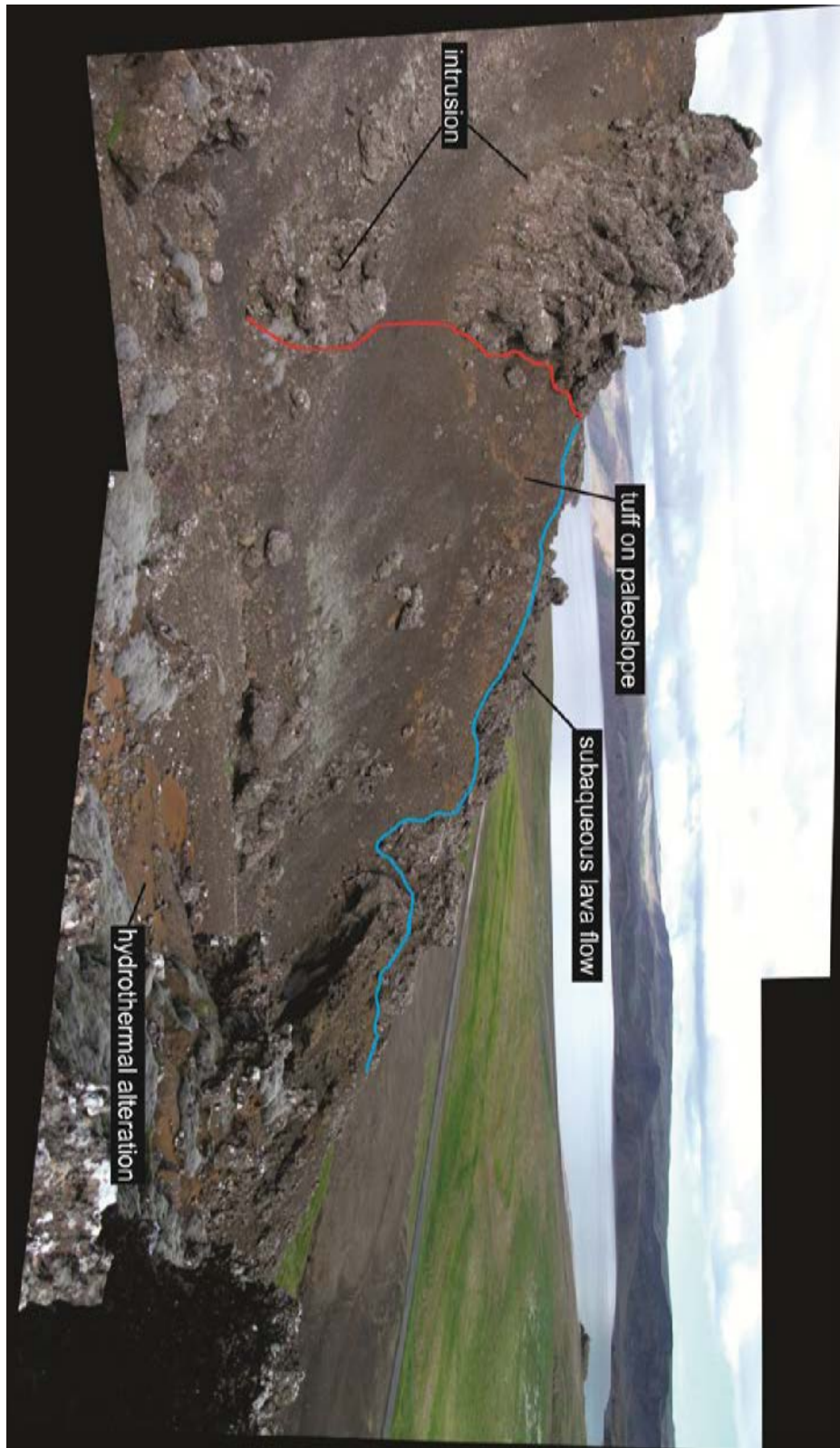


**Figure 24. Intrusion (red) and subaqueous lava flow (light blue) at Station 1d at Sveifluhals, Iceland.**  
**Note hydrothermal alteration and the high-level nature of the intrusion in reference to the paleoslope.**



One dike with apparently compressed pillow margins displayed “ooze-out” structures along polygonal cooling joints developed in the compressed pillows (Figure 25).



**Figure 25. “Ooze-outs” along polygonal cooling joints, developed along compressed dike-margin pillows, located at Station 8a at Sveifluháls, Iceland. Such structures indicate characteristics of this intrusion’s cooling process where magma was later squeezed through fractures in the previously chilled margin.**

### **4.2.3 Dike-Induced Deformation of Host Lapilli Tuff**

Dike-related ductile and brittle deformation of host lapilli tuff is very common at Sveifluháls, and can be subdivided into two types, drag-folded and faulted domains within a few meters of the dike margin, and more distal (up to 200m) away, rotated and slumped blocks and domains of host. Rotated bedding in the host can most easily be identified where it is greater than the angle of repose (about 35 degrees). Such oversteepened bedding occurs in both the drag-folded proximal domains and in the more distal angular blocks and irregular domains. Vertical, near-vertical bedding, overturned bedding and syn-sedimentary faulting and folding is particularly common in the proximal domains.

A view of overturned drag folded lapilli tuff may be seen near an intrusion in Figure 26.

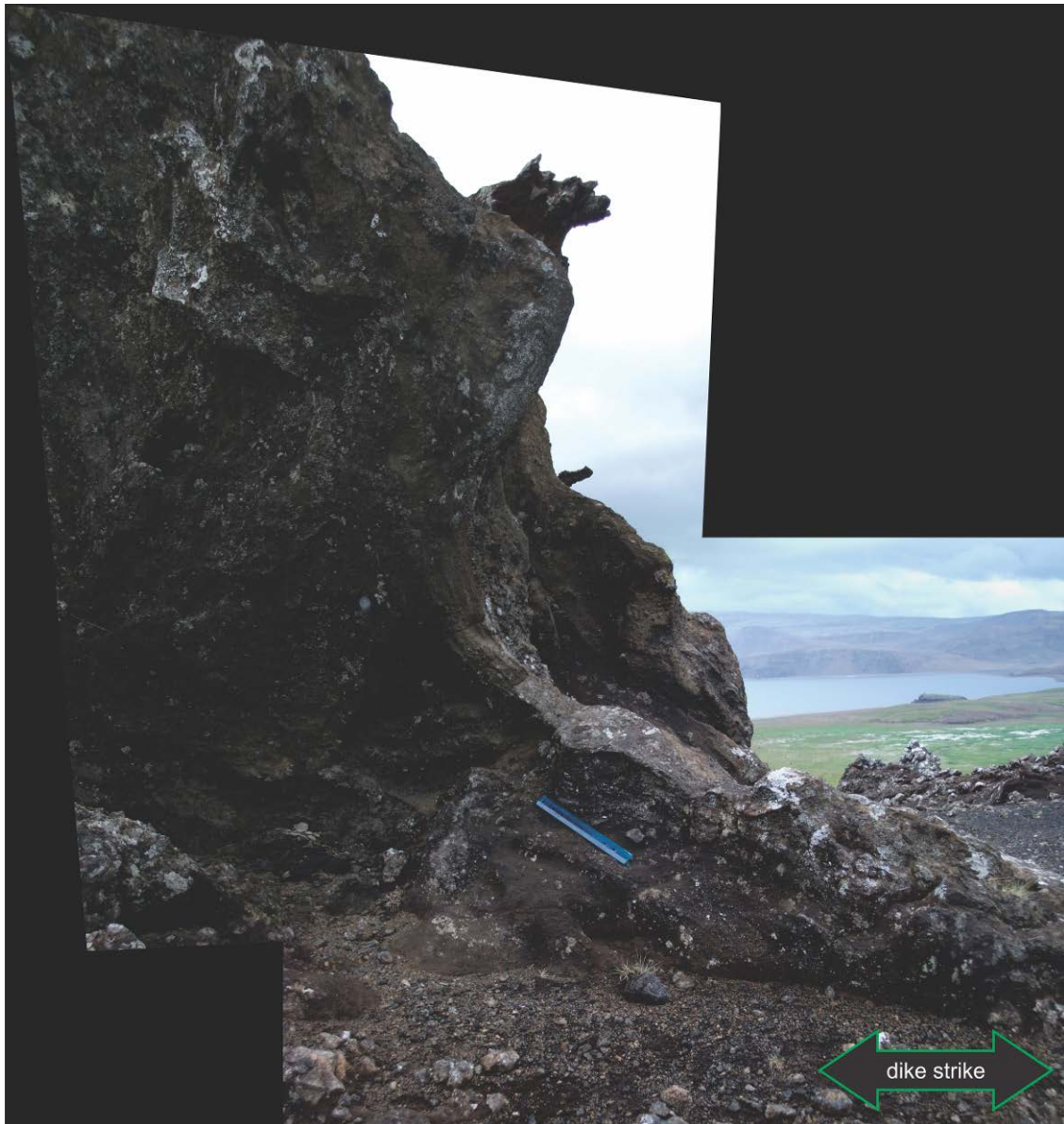


**Figure 26. Drag-folded overturned lapilli tuff adjacent to dike at Station 2j at Sveifluháls, Iceland. Note the deformed and nearly overturned nature of the host lapilli tuff.**

Figure 27 shows drag-folded lapilli tuff domains adjacent to a dike with cross-lamination, scours, overturned beds and a possible synsedimentary fault.





**Figure 27. Drag-folded lapilli tuff domains adjacent to a dike at Station 1c at Sveifluháls, Iceland. Note area of cross-lamination, scours, and overturned beds. A possible synsedimentary fault is outlined in orange.**

An instance of dike-induced deformed lapilli tuff may be seen in Figure 28.





**Figure 28. Synsedimentary deformation observed within host lapilli tuff near a dike at Station 2k at Sveifluháls, Iceland.**



Drag-folded (rotated and overturned) deformation of lapilli tuff adjacent to a dike is illustrated in Figure 29.



**Figure 29. Drag-folded and overturned bedding in lapilli tuff adjacent to a dike at Station 1c at Sveifluháls, Iceland.**

Figure 30 shows deformation of lapilli tuff adjacent to a dike. The lapilli tuff here also displays scours and well-developed parallel laminae.



**Figure 30. Deformation of lapilli tuff adjacent to dike at Station 1c at Sveifluháls, Iceland. The lapilli tuff here displays scours and horizons of well-developed parallel laminae.**

Figure 31 shows laminae within drag-folded domains of lapilli tuff adjacent to a dike.





**Figure 31. Laminae within drag-folded domains of lapilli tuff adjacent to a dike at Station 2j at Sveifluháls, Iceland. Note the fan-like and arch-like patterns of the laminae. An approximate axis of the fold is outlined in orange.**

Figure 32 shows distal rotation of blocks of host lapilli tuff further away from an intrusion.





**Figure 32. Distal rotation of host lapilli tuff at Sveifluhals, Iceland. The intrusion in this area is less than 200m to the left of this image. (Mercurio, shared data)**

Some areas display lapilli tuff that clearly post-dates emergent intrusions, such as the area in Figure 33.

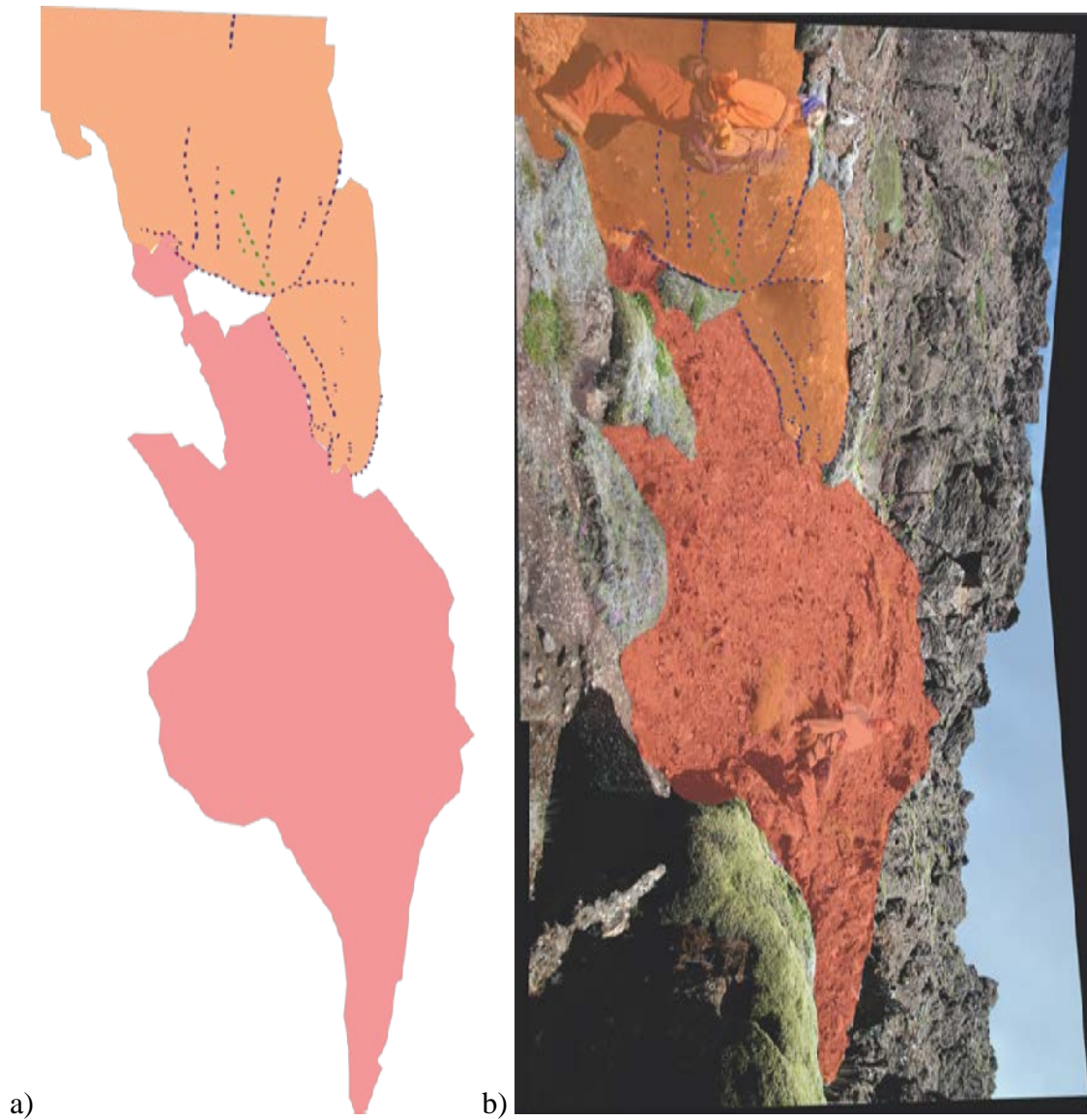


**Figure 33. Tephra may post-date the intrusions for this site at Station 5g at Sveifluháls, Iceland. Suspected post-intrusive tephra (orange) and intrusive mixing with lapilli tuff (peperite) (red) are shown. Note fractures (blue) and bedding (green).**



#### 4.2.4 Dike-Margin Peperite

Studied dike-margin peperite at Sveifluh  ls, Iceland displayed a range of structures and characteristics that varied with location. A combination of several of the following were observed within examples of dike-margin peperite found at Sveifluh  ls: fluidal peperite, blocky peperite, and clasts derived from pillow rinds.

Figure 34 highlights fluidal and blocky peperite domains along the margin of an intrusion at Sveifluh  ls, Iceland (Skilling, unpublished).

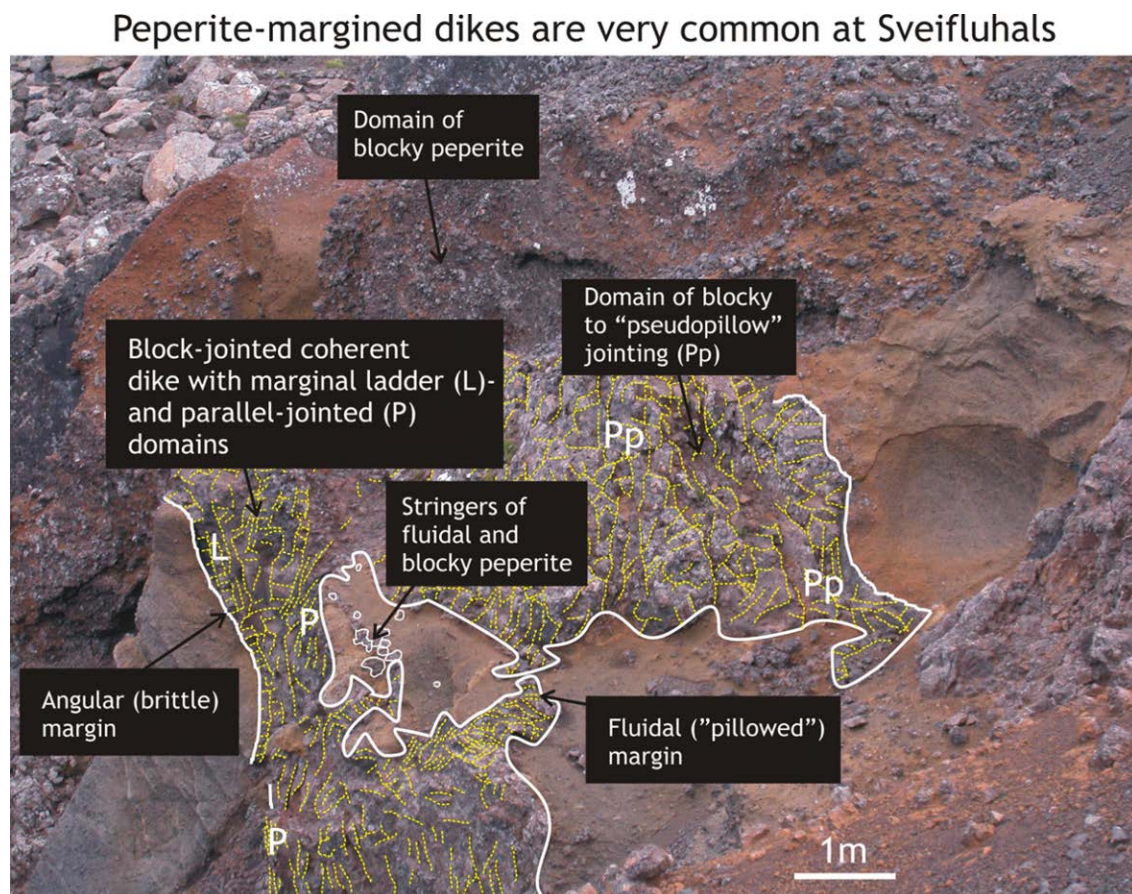


**Figure 34. Fluidal and blocky peperite domains along the margin of an intrusion at Sveifluh  ls, Iceland. (Skilling, unpublished)**

Figure 34 displays a brittle contact on one side and a fluidal contact on the other. Such contacts may indicate a temperature and/or moisture differential within the host from one side to the other. Pseudopillow joints are seen in Figure 34 as well. Such structures may originate as curved fractures perpendicular to the margin that expand as liquid water or steam invade.

The peperite in Figure 35 displays a variety of jointing patterns, including blocky, “pseudopillow”, and parallel jointing. Figure 35 illustrates a blocky dike-margin peperite that displays several juvenile clasts clearly derived from the rinds of pillows.



**Figure 35. Blocky dike-margin peperite at Station 9b at Sveifluháls, Iceland, that displays several clasts clearly derived from pillow rinds. Note pillow joint blocks and cubes breaking off from the dike.**

Figure 36 shows a blocky peperite-drag folded lapilli tuff contact at Sveifluháls, Iceland.





**Figure 36. Blocky peperite associated with drag-folded host lapilli tuff at Station 9a at Sveifluháls, Iceland. Note adjacent host lapilli tuff deformation.**

Figure 37 shows a dike emplaced into lapilli tuff with fractured angular blocks, pillow forms, and peperite.



**Figure 37. Dike emplaced into lapilli tuff featuring fractured angular blocks, pillow forms, and marginal blocky peperite at Station 2a at Sveifluháls, Iceland.**



Figure 38 shows a blocky-jointed dike interior with peperite.

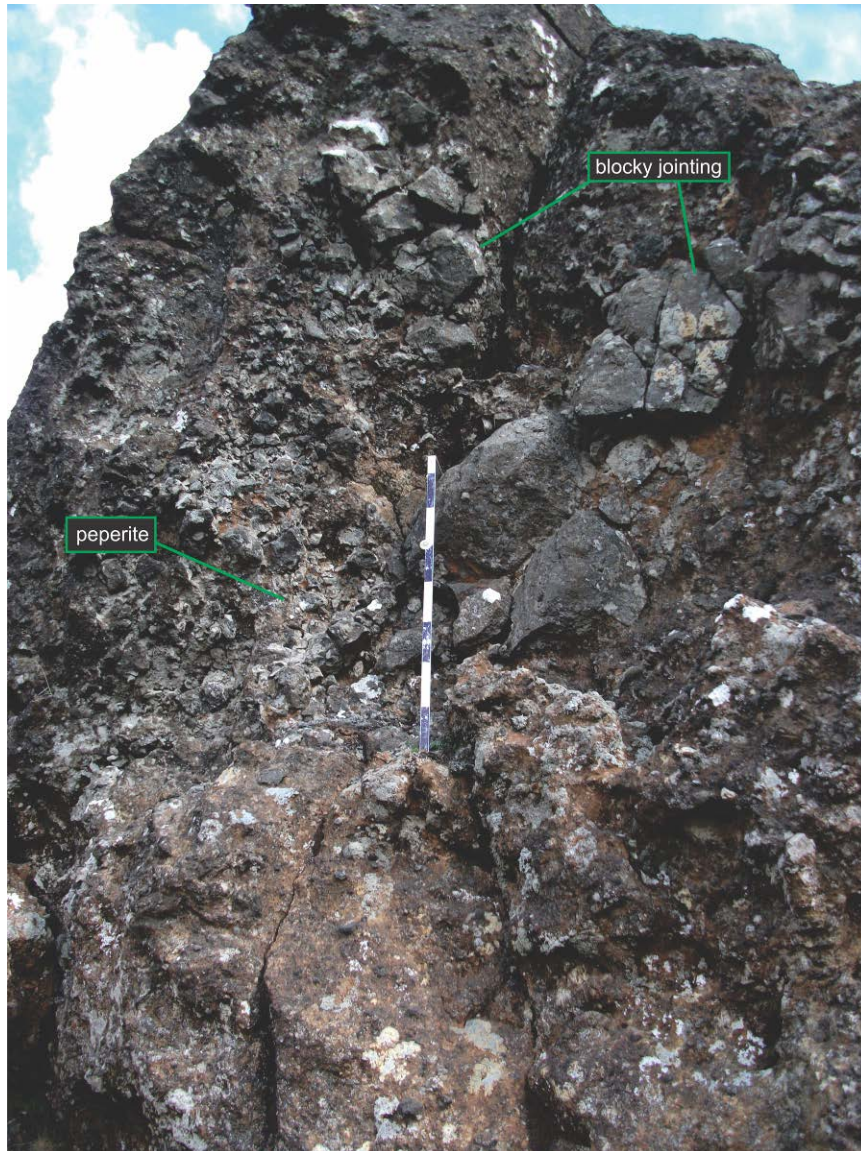


**Figure 38. A blocky-jointed dike interior with peperite at Sveifluháls, Iceland, located at Station 5d.**

Figure 39 shows a close-up of dike-margin blocky peperite with blocky to ragged juvenile clasts as seen at Sveifluháls.





**Figure 39. Blocky to ragged juvenile vesicular clasts (black/grey) in dike-margin peperite at Station 2c at Sveifluháls, Iceland surrounded by host lapilli tuff (orange). Moss patch (bottom right) is about 10 cm. Note the scoriaceous/highly vesicular nature of these juvenile clasts.**

#### **4.2.5 Dike-Related Hydrothermal Alteration of Host Lapilli tuff**

Studied dike-related hydrothermal alteration of host lapilli tuff at Sveifluháls, Iceland displayed a range of structures and characteristics that varied with location. A combination of several of the following were observed: deep reddening of host lapilli tuff (which differed from the buff coloring of the non-hydrothermally altered host lapilli tuff), potential hematite lining vesicles, and red soils.

Figure 40 shows common hydrothermal reddening of lapilli tuff adjacent to dike margin.



**Figure 40. Hydrothermal reddening of tephra adjacent to dike margin at Station 2j at Sveifluháls, Iceland with deformed lapilli tuff. Note the deep shade of red to the hydrothermal alteration, indicating a possible higher temperature of the hydrothermal fluids in this area.**



Figure 41 shows an example of an intrusion (light gray) associated with distinctive hydrothermally altered adjacent lapilli tuff (dark red).



**Figure 41. Dike-like intrusion into hydrothermally reddened lapilli tuff at Station 2i at Sveifluháls, Iceland. The lapilli tuff displays a reddening that is distinct from the “background” buff palagonitization.**

Figure 42 and Figure 43 show microscopic views of possible hematite lining vesicles within a dike at Sveifluháls.

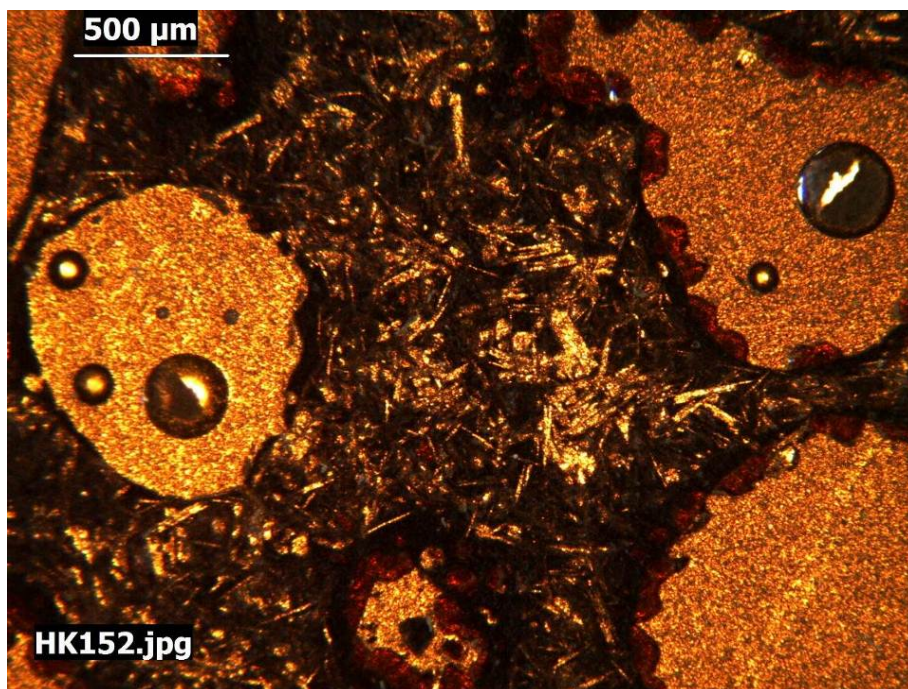


Figure 42. Microscopic view of possible hematite lining vesicles within a dike at Sveifluháls, Iceland.  
The thin section was taken from Sample 5 at Station 2d.

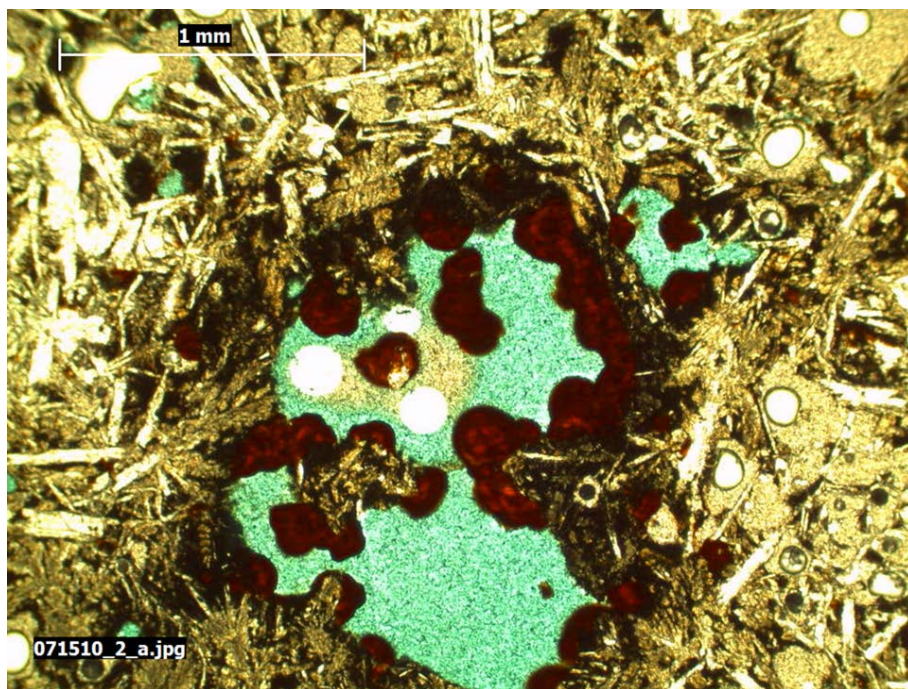


Figure 43. Possible hematite spherules infilling a vesicle at Sveifluháls, Iceland. (Mercurio, shared data)



Similar Fe-rich minerals can be seen in vesicles in pore space of host lapilli tuff glass. This secondary mineralization is presumably the cause of the reddening. Figure 44 shows red soils developed near areas of hydrothermal reddening of lapilli tuff along dike margins.



**Figure 44. Red soils developed near areas of hydrothermal reddening of lapilli tuff along dike margins at Station 2a at Sveifluhál, Iceland. Note the plateau region along the strike of the dike.**



### **4.3 INTERPRETATION AND MODEL OF DIKE EMPLACEMENT INTO WET LAPILLI TUFF AT SVEIFLUHÁLS, ICELAND**

Clifton and Kattenhorn (2006) produced a map of fractures and normal, oblique, and strike-slip faults of the Reykjanes Peninsula. Fractures near volcanic fissure swarms tended to strike parallel to the complexes, and are thought to be normal faults and tension fractures (Clifton and Kattenhorn, 2006). These fractures were interpreted by Clifton and Kattenhorn (2006) to indicate extensional structures formed above and flanking dikes.

Many of the confirmed dikes at Sveifluháls are sub-parallel, with some curved areas of the dikes (in plain view) and some apparent bifurcations seen in aerial imagery. Figure 5 shows exposures of confirmed and inferred dikes at Sveifluháls, which reveals that overall the dikes largely trend from SW to NE, consistent with the main ridge trend. The overall dike trends at Sveifluháls are consistent with the overall trend of fractures on the Reykjanes Peninsula, which largely strike NE (Figure 45) (Clifton and Kattenhorn, 2006).

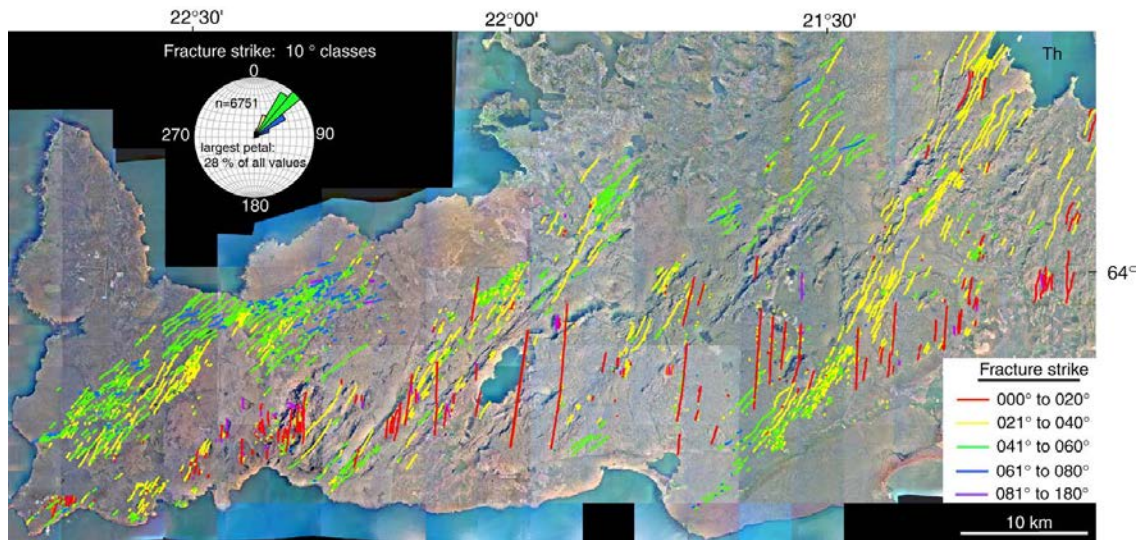


**Figure 45. Fracture trends of the Reykjanes Peninsula, SW Iceland. The rose diagram indicates an overall NE trend among the fractures. Strike trends are denoted by color: 000°- 20° (red), 021° - 040° (yellow), 041° - 060° (green), 061° - 080° (blue), 081° - 180° (purple). (Clifton and Kattenhorn, 2006)**

Locally a variety of dike trends are observed, with a few segments trending SE to NW (Figure 5). Locally some dikes also appear to be offset when observed in aerial photography, and may be indicative of transform faults that postdate the dike (Figure 5). Clifton and Kattenhorn (2006) marked the likely placement of strike-slip faults at Sveifluháls, Iceland as well (Figure 46).

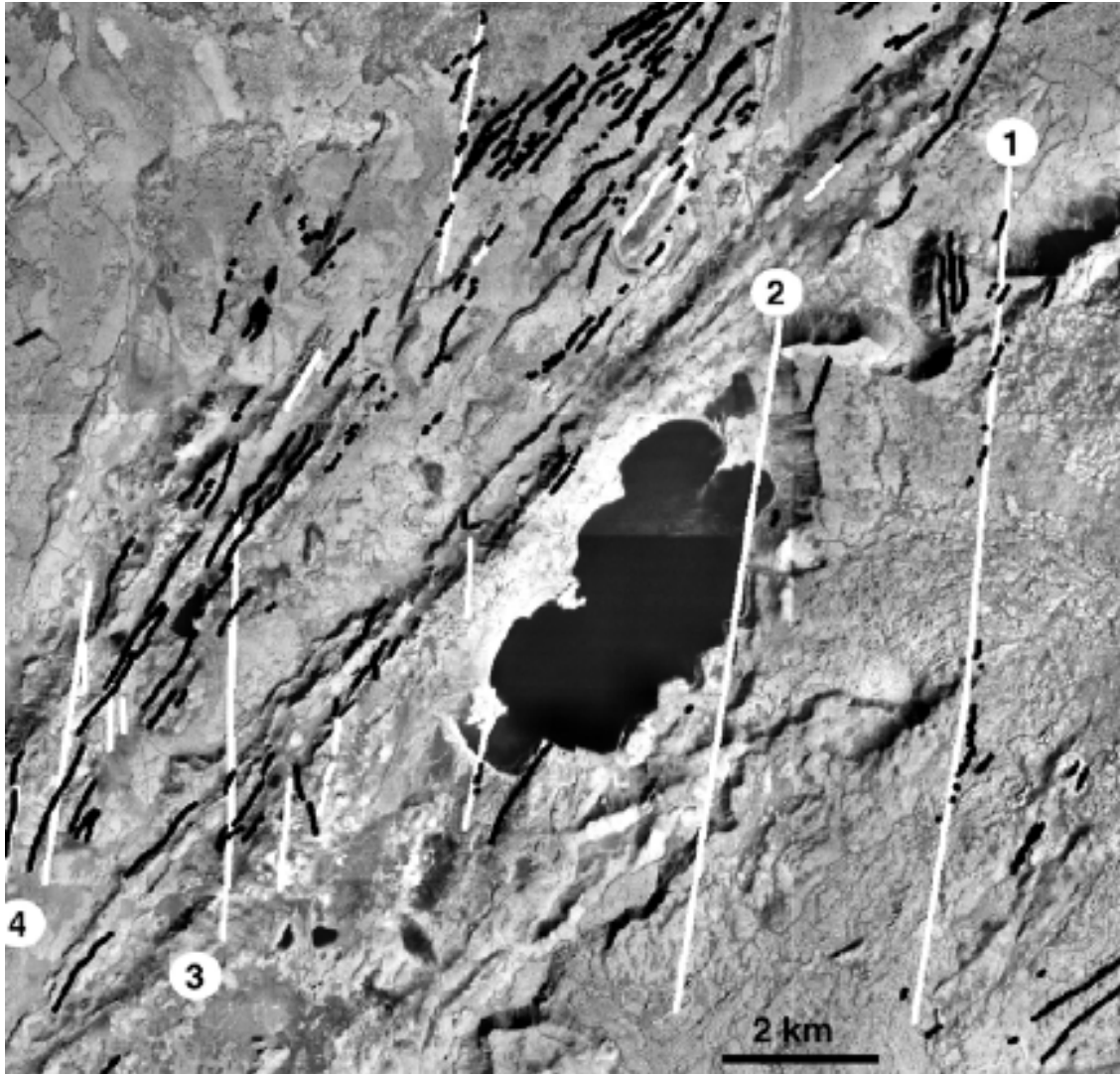


**Figure 46. Strike-slip faults (white) and fractures (black) at Sveifluháls, Iceland were interpreted from photographic and field data (fault 1). Faults 1 - 4 were identified with the aid of seismic data. (Clifton and Kattenhorn, 2006)**

The strike-slip faults indicated by Clifton and Kattenhorn (2006) in Figure 46 were largely identified via seismic analysis. Only Fault 1 in Figure 46 was interpreted by photographic and field data.

The dikes at Sveifluháls observed in this study largely fell within Clifton and Kattenhorn's fracture strike green range on Figure 45. A few of the dikes of this study fell

within the blue range of Clifton and Kattenhorn's fracture strike range, and one dike fit within the purple strike range seen in Figure 45.

The origin of the dike plateaus at Sveifluháls is most likely due to two or more sub-parallel dikes that have developed a more highly resistant hydrothermally altered zone between them and/or have trapped dike-derived talus or later phreatomagmatic tephra in the same area. Topographic profiles drawn perpendicular to strikes of potential dikes on Mars obtained via MOLA data may aid in the identification dike plateaus and possible dikes in the future.

Distinctive cavities observed within the dikes are of two possible origins. The larger cavities (Figure 16), are interpreted as “cryoliths” or as Skilling (2009) describes them, “ice-block meltout cavities”, which were interpreted by Skilling (2009) from sub-ice lava mounts at Höðufell, Iceland (Figure 47 and Figure 48). “Cryoliths” were also described and interpreted by Graettinger et al. (submitted).

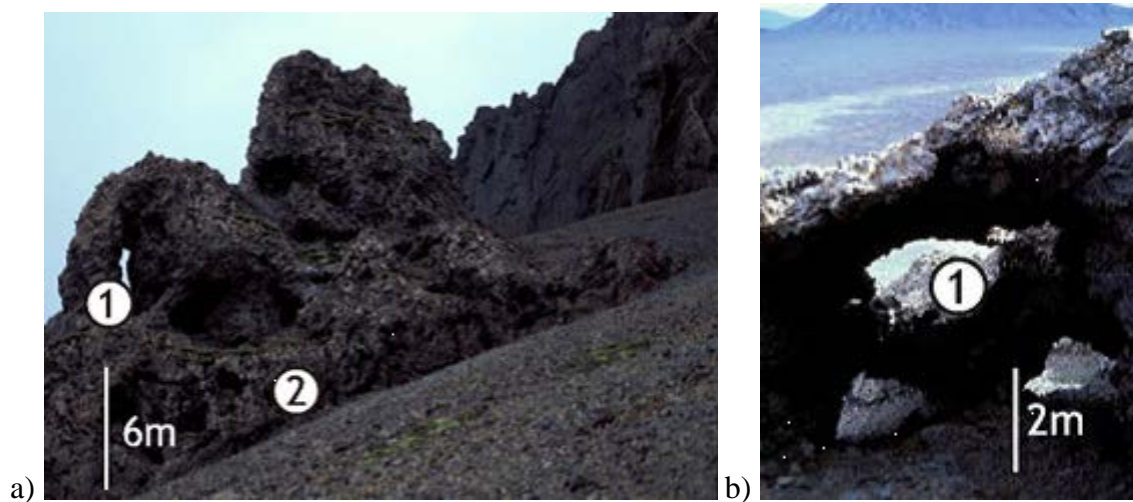


**Figure 47. “Ice-block meltout cavities” at Höðufell, Iceland. (Skilling, 2009)**

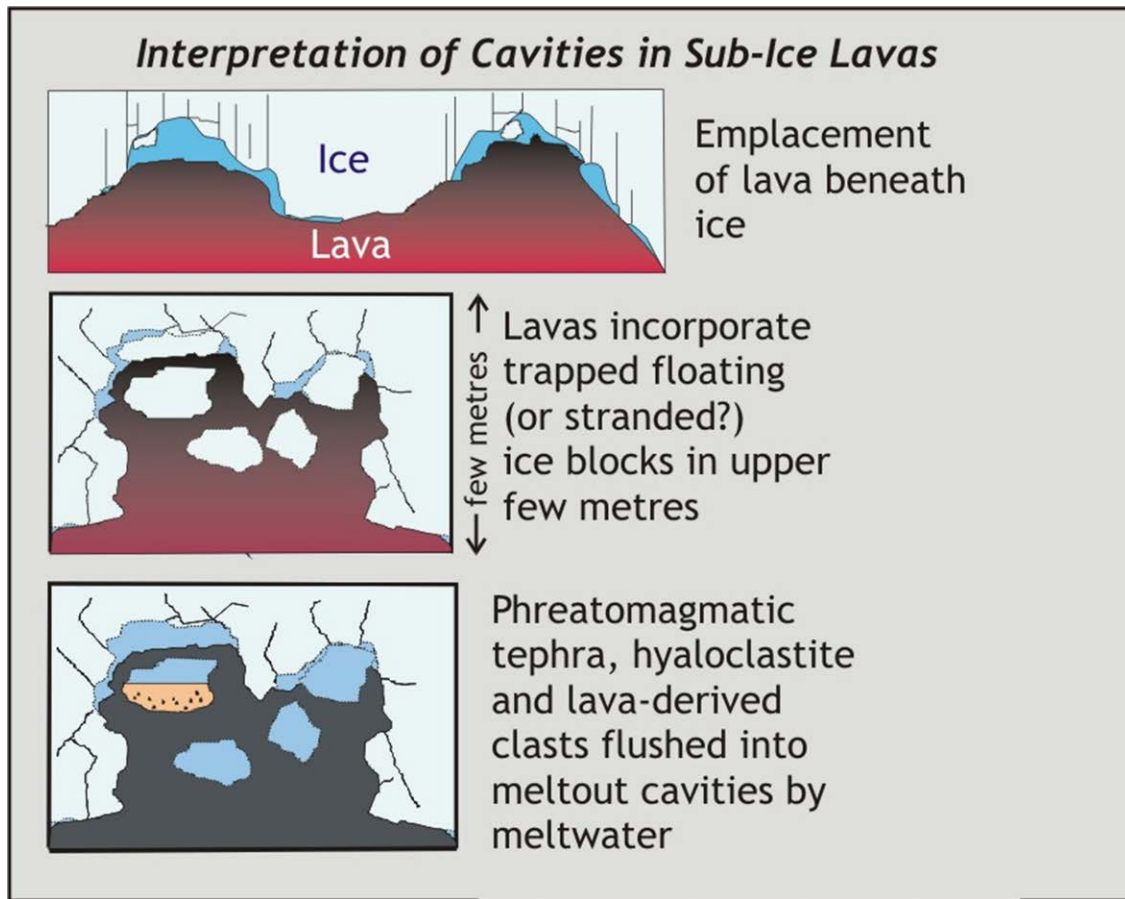


**Figure 48. Model of the evolution of “ice-block meltout cavities” at Höðufell, Iceland. (Skilling, 2009)**

The smaller cavities (Figure 17) in pillowed areas of the dikes are interpreted as cavities arising from stacking of cylindrical pillow tubes and drainage cavities in the centers of pillows tubes. The pillows (Figure 17) appear to also have been compressed against solid material, interpreted as ice or ice-cemented sediment (Skilling, 2009).

Features interpreted as pillow haystacks at Sveifluháls (Figure 9 and Figure 23) consisted of steep-sided conical structures of radiating pillow tubes. These pillow haystacks are interpreted to have originated when a dike emerged through the vault’s subaqueous paleoslope, in a manner analogous to submarine pillow haystacks. Pillow haystacks were observed at Sveifluháls as well by Mercurio (2011) within non-peperitic pillowed dikes. The pillow



haystacks described by Mercurio (2011) at Sveifluháls were approximately 2-3 m tall. A feature interpreted by Stakes et al. to be a submarine pillow haystack was observed along the southern Juan de Fuca Ridge may be seen in Figure 49 (Stakes et al., 2006).



**Figure 49. Submarine pillow haystack on the Juan de Fuca Ridge. (Stakes et al., 2006)**

Another pillow haystack found via a dive to the Juan de Fuca Ridge by Stakes et al. may be observed in Figure 50 (Stakes et al., 2006).

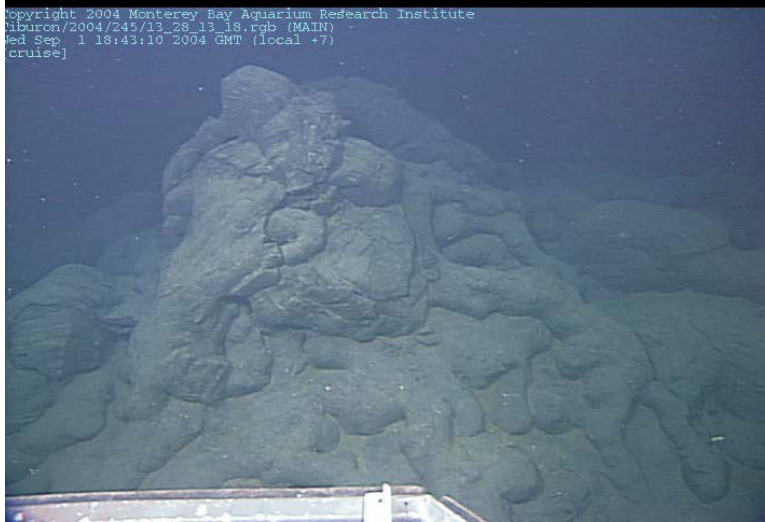


**Figure 50. Submarine pillow haystack on the Juan de Fuca Ridge. (Stakes et al., 2006)**

A subaqueous pillow haystack photographed by Stakes et al. may be seen in Figure 51 (Stakes et al., 2006).



**Figure 51. Subaqueous pillow haystack found in a dive on the Juan de Fuca Ridge. (Stakes et al., 2006)**

In addition, a young subaqueous pillow haystack was observed 3,183m below sea level along the Mid-Atlantic Ridge on the rift valley floor by Bideau et al. (1998).

Such structures are the subaqueous equivalents of spatter cones or hornitos in subaerial basaltic lava fields, but have never been described from near-surface or emergent dike tips before. Further evidence of the very high level of some dikes at Sveifluháls is that some of the dikes also clearly emerged on the former subaqueous tuff cone slope and fed lava flows (Figure 24). The dikes at Sveifluháls were clearly responsible for a variety of deformation of the host lapilli tuff. Domains of well-bedded/laminated tephra immediately adjacent to the dike margins appear to have been dragged upwards, folded, rotated and in some cases, detached during dike emplacement.

Folding of the host sediment in response to intrusion propagation is mentioned by Skilling et al. (2002) with respect to peperite formation, and Duffield et al. (1986) as a product of sill propagation. An interesting aspect of the domains at Sveifluháls is that they are typically much better bedded or laminated than the bulk of the host lapilli tuff and contain more small scour and fill structures. This implies that the bedding represents new structures formed during dike emplacement or that they have been dragged from depth from deeper better bedded lapilli tuff. It is possible that some of these structures may be formed by liquid or water vapor moving along the dike margins during their emplacement. The dikes have also clearly induced rotation and slumping of much more distal lapilli tuff (Figure 32), and were hence an important control on slope failure, and acted as topographic barriers to future tephra deposition.

The presence of peperite along the margins of some of the dikes at Sveifluháls is important because it clearly indicates that the host lapilli tuff was at least locally unconsolidated at the time of dike emplacement. Both blocky and fluidal peperite types (Busby-Spera and White, 1987) are present, which is probably a function of different magma rheologies as a consequence of different degrees of cooling.

The host lapilli tuff along intrusive margins at Sveifluháls commonly displays hydrothermal alteration that is clearly different from the “background” palagonitization, namely a distinctive reddening. This reddening may be due to the presence of hematite. Figure 42 and Figure 43 show thin section samples with possible hematite spherules concentrically lining vesicles at Sveifluháls, Iceland. The model in Figure 52 provides an overall image of the evolution and morphologies of the dike-wet lapilli tuff system at Sveifluháls, Iceland (Skilling, unpublished).

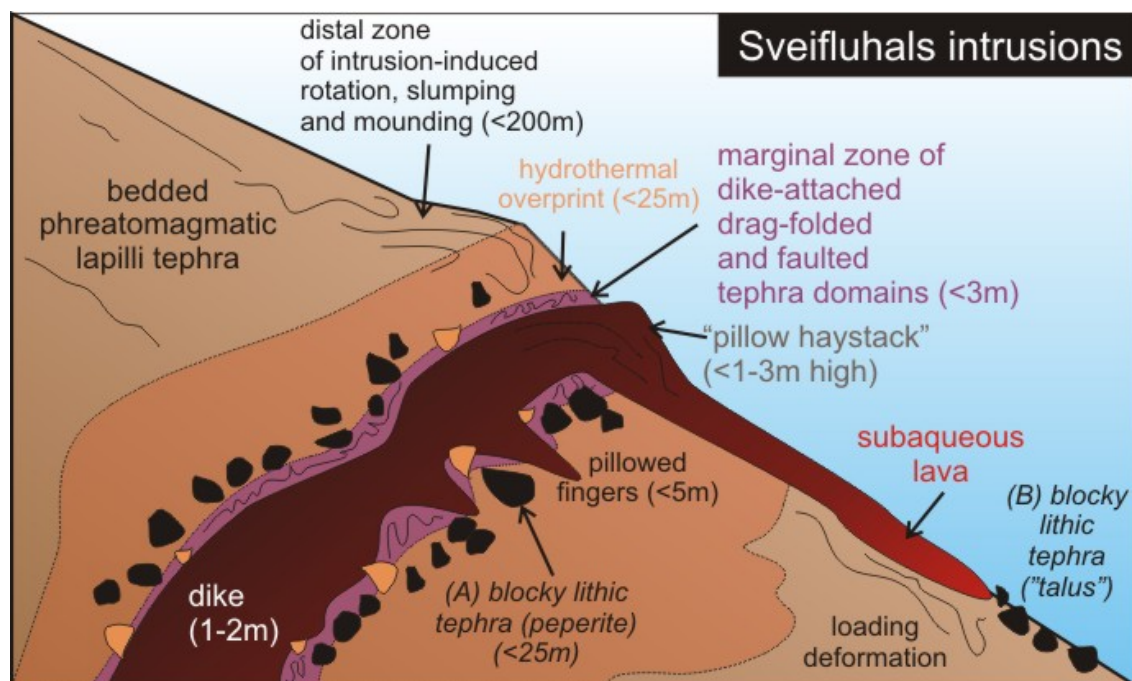


**Figure 52. Evolution and morphologies of the dike-wet lapilli tuff system at Sveifluháls, Iceland.**  
(Skilling, unpublished)

Propagation of the dike first distorts the distal lapilli tuff, resulting in mounding, rotation, and slumping. The lapilli tuff nearer the dike becomes further altered by the circulation of hydrothermal fluids and obtains a dark orange or deep red tint. Lapilli tuff immediately adjacent

to the dike undergoes drag-folding and faulting as it is deformed to make way for the propagating dike. With magma now present, the wet lapilli tuff and magma intermingle, forming peperite. When the dike breaches the paleosurface and thus interacts with water in the vault, “pillow haystacks” may form. In the final stages a subaqueous lava flow may result, flowing along the paleo-surface within the water-filled vault.



## **5.0 SUMMARY OF VOLCANO-ICE INTERACTION ON MARS**

The products of volcano-ice interaction are potentially very common on Mars, where volcanism is the dominant surface process, and evidence of near-surface water ice is now widespread (Hartmann, 2003). In the summer of 2008 the existence of water ice in the subsurface of Mars was confirmed with the Phoenix mission (Smith et al., 2009). During the mission Martian water ice sublimation was observed over the course of several days (Smith et al., 2009). For the first time in history, a lander obtained some water ice from the soil of Mars and placed it into a mass spectrometer for analysis (Smith et al., 2009). This instrument on the Phoenix lander, known as TEGA (Thermal and Evolved Gas Analyzer), was a mass spectrometer combined with a high temperature oven in which to cook gasses out of the sample, and was instrumental in confirming the existence of water ice in the sample (Smith et al., 2009). The landing thrusters of the spacecraft uncovered a layer of ice a mere few centimeters from the surface (Smith et al., 2009). Volcano-ice interactions may provide favorable conditions for life on both Earth and Mars (Hartmann, 2003, Warner and Farmer, 2010).

While there are aspects of basaltic volcano-ice interaction that are similar on Earth and Mars, the different environmental conditions on Mars could cause important differences to processes, products and resultant edifices. Basaltic intrusions on Mars are thought to be emplaced faster than on Earth (Wilson and Head, 2002) and magma flowing through subsurface dikes on Mars may be able to travel greater distances than on Earth (Wilson and Head, 2002).

There are many areas on Mars where products generated by volcano-ice interaction have been postulated. Utopia Planitia has some possible tuyas (Zimbelman and Gregg, 2000) and Elysium Mons displays possible hyaloclastic ridges about its flanks (Chapman et al., 2007). The Dorsa Argentea Formation is a circumpolar ice sheet with marginal features that show evidence of significant melting such as lakes, channels, and eskers (Head and Wilson, 2007). This formation also displays features that have been interpreted as having formed from volcano-ice interactions, such as subglacial volcanic edifices, pits, basins, and eskers (Head and Wilson, 2007). Chapman et al. (2007) identified possible jökulhlaups, lahars, hyaloclastic ridges, and tuyas in Acidalia Planitia, but they are not near any volcanic fields. Kadish et al. (2008) indicated a possible glacier and some nearby ridges at Ascraeus Mons. Chaotic terrain, outflow channels, and subdued craters are seen in the Xanthe and Margaritifer Terrae regions and near Valles Marineris (Chapman and Tanaka, 2002). Chapman and Tanaka (2002) suggest that these features may all be related to sub-ice volcanism. Pedersen and Head (2008) state that the transition between Elysium and Utopia displays outflow channels, eskers, and mega-lahar deposits. Meresse et al. (2008) infer the Aureum and Hydraotes Chaos regions to be a result of intrusion-ice interaction.

In Acidalia Planitia, jökulhlaups, lahars, hyaloclastic ridges, and tuyas have been identified (Chapman et al., 2007). Chapman et al. (2007) writes that these volcano-ice features are generally found to the north and northwest of Elysium Mons. They have also been observed in Ares Valles near the Mars Pathfinder Lander (Chapman et al., 2007). Chapman et al. (2007) states that these volcano-ice features of Mars are similar to Icelandic sub-ice volcanoes in size and morphology. Chapman et al. (2007) also describes a steep-sided flat-topped volcano-ice feature at 45°N and longitude 21° in Acidalia Planitia. Its plateau is similar in size to tuyas on

Earth in Iceland (Chapman et al., 2007). The height of terrestrial tuya plateaus are used to extrapolate thickness of the past overlying ice (Chapman et al., 2007). A similar technique could be utilized to estimate past ice features on Mars. Chapman et al. (2007) writes that photoclinometric measurements of ridges northwest of Elysium suggest a paleo-ice sheet thickness of approximately 200m in the Utopia region. Chapman et al. describes another volcano-ice feature at 38°N, and longitude 13° (Chapman et al., 2007). This feature displays a ridge of steep-sided relief similar to hyaloclastic ridges in Iceland (Chapman et al., 2007).

Ridges and mesas on the flanks of Elysium Mons have also been interpreted to be of volcano-ice origin (Chapman et al., 2007). This idea is supported by a comparison with the terrestrial tuya Herdubreidartögl in Iceland (Chapman et al., 2007). This sub-ice volcano displays a narrow central ridge from fissure eruptions (Chapman et al., 2007). The Martian ridges are also comparable to tindar southwest of the Icelandic Vatnajökull icecap (Chapman et al., 2007). Chapman et al. (2007) attests the linear ridges and pits in combination with the alignments of mounds with Elysium Fossae point to a fissure eruption origin. There may be hyaloclastic ridges formed of palagonite and breccias in Elysium (Chapman et al., 2007). According to Chapman et al. (2007) mesas in northeastern Utopia Planitia may be tuyas erupted from central point sources, which compare well to the Icelandic tuya Gaesafjöll.

Shean et al. (2005) proposed paleo-glaciers that interacted with magma on the northwestern flank of Pavonis Mons. This interpretation was based on observed fan-shaped deposits with flow features and radial ridges (Figure 53, Figure 54, and Figure 55) (Shean et al, 2005).

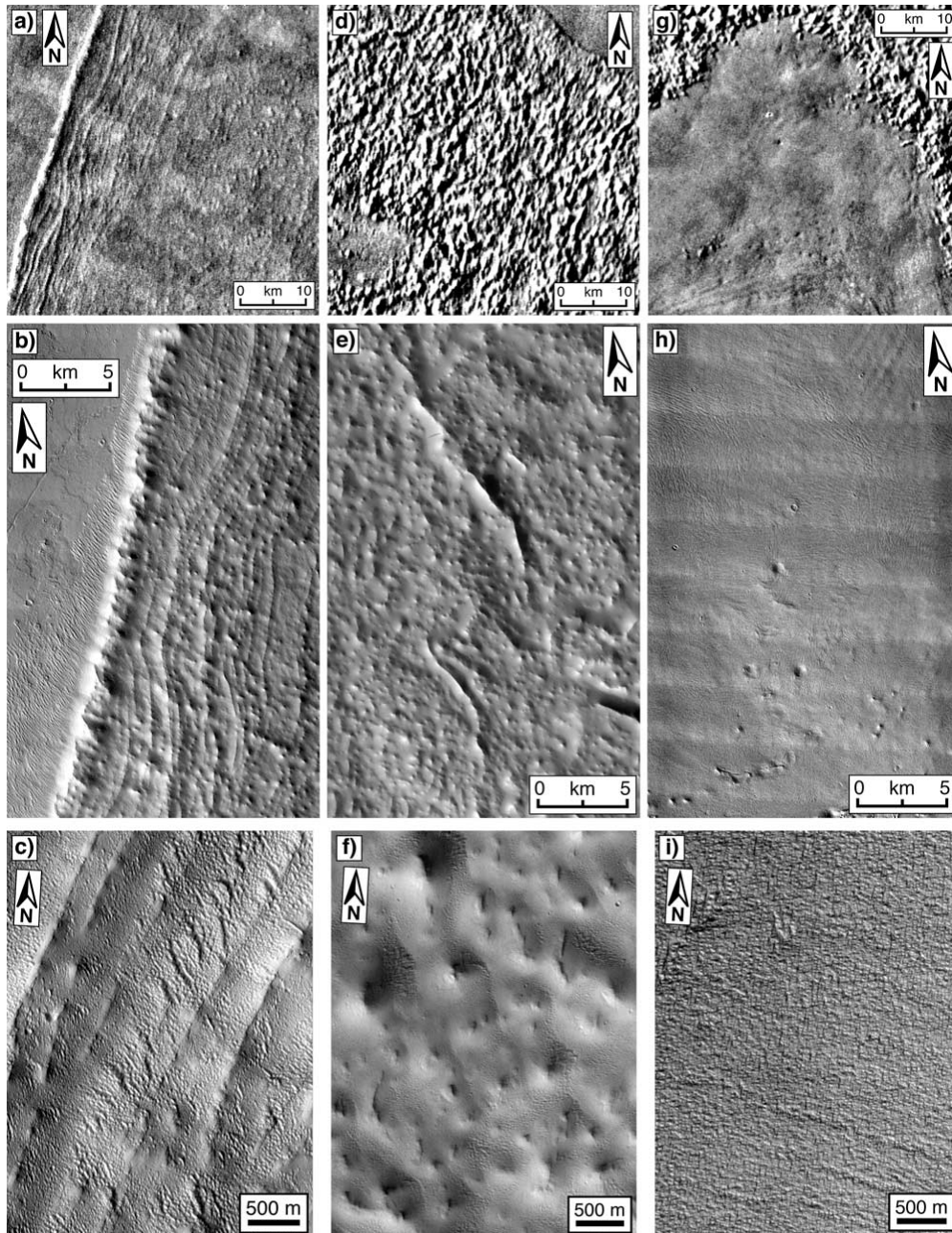


**Figure 53. a) Viking image of ridges at Pavonis Mons. b) THEMIS VIS image of potential drop moraines. c) MOC narrow-angle image of ridges at Pavonis Mons. d) Viking image of knobby features at Pavonis Mons. e) THEMIS VIS image of ridges thought to be lobate flow features, and knobby features over flow-like features. f) MOC narrow-angle image of the knobby features and dune fields. g) Viking image of the main smooth facies deposit at Pavonis Mons. h) THEMIS VIS image of the main smooth facies deposit at Pavonis Mons. Circular depressions may be softened impact craters. i) MOC narrow-angle image of smooth facies and dune fields at Pavonis Mons. (Shean et al., 2005)**



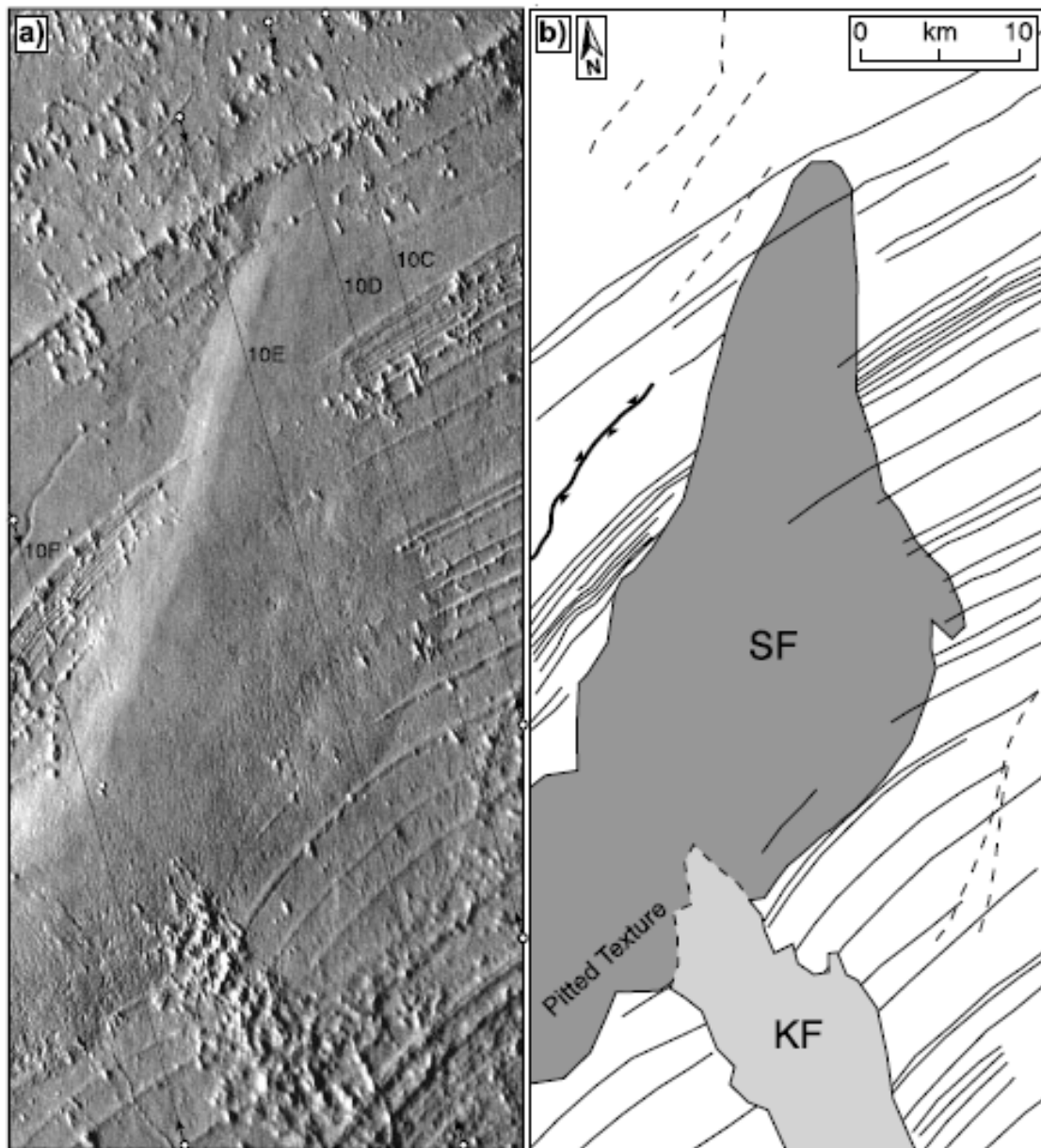


**Figure 54. a) THEMIS daytime IR image of the Pavonis fan-shaped deposit. Some knobs in the upper portion on this image may be drumlins (Scott et al., 1998). b) Sketch of the image in a) showing smooth facies (SF, dark gray), knobby facies (KF, light gray), primary ridges (solid lines), and secondary ridges (dashed lines). The thick solid line with triangles shows possible meltwater channel. (Shean et al., 2005)**

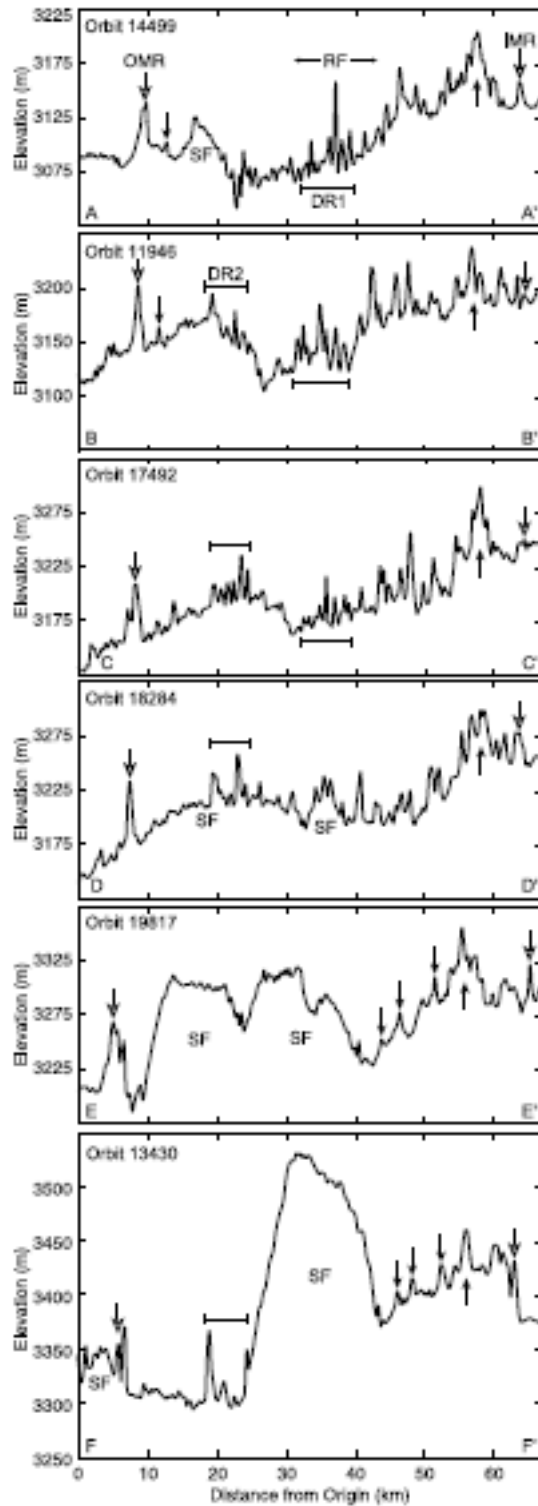
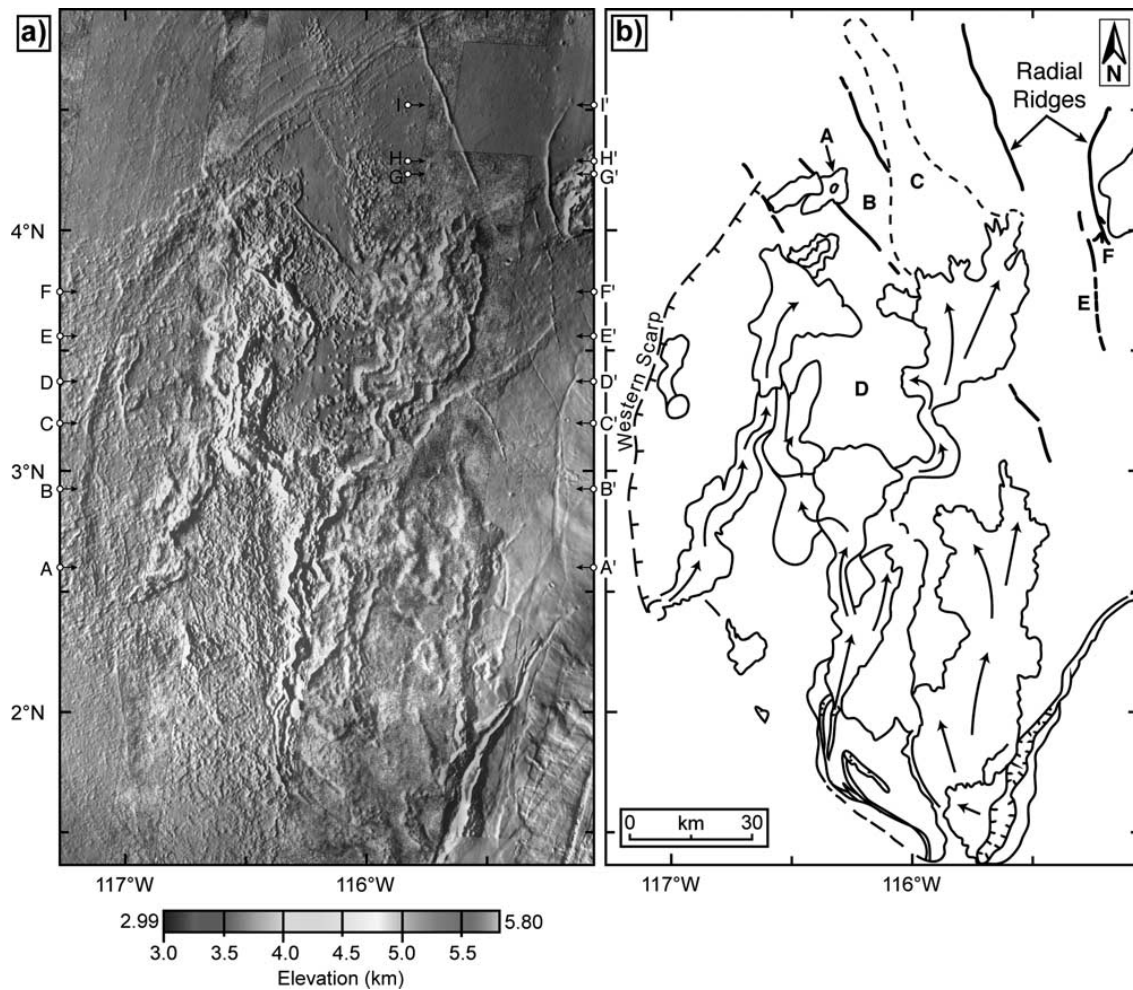


Figure 55. MOLA profiles of ridges at Pavonis Mons. DR1 and DR2 show clustered central ridges.

The smooth facies (SF) is present in some profiles. Vertical exaggeration is approximately 158X. (Shean et al., 2005)

Shean et al. (2005) interprets the radial ridges around volcanoes in the area to be dikes which may have erupted beneath the glacier (Figure 56).



**Figure 56. (a) THEMIS daytime IR and Viking data with MOLA overlay of radial ridges. b) Sketch of flow features (arrows) that may be subglacial flows. Thick solid lines show radial ridges that are interpreted as dikes that once interacted with ice. One radial ridge transitions into a pancake-like feature and was interpreted as a potential subglacial sill. (Shean et al., 2005)**

They also identified potential fluvial features in the area of meltwater outflow (Figure 57) (Shean et al., 2005).



**Figure 57. THEMIS daytime IR image showing possible meltwater outflow features northeast of the Pavonis fan-shaped deposit. These features may originate from eruptions beneath a glacier at Pavonis Mons. (Shean et al., 2005).**



## **6.0 DIKE RECOGNITION ON MARS**

Unequivocal dikes on Mars are somewhat elusive, most likely due to dust cover, erosion and difficulties disproving other plausible origins for elongate features. Evidence of volcanism on Mars is ubiquitous, and like Earth, basaltic magma must be emplaced at the sub-volcanic level dominantly as dikes. Hence, dikes must be very common at the surface of Mars, especially given the prolonged period of erosion to which many ancient volcanic centers have been subjected.

Mège (1999), details guidelines for determining the presence of Mars dikes using satellite data. Mège (1999) discusses likely dike distribution and geometry about volcanic features on Mars. Radial dikes are likely to be found around/in the areas of Syria Planum, Tharsis Montes, Alba Patera, and possibly Thaumasia (Mège, 1999). Concentric dikes may be found around the largest volcanoes in these regions, likely with radial dikes intersecting them (Mège, 1999). Mège (1999) suggests utilizing promontories on cliff walls as potential indicators of dikes. The albedo of dikes should appear a medium to dark gray on high resolution MOC images according to Mège (1999). The linearity of features is not a reliable indicator for determining dikes, although it may be of some use in combination with other indicators (Mège, 1999). Two rules of thumb exist concerning Martian dikes associated with graben; the first rule says that dike thickness correlates with the amount of vertical subsidence in the graben above it by a ratio

around 1.5 (Gibbons et al., 2001). The second rule correlates graben width with depth to the subsurface dike by a ratio of 2.5 to 3 (Gibbons et al., 2001).

Graben are another tracer of dike emplacement, however, they may originate from tectonic extension rather than intrusive activity (Schultz et al., 2004). HiRISE imagery of Memnonia Fossae, Mars, reveals graben which may possibly be related to past intrusive activity (Figure 58a) (NASA/JPL/University of Arizona). In addition, a HiRISE image shows graben and collapse pits at Cyane Fossae, Mars, which may be related to intrusions (Figure 58) (NASA/JPL/University of Arizona).

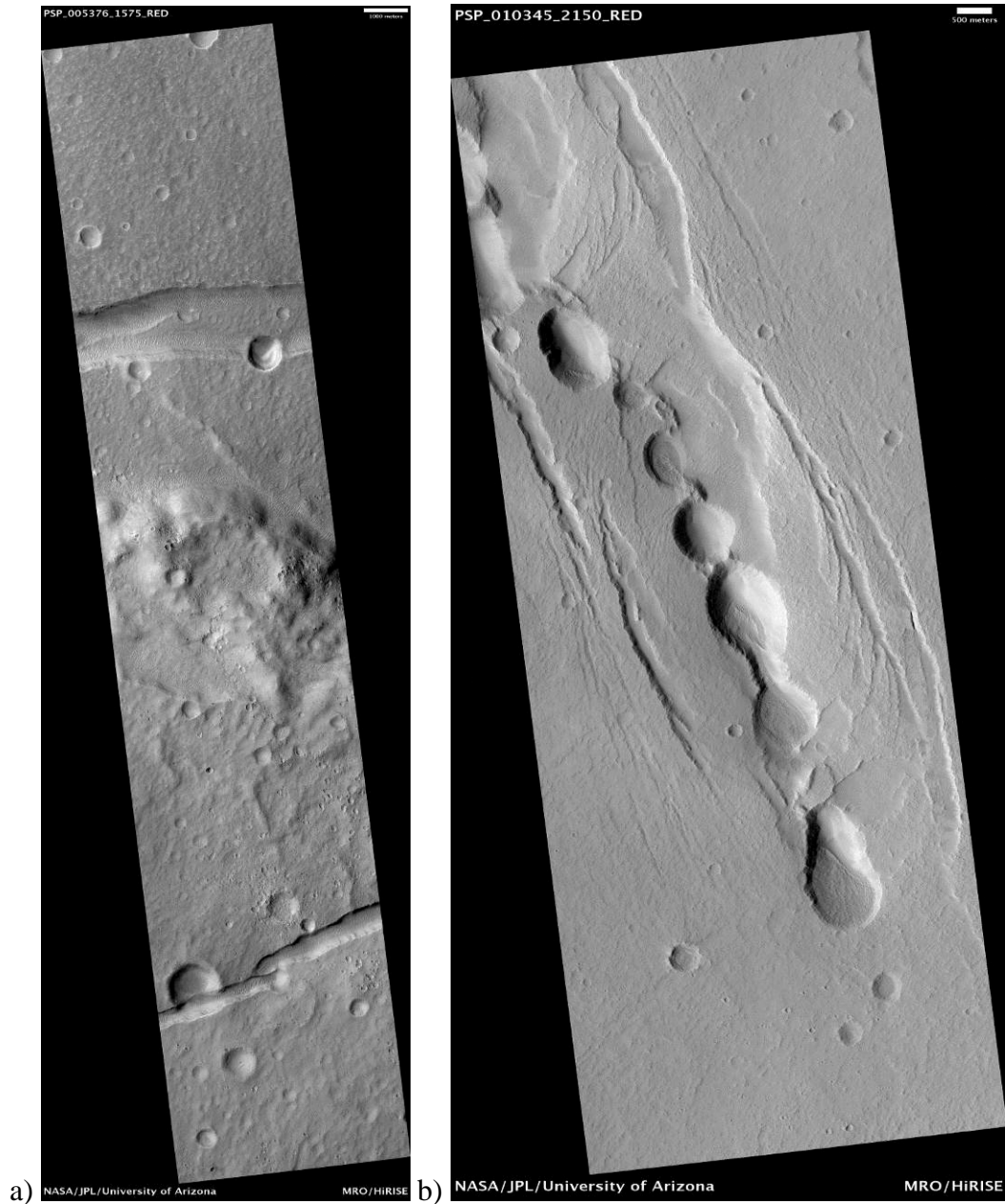
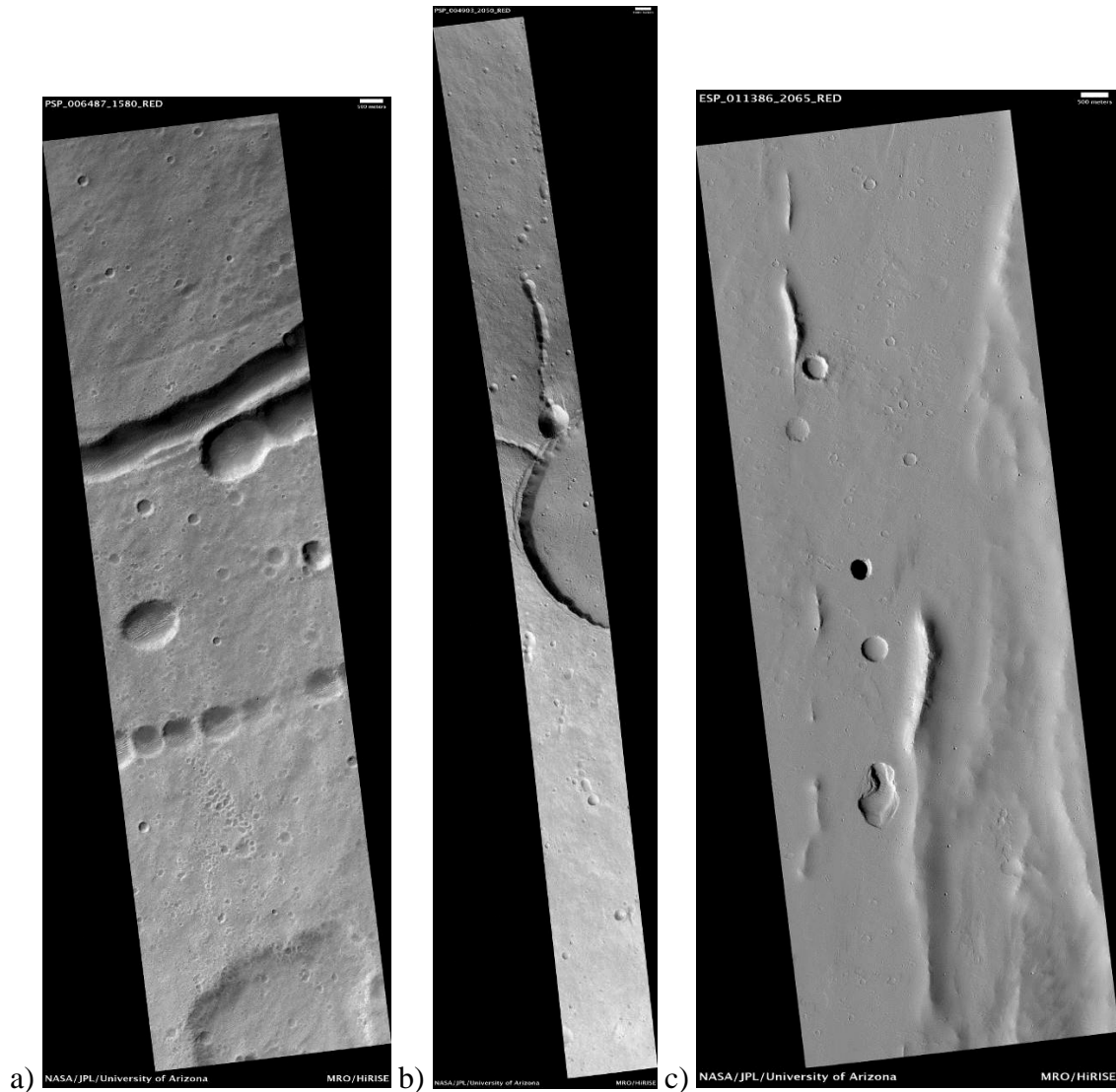


**Figure 58. HiRISE images (NASA/JPL/University of Arizona) of a) graben within Memnonia Fossae, Mars, that may be due to an underlying dike. White scale bar (top right) = 1,000m. (PSP\_005376\_1575) b) graben and collapse pits at Cyane Fossae, Mars. White scale bar (top right) = 500m. (PSP\_010345\_2150)**

Pit crater chains may be related to dike-ice/wet sediment interaction and indicate a sudden release of volatiles (Korteniemi et al., 2009) such as liquid water, water ice, or carbon

dioxide ice. Such volatiles may form small craters in a linear fashion (Korteniemi et al., 2009) along the flanks of intrusions via their associated hydromagmatic explosions. Terra Tyrrhena, Mars, displays several possible indicators of dike presence, such as the pit crater chains and depressions observed in a HiRISE image near the summit of Tyrrhena Patera, Mars (Figure 59a) (NASA/JPL/University of Arizona). Pit crater chains which may be dike-related have also been observed at Elysium Mons, Mars, in HiRISE imagery (Figure 59b) (NASA/JPL/University of Arizona). The HiRISE image in Figure 59c displays a collapse pit and possible dikes at Tractus Fossae on Mars (NASA/JPL/University of Arizona).

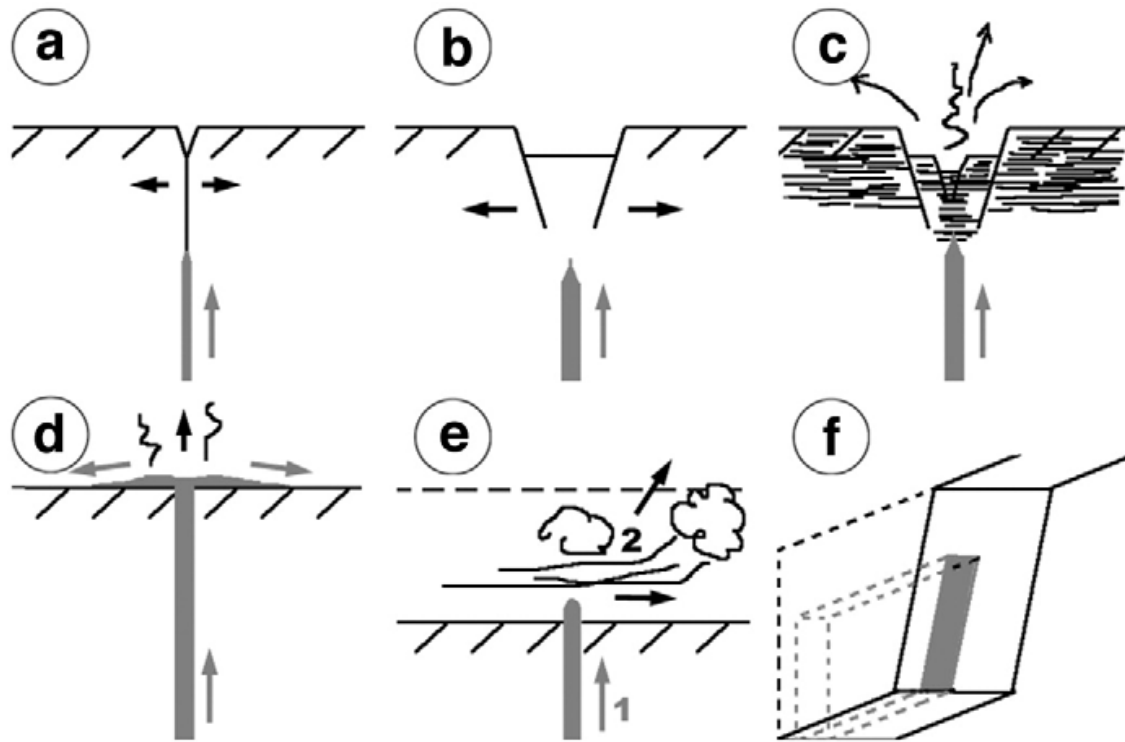




**Figure 59. HiRISE images (NASA/JPL/University of Arizona) of a) pit crater chains near the summit of Tyrrhena Patera, Mars. White scale bar (top right) = 500m. (PSP\_006487\_1580) b) pit crater chains at Elysium Mons Caldera, Mars. White scale bar (top right) = 1,000m. (PSP\_004903\_2050) c) a collapse pit and possible dikes in Tractus Fossae, Mars. White scale bar (top right) = 500m. (ESP\_011386\_2065)**

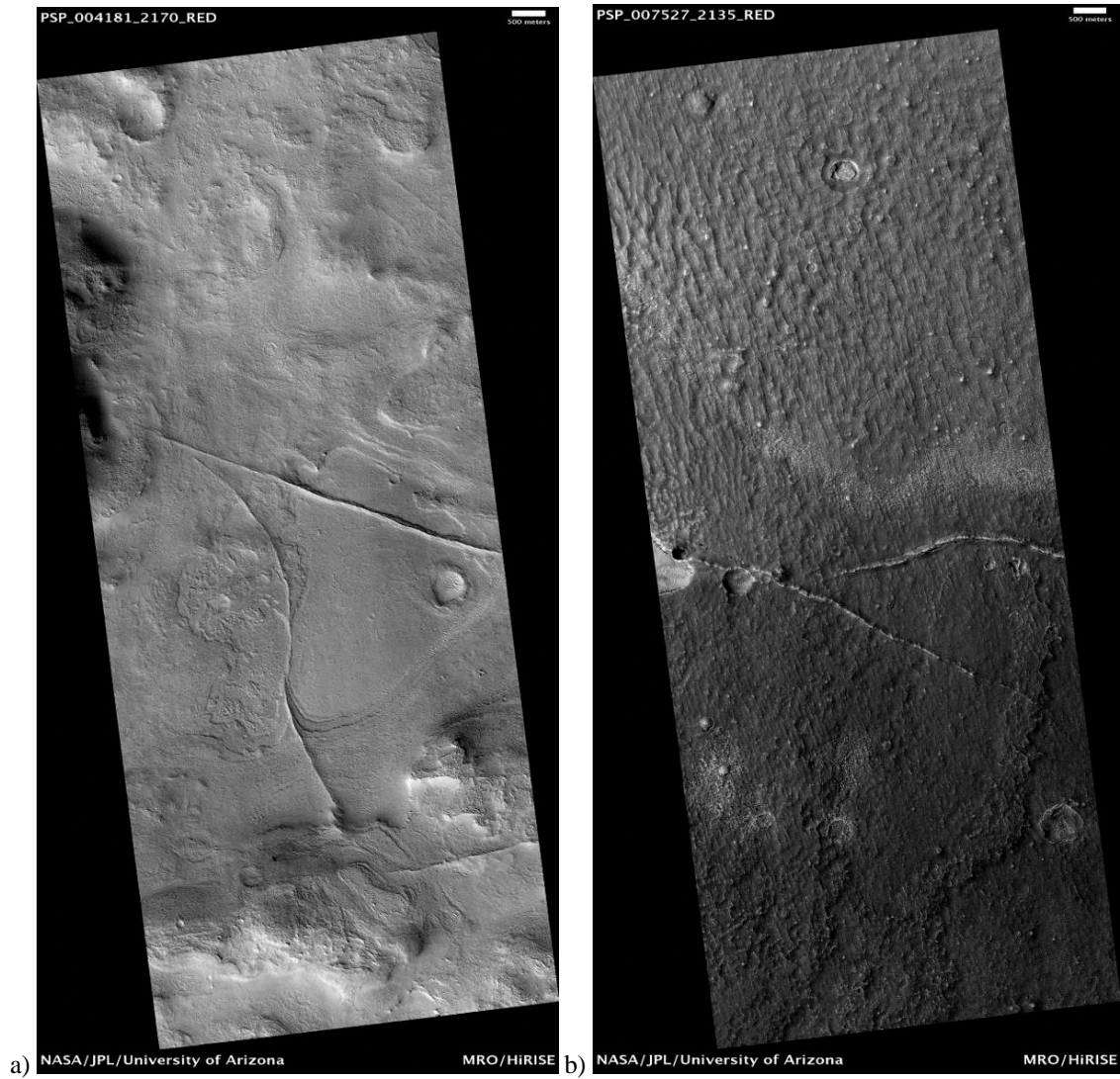
In Valles Marineris, there are indications of dikes (Flahaut et al., 2011) and interior layered deposits (ILDs) possibly related to dike emplacement (Komatsu et al., 2004).

Figure 60 shows a model of dike emplacement on Mars involving graben and pit crater chains by Kortenienmi et al (2009).



**Figure 60. Model of dike emplacement on Mars. a) Fracturing via propagation of the dike. b) Graben formation. c) Pit crater chain formation as volatiles escape. d) Fissure eruption related to a dike. e) Erosion of country rock. f) Model of a partially eroded surface. (Korteniemi et al., 2009)**

Shows some potential dike splays at Coloe Fossae, Mars (Figure 61a) (NASA/JPL/University of Arizona), and Hrad Vallis (Figure 61b) (NASA/JPL/University of Arizona) on Mars, shown in HIRISE imagery.



**Figure 61. HiRISE images (NASA/JPL/University of Arizona) of a a) possible dike splay in the Coloe Fossae Region of Mars. White scale bar (top right) = 500m. (PSP\_004181\_2170) b) possible dike in Hrad Vallis, Mars. White scale bar (top right) = 500m. (PSP\_007527\_2135).**

## **6.1 PUBLISHED EXAMPLES OF DIKES ON MARS**

Linear basaltic dikes on Mars have been interpreted in several regions, on the basis of grabens (Schultz and Fori 1996; Liu and Wilson, 1998; Schultz et al., 2004), ridges (Korteniemi et al. (2009); Pedersen and Head, 2008), and collapse pits (Liu and Wilson, 1998). Radial dikes around volcanoes have been interpreted in Syria Planum, Tharsis Montes, and Alba Patera (Mège, 1999). Concentric dikes are also likely to be found about the largest volcanoes, possibly with radial dikes intersecting them (Mège, 1999).

Schultz and Fori (1996) identified graben sets in Candor Mensa, which they interpreted as dikes. Schultz et al. (2004) compared terrestrial grabens to the surface manifestation of Martian dikes. Studies of terrestrial grabens demonstrate that a characteristic topographic signature at the surface develops above a near-surface igneous dike (Schultz et al., 2004). Schultz et al. (2004) also described Tharsis-radial graben in the Memnonia region of Mars. They analyzed images from the Mars Orbiter Camera (MOC) and topographic data provided by the Mars Orbiter Laser Altimeter (MOLA) Precision Experiment Data Record (PEDR) of radial graben around the Tharsis Bulge (Schultz et al., 2004). The graben in their study displayed a concave floor morphology, talus fans, and dunes along their lower slopes in MOC images (Schultz et al., 2004). PEDR was used specifically in their study to examine the cross-strike topography of the Tharsis-radial graben with spot elevations (Figure 62) (Schultz et al., 2004).



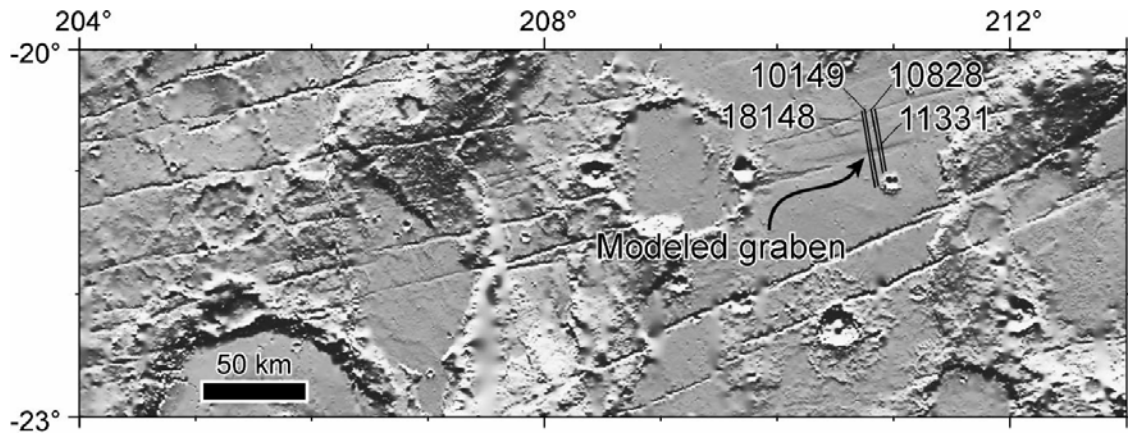


**Figure 62. Shaded relief map of Tharsis-radial graben in the Memnonia region. (Schultz et al., 2004).**

Spot elevations were collected via the Mars Global Surveyor (MGS) and were spaced approximately every 300 m (Schultz et al., 2004). They concluded that a 10 km long Tharsis-radial graben in Memnonia Fossae coincides with a subsurface dike beneath the feature (Schultz et al., 2004). A depth of 18 km is estimated to reach the mentioned underground dike (Schultz et al., 2004). This dike created a positive relief feature which may be detected with MOLA data, with uplifts of 15 - 20m (Figure 63) (Schultz et al., 2004).

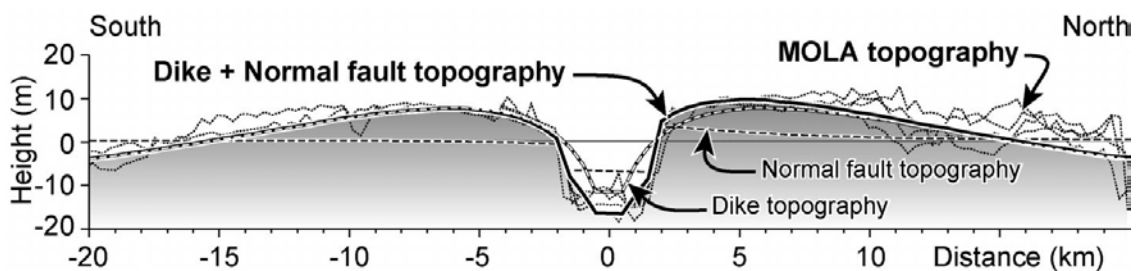


**Figure 63. Mars Orbiter Laser Altimeter (MOLA) topographic profiles of graben. (Schultz et al, 2004)**

The other graben studied were not consistent enough in topographic signatures to confirm additional subadjacent dikes and may have originated from other processes, such as tectonic extension and collapse (Schultz et al., 2004).

Korteniemi et al. (2009) identified 500 dike segments in the Hadriaca Patera and Promethei Terra regions, with about 90% of them displaying a ridge morphology. Pedersen and Head (2008) conducted an analysis of possible dikes in the Utopia Basin from CTX, MOLA, and HiRISE imagery. In the CTX imagery, which shows 6m/pixel, ridges had sharp ridge summits (Pedersen and Head, 2008). The ridges ranged from 200m - 400m wide (CTX) and had heights of 5 - 30m according to MOLA (Mars Orbiter Laser Altimeter) data (Pedersen and Head, 2008). Five multiple ridge systems were identified, 15 - 45km long with widths of 1 - 7km (Pedersen and Head, 2008). Pedersen and Head (2008) also found yardangs and inverted craters in the area, which suggest adequate erosion to exhume dikes.

The upper flanks of Pavonis Mons display grabens that have been interpreted as related to underlying dikes (Liu and Wilson, 1998). Collapse pits along the graben and are thought to be related to dike emplacement and escaping gas (Liu and Wilson, 1998). Liu and Wilson (1998) describe some of these features on Mars and their model of dike emplacement with pressurized gas. They contend that the pits are formed when overlying host rock subsides or collapses into the void left by escaping volatiles (Liu and Wilson, 1998). Liu and Wilson (1998) go on to state that the widths of the dikes allowed for the accumulation of large amounts of gas; enough to support convection within the magma.

Ernst et al. (2001) discussed possible dike swarms in the Syrtis Major region and in Valles Marineris. In Syrtis Major Ernst et al. (2001) recognized graben that they believe to be indicators of radial dikes. In the walls of Ius Chasma, part of the Valles Marineris system, Ernst

et al. (2001) observed graben that have been eroded during the formation of Louros Valles, which they site as a potential indicator of subsurface dikes.

Gibbons et al. (2001) describes possible giant radial dikes beneath graben in northern Tharsis. Many graben radiate from central Tharsis and aid in the identification of subsurface dikes on Mars (Gibbons et al., 2001). The patterns made by the graben in this area suggest that the dikes are part of giant dike swarms that traveled laterally out from central Tharsis (Gibbons et al., 2001). The system of Tharsis graben extends north into the flanks of Alba Patera (Gibbons et al., 2001). Generally pit craters follow the graben and are thought to originate from explosive magma eruptions (Gibbons et al., 2001). Gibbons et al. (2001) observed and measured the morphologies of graben and associated pit craters in the Tharsis region of Mars to indirectly determine properties of subsurface dikes. Gibbons et al. (2001) argued that dike thickness correlates with the amount of vertical subsidence in the graben above it by a ratio around 1.5 (Gibbons et al., 2001). Graben width correlates with depth to the subsurface dike by a ratio of 2.5 to 3 (Gibbons et al., 2001). Utilizing such rules, Gibbons et al. concluded that dikes in the Tharsis region range from 150 to 700 m thick, with depths from 800 m to 4 km (Gibbons et al., 2001).

Head et al. (2006) describes a possible giant dike system in the Huygens-Hellas region. Two arc-shaped ridges about 600 - 700 km long exist in western Terra Tyrrena and are thought to be very old dikes, possibly as old as 3.6 - 3.8 Gya (Head et al., 2006). Mars orbiter laser altimeter (MOLA) data suggests that the ridge heights are 6.2 - 24.3 m with an average height around 14 m (Head et al., 2006). The dikes appear linear on a local scale with occasional slight curves (Head et al., 2006). The two giant dikes overly Noachian terrain and are thought to have been emplaced in the Early Hesperian (Head et al., 2006). The dikes have been exposed to

various types of erosion, likely a combination of aeolian, fluvial, and sublimation processes (Head et al., 2006). Eskers have been suggested as an alternative interpretation of these ridges, but the ridges are much too long (Head et al., 2006). A giant dike system is the most likely interpretation of these ridges as dikes can travel for thousands of kilometers and are typically linear and/or broadly arcing (Head et al., 2006).

Ernst et al. (2001) focused on evidence for giant dike swarms on Mars. They asserted that ten giant dike swarms were present in the Tharsis region, four of which are possibly concentric dikes, and the other six are likely radiating. Ernst et al. (2001) also discussed possible dike swarms in the Syrtis Major Region and in Valles Marineris. In Syrtis Major, graben are observed that may be indicators of radial dikes (Ernst et al., 2001). They also suggested that in the walls of Ius Chasma in Valles Marineris there are some graben that have eroded during the formation of Louros Valles which may indicate the presence of subsurface dikes (Ernst et al., 2001).



## **7.0 RECOGNITION OF DIKES EMPLACED INTO ICE OR WET SEDIMENT ON MARS**

Dikes interacting with wet/icy sediment rather than rock behave in several different ways. Traditional dikes (dike-dry rock interaction) cause brittle fracturing in the country rock. In these dikes, the magma and country rock remain distinct and form sharp margins with no incorporation of dike-derived clasts in the host. Dikes interacting with wet sediment deform the host sediment both brittely and ductily. The two fluids (magma and wet sediment) intermingle and often pillowed, fluidal margins and peperite result.

Dikes emplaced into wet/icy sediment on Mars are difficult to directly identify with the current resolution of satellite imagery. Identification should be enhanced in the future by HiRISE and developing technologies. While direct observation and accurate identification of dikes is challenging, if they can be identified, then several factors can aid in the identification of their emplacement into wet sediment. The best place to look for dikes emplaced into wet sediment is in areas where evidence of other volcano-ice interaction, such as the areas displaying possible volcano-ice interaction features as in: Allen, 1979; Chapman et al., 2007; Chapman and Tanaka, 2002; Kadish et al., 2008; Meresse et al., 2008; Pedersen and Head, 2008; and Shean et al., 2005. Adjacent edifices and deposits interpreted to be produced by volcano-ice interaction increase the likelihood of intrusion into icy or wet sediment in the same area. These potential volcano-ice features include lahar deposits (Pedersen and Head 2008; Chapman et al., 2007),

chaos terrain (Chapman and Tanaka, 2002), outflow channels (Chapman and Tanaka, 2002; Pedersen and Head 2008), tuyas (Chapman and Tanaka, 2002), and tindars (Chapman and Tanaka, 2002). Areas with postulated glaciers (Kadish et al., 2008; Shean et al., 2005), moraines (Shean et al., 2005), and lobate features (Shean et al., 2005) could be used to support presence (or former presence) of wet sediment. Generally, a combination of several indicators is desirable for the proper identification of dikes emplaced into wet/icy sediment on Mars, though currently identifiable dikes on Mars may not be as common as predicted due to erosion and dust covering.

Shean et al. (2005) also illustrated views of a couple of the radial ridges with elongate collapse pits, thought to be indicative of magma-ice interaction (Figure 64).

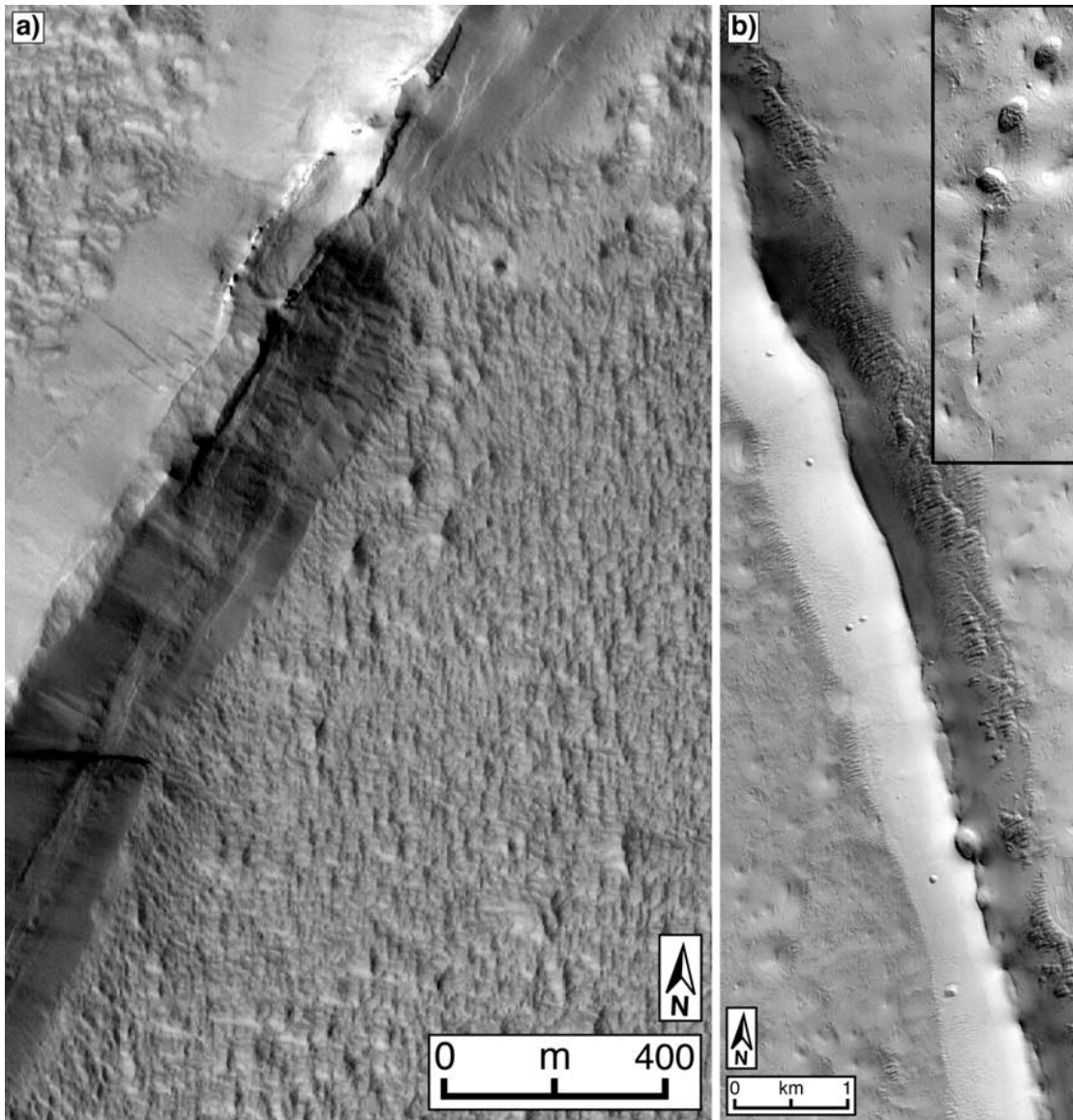


**Figure 64. MOC narrow-angle images of radial ridges: a) A curvilinear radial ridge possibly formed via volcano-ice interaction. b) A radial ridge with collapse pits along the ridge axis. (Shean et al, 2005)**

Pedersen et al. (2010) identified dike swarms and possible associated subglacial eruptive features in the Elysium Rise and Utopia Basin region. Wilson and Mouginis-Mark (2003) suggested phreato-magmatic dike-cryosphere interactions as the cause of ridges north of Olympus Mons.

Gregg (2007) discusses dry and wet sediment interactions with lava on Mars. Gregg argues that sediment intermixed with interstitial ice would behave similarly to solid rock or a glacier (Gregg, 2007). Gregg (2007) predicts the presence of peperites on Mars if such a case occurred in conjunction with an intrusion. Gregg (2007) further asserts that evidence of volcano-ice interaction should be observed in such as case, such as pseudo-craters on the basis of research conducted by Fagents et al. (2002).

It is important to note that the identification of dikes from aerial imagery of Earth of similar scales to current Martian imagery is difficult. Even on Earth, as seen at Sveifluháls, Iceland in this study, chaotic domains of peperite, multiple diking, and tephra ridges can complicate the identification of dikes which intruded wet or icy sediment. On both Earth and Mars, the identification of dikes benefits from the association of several magma-ice indicators when available. A chemical signature of a hydrothermal overprint adjacent to suspected dikes on either planet is beneficial for the identification of dikes which intruded wet or icy sediment. The identification of pillow lava in Martian imagery within suspected magma-cryosphere interaction dikes would greatly aid the identification process.



## **8.0 COMPARISON OF SVEIFLUHÁLS DIKES WITH DIKES ON MARS**

Martian and terrestrial dikes emplaced into wet/icy sediment are likely to be similar in many ways, therefore terrestrial analogs are imperative to understanding their Martian equivalents. In this part of the study, dikes emplaced into wet lapilli tuff at a glaciovolcanic center on Earth (Sveifluháls, Iceland) are compared with putative dikes on Mars. These dike comparisons provide an association of observations that could be used to confirm dike-ice or wet sediment interaction on Mars. Peperite should be present on Mars as wet/icy sediment interactions with magma are likely to be common due to the postulated cryosphere (Clifford, 1993; Clifford and Parker, 2001; Murray et al., 2005, Russell and Head, 2002) and glaciers (Shean et al., 2005) in the past. Volcano-ice interaction dikes should appear wider due to their peperitic margins, which may aid in their detection.

Some of the dikes at Sveifluháls, Iceland, clearly emerged on the former subaqueous tuff cone slope and fed haystack-like structures and subaqueous lava flows (Figure 24). Such slopes likely became loaded with lava, which may have induced slope failure. The geomorphic expression of high-level (close to the paleosurface) dikes may appear wider on aerial or satellite imagery on Earth or Mars due to peperitic margins. Dikes in the study by Gibbons et al. (2001) were estimated to be 150m-700m thick, an extremely thick estimate by terrestrial standards. It is important to note that Martian dikes may appear wider in satellite imagery due to peperite and talus.

The tephra ridges at Sveifluháls, Iceland look similar to the dike swarms recognized by Pedersen et al. (2010) in THEMIS IR imagery (Figure 65) in their curvilinear shape.

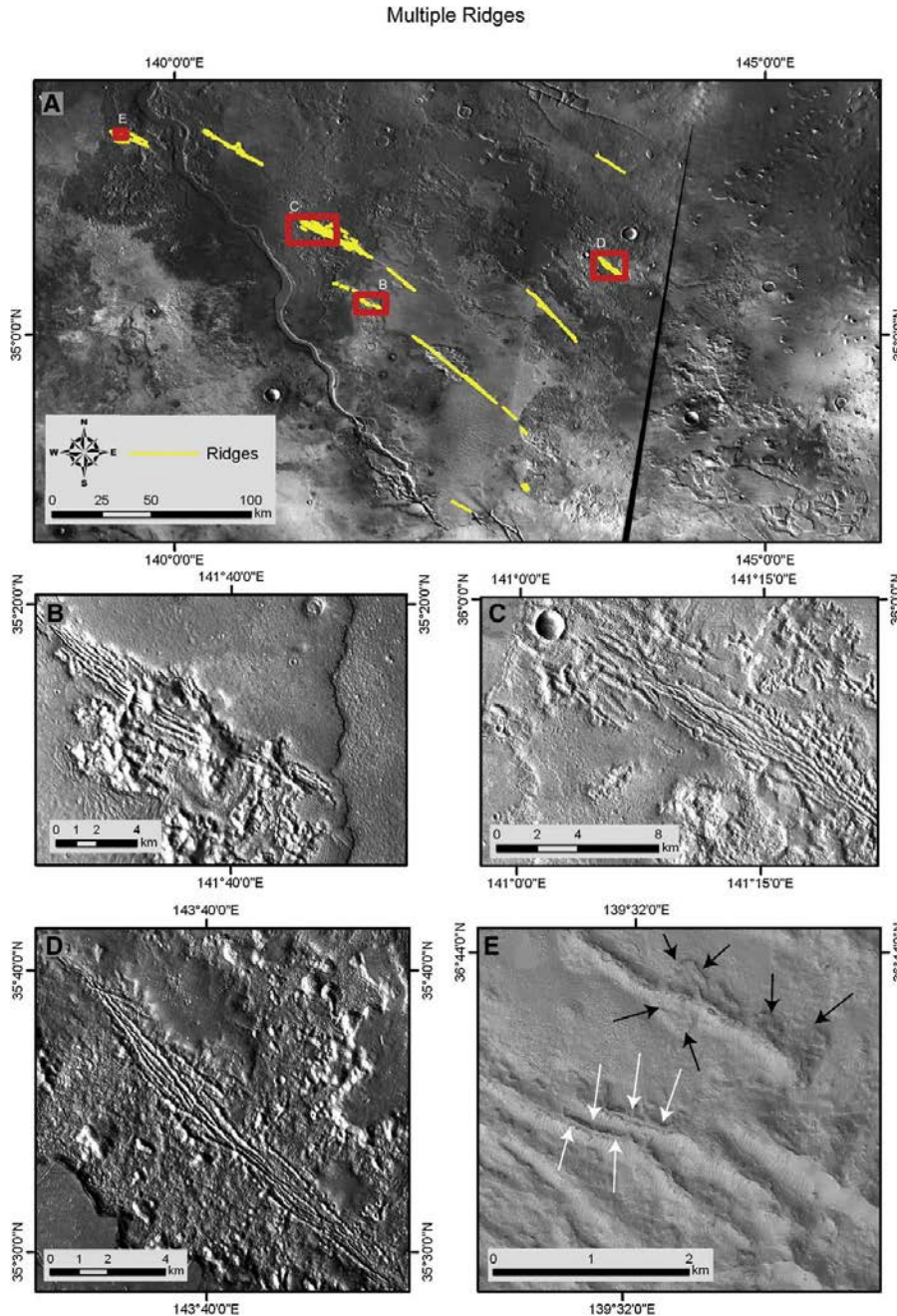


**Figure 65. THEMIS IR images of dike swarms in the Elysium Rise and Utopia Basin regions of Mars. Red boxes show locations for B, C, D, and E. Black arrows show “stubby flows” and white arrows show symmetric fractures atop ridges. (Pedersen et al., 2010)**

The dike swarms recognized by Pedersen et al. (2010) (Figure 65) displayed lengths of 10-45km and widths of 1-7km, with individual ridges of lengths 47m-13km and widths 45m-341m (Pedersen et al., 2010). The glaciovolcanic ridge complex of Sveifluháls, Iceland, is approximately 21km long and 2.5km wide. The coherent parts of the dikes at Sveifluháls, however, displayed widths of 1-5m.

Pedersen et al. (2010) also interpreted THEMIS IR imagery of several single ridges in the Elysium Rise and Utopia Basin of Mars as dikes (Figure 66). These dikes identified by Pedersen et al. (2010) look similar to the tephra ridges at Sveifluháls as well in their curvilinear shape.

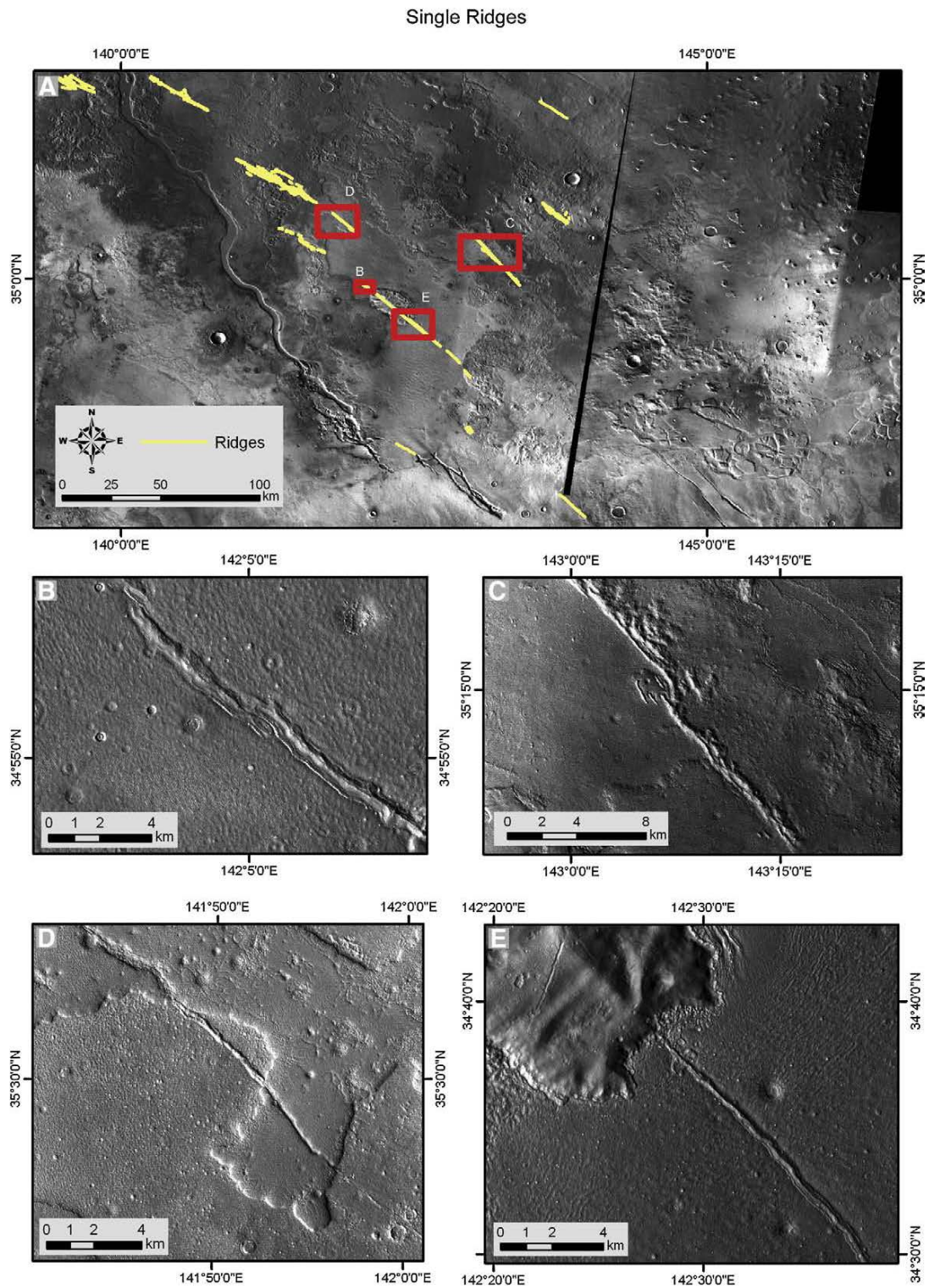


**Figure 66. THEMIS IR imagery of single dikes in the Elysium Rise and Utopia Basin of Mars. Red boxes show locations for B, C, D, and E. (Pedersen et. al, 2010)**

The single ridges studied by Pedersen et al. (2010) (Figure 66) had a mean length of 5770m and widths of 13-500m. The glaciovolcanic ridge complex of Sveifluháls, Iceland, is approximately 21km long and 2.5km wide. The dikes at Sveifluháls, Iceland ranged from 1-5m wide.

Possible hematite spherules within dike interiors at Sveifluháls, Iceland (Figure 42 and Figure 43) are similar in shape and suspected composition to the Martian “blueberries” albeit on a smaller scale. The hematite “blueberries” on Mars mostly ranged in size from 1.5mm – 5mm (Gánti, T. et al., 2005). The spherules of possible hematite within vesicles at Sveifluháls mostly ranged in size from 0.125mm – 0.25mm.

Figure 67 compares THEMIS IR imagery of dike swarms in the Elysium Rise and Utopia Basin regions of Mars interpreted by Pedersen et al. (2010) to the tephra ridges and dikes of the tindar at Sveifluháls, Iceland at the same scale.



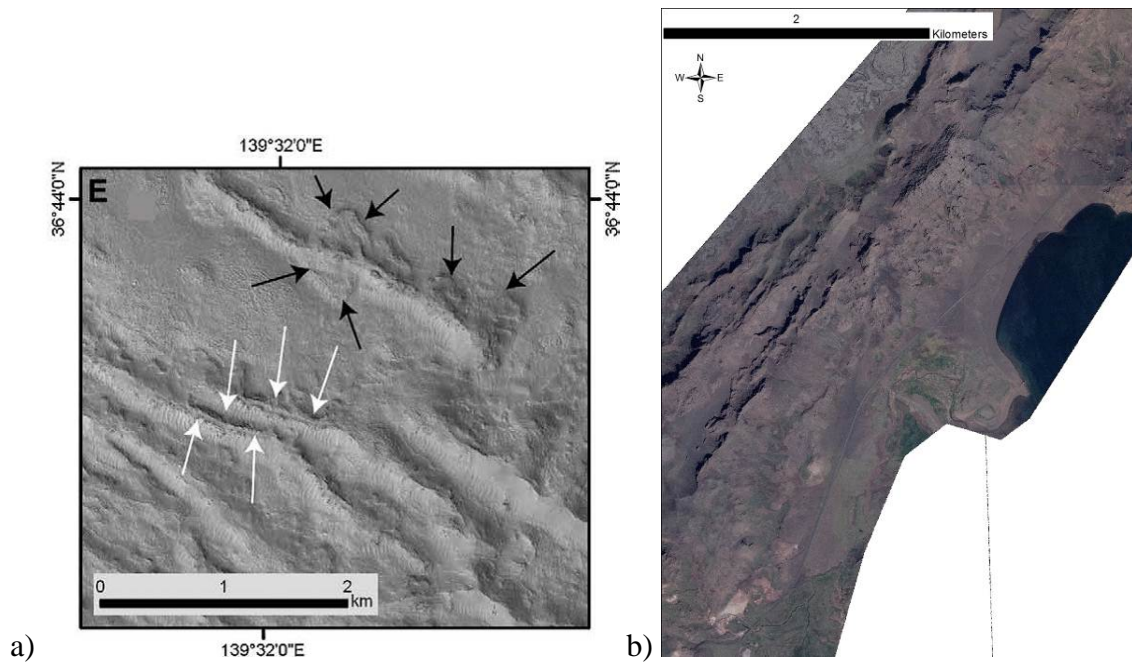


**Figure 67. Comparison at the same scale of THEMIS IR imagery of dike swarms in the Elysium Rise and Utopia Basin regions of Mars in a) by Pedersen et al. (2010) to the tendar b) comprised of phreatomagmatic tephra ridges and dikes at Sveifluh  ls, Iceland, seen in Loftmyndir color orthophotos. Black arrows show “stubby flows” and white arrows show symmetric fractures atop ridges. (Pedersen et al., 2010)**

The Pedersen et al. (2010) Martian dike swarms in Figure 67a appear to more closely resemble the terrestrial tephra ridges (Figure 67b) of the Sveifluh  ls, Iceland tendar in width ranges than the much smaller-scale dikes at Sveifluh  ls (widths 1-5m), which are barely discernable at this scale.

Figure 68 compares at nearly the same scale a curvilinear radial ridge of potential volcano-ice interaction origin interpreted by Shean et al. (2005) to the tephra ridges and dikes at Sveifluh  ls, Iceland.

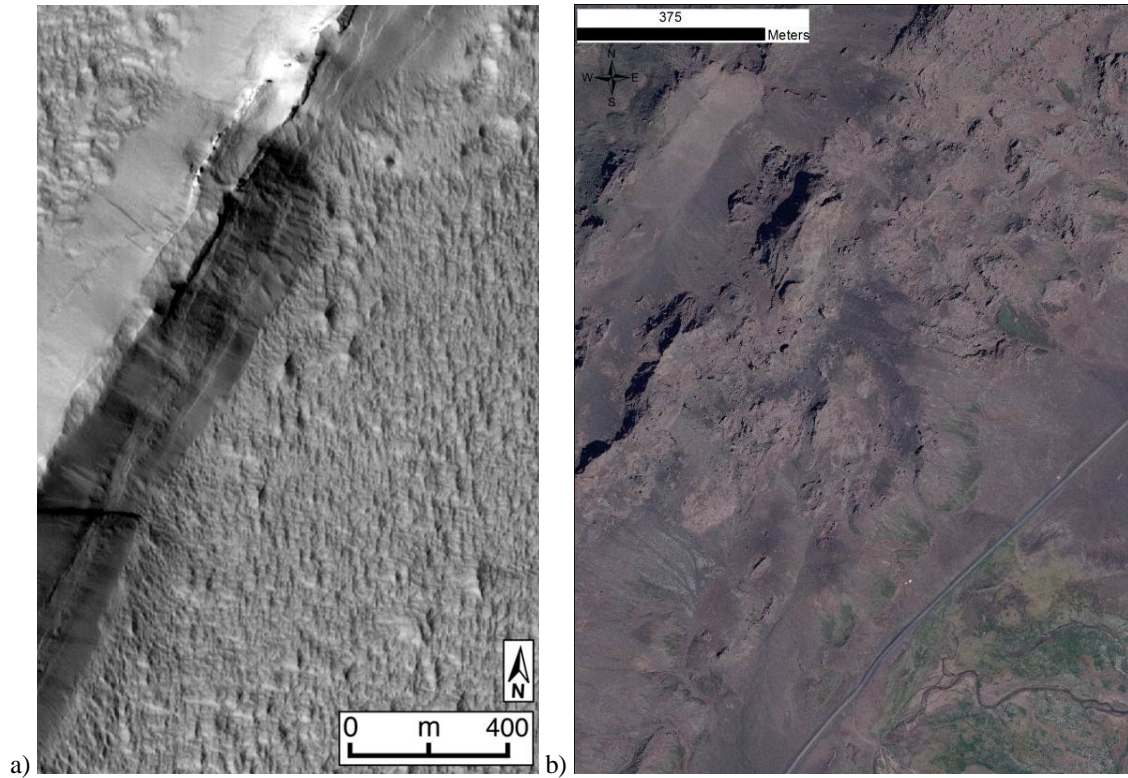


**Figure 68. Comparison at nearly the same scale of a Martian curvilinear radial ridge of potential volcano-ice interaction origin in a) from Shean et al. (2005) to tephra ridges and dikes at Sveifluháls, Iceland, seen in Loftmyndir color orthophotos.**

The Martian curvilinear radial ridge interpreted to have a possible volcano-ice origin by Shean et al. (2005) in Figure 68a resembles the terrestrial tephra ridges (Figure 68b) of the Sveifluháls, Iceland tindar in shape and widths. The terrestrial dikes found at Sveifluháls in Figure 68b appear to be much smaller linear features (widths 1-5m) in comparison to the Martian ridge in Figure 68a.

Figure 69 compares at the same scale a CRISM-confirmed olivine dike in the Coprates Chasma central horst of Valles Marineris on Mars interpreted by Flahaut et al. (2011) with dikes at Sveifluháls, Iceland.

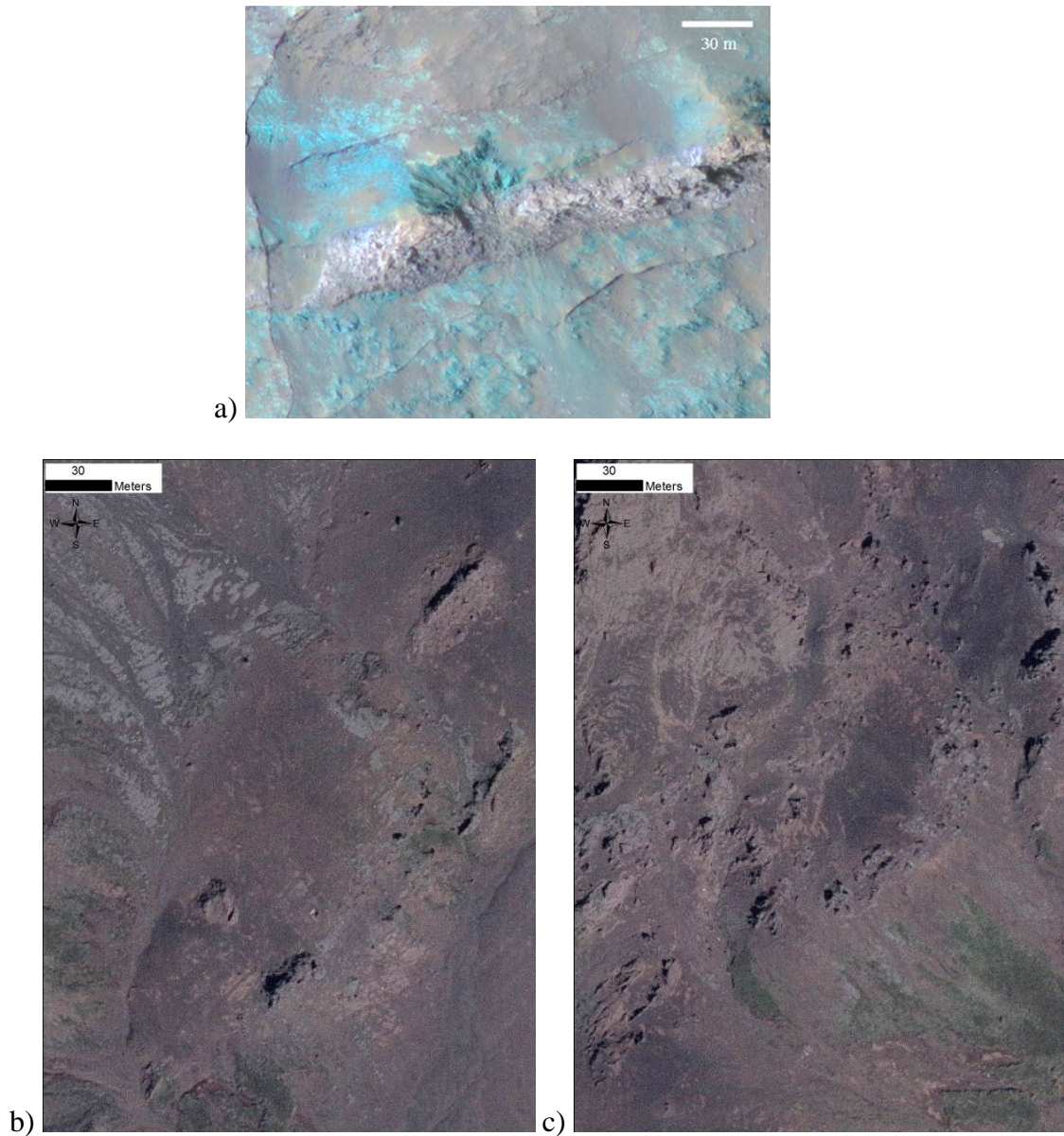


**Figure 69. Comparison at the same scale of a color HiRISE image (ESP\_013903\_1650) of a CRISM-confirmed olivine dike in the Coprates Chasma central horst of Valles Marineris on Mars (Flahaut et al., 2011) in a) to dikes at Sveifluh  ls, Iceland seen in Loftmyndir color orthophotos in b) and c).**

The Martian olivine dike in Figure 69a interpreted by Flahaut et al. (2011), is much wider (30m) than the terrestrial dikes (widths 1-5m) at Sveifluh  ls, Iceland (Figure 69b). The thinner ridges on either side of the Martian olivine dike from Flahaut et al. (2011) in Figure 69a,

however, more closely resemble the terrestrial dikes at Sveifluháls, Iceland (Figure 69b) in terms of width, and may be dikes themselves.

## **8.1 CAN WE USE DIKES ON MARS TO INFER PALEOCLIMATE?**

Volcano-ice interaction products have the potential to provide an important paleoclimate proxy via records of former ice presence and thickness (Smellie, 2009; Tuffen et al., 2010).

The history of ice on Mars is largely accepted, but disputed as to its extent during certain periods of Mars' paleoclimate. Some assert that Mars once maintained a hydrosphere with oceans in addition to a cryosphere (Clifford, 1993; Clifford et al., 2010), perhaps with sub-permafrost groundwater (Clifford et al., 2010). Another theory suggests the existence of a hydrosphere beneath the cryosphere on Mars currently and in the past (Clifford and Parker, 2001; Murray et al., 2005, Russell and Head, 2002).

It is difficult to identify dikes and dikes emplaced into ice-cemented or wet sediment on Mars confidently, but could theoretically be used as a Martian climate proxy if dikes which interacted with ice-cemented or wet sediment were confirmed. Future identification of pillows in Martian imagery would aid in the confirmation of dikes which interacted with icy or wet sediment.

## 9.0 CONCLUSIONS

- Basaltic dikes emplaced into formerly wet unconsolidated phreatomagmatic tephra deposits serve as excellent terrestrial analogs for high-level basaltic dike-cryosphere interactions on Mars.
- Such dikes at Sveifluháls, SW Iceland typically have narrow (<1.5m wide) coherent cores of both pillowed and non-pillowed types, but develop blocky and fluidal peperitic margins with a geomorphic expression that is often an order of magnitude larger than the coherent dike. This has important implications for recognizing dikes emplaced into the cryosphere, interpreting past climates on Mars, estimating dike widths from remote imagery, and calculating magma flux rates on Mars.
- Large-scale geomorphological features of the Sveifluháls dikes include local dike-bounded plateaus, adjacent and at lower elevation to phreatomagmatic tephra ridges, that display surfaces of dark dike-derived talus, often of uniform (lapilli) size. Such dike plateau regions were likely formed through the emergence of several dike fingers or separate dikes with nearly parallel strikes. This configuration could create a dam effect in which eroded tephra



and talus collect against the dikes until a shallower slope than the surrounding ridge is obtained with the local area (dike-related plateau zone).

- The dikes at Sveifluháls are associated with broad bounding areas of orange to reddish-brown host lapilli tuff (“hydrothermal reddening”), that extends for up to 20m on either side of the dikes, and contrasts with the more typical buff-colored palagonitized lapilli tuff that has not been intruded by dikes.
- The hydrothermal reddening of the host lapilli tuff at Sveifluháls is probably caused by the presence of concentrically banded zones of hematite(?) in vesicles and pore-spaces. Such reddening zones may aid in the identification of dikes which interacted with the cryosphere on Mars.
- At Sveifluháls, drag-folded, rotated and slumped blocks or domains of the host extend up to 30m from dike margins.
- The dikes at Sveifluháls have a gross tabular morphology, but are locally pillowed or billowy along their margins, and also include finger-like or elongate pillowed projections up to 5m in length from their margins into the host lapilli tuff.
- At Sveifluháls, narrow steep conical mounds of pillow lavas were observed, resembling pillow-like haystacks, described from the submarine environment, and are interpreted as areas where the dikes emerged on the substrate surface. Identification of such features on Mars is limited by the currently available resolution of satellite data.
- The identification of such dikes on Earth and Mars may be aided by erosion on the flanks of tindars (sites of former fissure eruptions beneath an ice sheet),

which may expose dikes with associated plateau regions. The observation of raised linear features cross-cutting tephra ridges would be beneficial as well. Dikes on Mars in particular are difficult to confidently identify due to the current resolution of satellite imagery and to erosion and dust covering the Martian surface. HiRISE imagery may greatly aid in this endeavor in the future with the observation and interpretation of more high resolution images of Mars. Graben, pit crater chains, collapse pits, and/or troughs in combination may be indicators of dike location on Mars. Each of these features alone may originate from other causes.

- The phreatomagmatic tephra ridges of eroded tinders, though they are likely to be cored with dikes, may be mistaken for exposures of dikes on Mars.
- CRISM observations of Mars with attention focused on ridges, hydrothermal zones, graben, pit crater chains, chaos terrain, nontronite, carbonates, and clays may aid in the identification of dikes which were emplaced into the cryosphere on Mars.
- XRD analyses from samples of dikes emplaced into wet/icy sediment on Earth would be useful to compare to CRISM geochemical signatures to aid in the identification of dikes emplaced into the cryosphere on Mars.
- Hydrothermal zones flanking ridges and their associated geochemical signatures may aid in the recognition of dikes on Mars. The detection of linear zones of zeolites, anhydrite, clays, and/or hematite may be indicators of hydrothermal alteration zones on Mars.

- Dikes emplaced into wet sediments on Earth may appear wider due to peperitic margins, hydrothermal zones, and dike-derived blocky talus. Dikes emplaced into ice-cemented sediment on Mars may also appear wider than their coherent cores. This may have implications for magma flux estimates within the intrusion. Overestimation of magma fluxes on Mars may result from the misinterpretation of dike geomorphic expressions for dike cores.

## REFERENCES

- Acocella, V., Cifelli, F., Funicello, R., Minore, L., Analogue Models of Dike Emplacement. EGS XXVII General Assembly, Nice, 21-26 April 2002, abstract #1144.
- Allen, C.C., Volcano-ice interactions on Mars. *Journal of Geophysical Research*, 1979. 84: p. 8048-8059.
- Allen, C.C., Jercinovic, M.J. and Allen, J.S.B., 1982. Subglacial Volcanism in North-Central British Columbia and Iceland. *Journal of Geology*, 90(6): 699-715.
- Befus, K.S., Hanson, R.E., Miggins, D.P., Breyer, J.A. and Busbey, A.B., 2009. Nonexplosive and explosive magma/wet-sediment interaction during emplacement of Eocene intrusions into Cretaceous to Eocene strata, Trans-Pecos igneous province, West Texas. *Journal of Volcanology and Geothermal Research*, 181(3-4): 155-172.
- Benn, K.; Odonne, F.; de Saint Blanquat, M., Pluton emplacement during transpression in brittle crust: New views from analogue experiments, *Geology*, vol. 26, Issue 12, p.1079, 1998.
- Bideau, D. et al., 1998. Contrasting volcanic-tectonic processes during the past 2 Ma on the Mid-Atlantic Ridge: submersible mapping, petrological and magnetic results at lat. 34°52'N and 33°55'N. *Marine Geophysical Research*, 20(5): 425-458.
- Busby-Spera, C.J. and White, J.D.L., 1987. Variation in peperite textures associated with differing host-sediment properties. *Bulletin of Volcanology*, 49(6): 765-776.
- Chapman, M.G., et al., HYALOCLASTIC RIDGES, TUYAS, LAHARS, AND JOKULHLAUPS ON MARS, in *The Geology of Mars: Evidence from Earth-based Analogs*, M.G. Chapman, Editor, 2007, Cambridge University Press. p. 60-63.
- Chapman, M. G. and Tanaka, K. L., Related Magma-Ice Interactions: Possible Origins of Chasmata, Chaos, and Surface Materials in Xanthe, Margaritifer, and Meridiani Terrae, Mars. 2002, *Icarus*, 155, 2, p. 324-339.
- Clifford, S.M., 1993. A Model for the Hydrologic and Climatic Behavior of Water on Mars. *J. Geophys. Res.*, 98(E6): 10973-11016.

- Clifford, S. M., and Parker, T. J., The Evolution of the Martian Hydrosphere: Implications for the Fate of a Primordial Ocean and the Current State of the Northern Plains. *Icarus*, Volume 154, Issue 1, pp. 40-79 (2001).
- Clifford, S.M. et al., 2010. Depth of the Martian cryosphere: Revised estimates and implications for the existence and detection of subpermafrost groundwater. *J. Geophys. Res.*, 115(E7): E07001.
- Clifton, A.E. et al., 2003. Surface effects of triggered fault slip on Reykjanes Peninsula, SW Iceland. *Tectonophysics*, 369(3-4): 145-154.
- Clifton, A. E., and Kattenhorn, S. A., “Structural Architecture of a Highly Oblique Divergent Plate Boundary Segment”, *Tectonophysics*, vol. 419, 27–40, 2006.
- Duffield, W. A., Bacon, C. R., and Delaney, P. T., “Deformation of Poorly Consolidated Sediment During Shallow Emplacement of a Basaltic Sill, Coso Range, California”, *Bulletin of Volcanology*, vol. 48, 97-107, 1986.
- Edwards, B.R. et al., 2009. Evolution of an englacial volcanic ridge: Pillow Ridge tindar, Mount Edziza volcanic complex, NCVP, British Columbia, Canada. *Journal of Volcanology and Geothermal Research*, 185(4): 251-275.
- Ernst, R.E., Grosfils, E.B. and Mège, D., 2001. Giant Dike Swarms: Earth, Venus, and Mars. *Annual Review of Earth and Planetary Sciences*, 29: 489-534.
- Fagents, S. A., Lanagan, P. D., and Greeley, R. (2002). Rootless cones on Mars: a consequence of lava-ground ice interaction., *Volcano-Ice Interaction on Earth and Mars*, ed. J. L. Smellie and M. G. Chapman. Geological Society of London Special Publication 202.
- Flahaut, J. et al., 2011. Dikes of distinct composition intruded into Noachian-aged crust exposed in the walls of Valles Marineris. *Geophys. Res. Lett.*, 38(15): L15202.
- Francis, P. and Oppenheimer, C., 2004. *Volcanoes*. Oxford University Press.
- Gánti, T., et al., MORPHOLOGICAL INVESTIGATIONS OF MARTIAN SPHERULES, COMPARISONS TO COLLECTED TERRESTRIAL COUNTERPARTS. *Lunar and Planetary Science XXXVI* (2005).
- Gibbons, H.L., Scott, E.D., Wilson, L. and Head, J.W., III, 2001. Inferred Properties of Giant Radial Dikes Beneath Graben in Northern Tharsis, Mars, *Lunar and Planetary Institute Science Conference Abstracts*, pp. 1154.
- Graettinger, A. H., et al., Intrusion of Basalt into Frozen Sediments and Generation of Coherent-Margined Volcaniclastic Dikes (CMVDs), *JVGR*, submitted.
- Gregg, T. K. P., Lava-sediment interactions on Mars: evidence and consequences, *The Geology of Mars: Evidence from Earth-Based Analogs*, edited by M. G. Chapman, 2007.



- Gudmundsson, M., Sigmundsson, F., Björnsson, H. and Högnadóttir, T., 2004. The 1996 eruption at Gjalp, Vatnajökull ice cap, Iceland: efficiency of heat transfer, ice deformation and subglacial water pressure. *Bulletin of Volcanology*, 66(1): 46-65.
- Harðarson, B. S., et al. (2008), Tertiary volcanism in Iceland, *Jökull*, 58, 161–178.
- Hartmann, W. K., *A Traveler's Guide to Mars: The Mysterious Landscapes of the Red Planet*. Workman, New York, 2003.
- Head, J. W., et al. The Huygens-Hellas Giant Dike System on Mars: Implications for Late Noachian-Early Hesperian Volcanic Resurfacing and Climatic Evolution. *Geology*, April 2006, v. 34, p. 285-288.
- Head, J.W. and Wilson, L., 2007. Heat transfer in volcano-ice interactions on Mars: synthesis of environments and implications for processes and landforms. *Annals of Glaciology*, 45(1): 1-13.
- HiRISE Image Catalog, NASA/JPL/University of Arizona.
- Kadish, S. A., et al., “The Ascraeus Mons fan-shaped deposit: Volcano–ice interactions and the climatic implications of cold-based tropical mountain glaciation”, *Icarus* 197 (2008) 84–109.
- Komatsu, G., Dohm, J.M. and Hare, T.M., 2004. Hydrogeologic processes of large-scale tectonomagmatic complexes in Mongolia--southern Siberia and on Mars. *Geology*, 32(4): 325-328.
- Komatsu, G., Gabriele Ori, G., Ciarcelluti, P. and D. Litasov, Y., 2004. Interior layered deposits of Valles Marineris, Mars: analogous subice volcanism related to Baikal Rifting, Southern Siberia. *Planetary and Space Science*, 52(1-3): 167-187.
- Korteniemi, J., et al., Dike indicators in the Hadriaca Patera-Promethei Terra region, Mars. *Earth and Planetary Science Letters*, 2009.
- Levi, S. et al., 1990. Late Pleistocene geomagnetic excursion in Icelandic lavas: confirmation of the Laschamp excursion. *Earth and Planetary Science Letters*, 96(3-4): 443-457.
- Liu, S.Y. and L. Wilson. Collapse Pits Due to Gas Release from Shallow Dikes on Mars. in *Lunar and Planetary Institute Science Conference Abstracts*. 1998.
- Mège, D., Dikes on Mars: (1) What to look for? (2) A First Survey of Possible Dikes During the Mars Global Surveyor Aerobreaking and Science Phasing Orbits., *Fifth International Conference on Mars*. 1999.
- Mège, D., Graben Morphology, Dike Emplacement, and Tension Fracturing in the Tharsis Igneous Province of Mars., *The Fifth International Conference on Mars*, 1999.

- Mercurio, E. C., Processes, Products and Depositional Environments of Ice-Confined Basaltic Fissure Eruptions: A Case Study of the Sveifluháls Volcanic Complex, SW Iceland, Ph.D. dissertation, University of Pittsburgh, Department of Geology and Planetary Science, 2011.
- Meresse, S., et al., Formation and evolution of the chaotic terrains by subsidence and magmatism: Hydraotes Chaos, Mars. *Icarus*, 2008, 194, 2, p. 487-500.
- Murray, J.B. et al., 2005. Evidence from the Mars Express High Resolution Stereo Camera for a frozen sea close to Mars' equator. *Nature*, 434(7031): 352-356.
- Pedersen, G.B.M., et al., "Formation, erosion and exposure of Early Amazonian dikes, dike swarms and possible subglacial eruptions in the Elysium Rise/Utopia Basin Region, Mars", *Earth Planet. Sci. Lett.* (2010), doi:10.1016/j.epsl.2009.08.010
- Pedersen, G. B. M., and Head, J. Geomorphic characteristics for Amazonian dike swarms emplaced in Utopia basin, Mars. *EPSC Abstracts*, 3, 2008.
- Russell, P.S. and Head, J.W., III, 2002. The martian hydrosphere/cryosphere system: Implications of the absence of hydrologic activity at Lyot crater. *Geophys. Res. Lett.*, 29(17): 1827.
- Schopka, H.H., Gudmundsson, M.T. and Tuffen, H., 2006. The formation of Helgafell, southwest Iceland, a monogenetic subglacial hyaloclastite ridge: Sedimentology, hydrology, and volcano-ice interaction. *Journal of Volcanology and Geothermal Research*, 152: 359-377.
- Schultz, R.A., et al., Igneous dikes on Mars revealed by Mars Orbiter Laser Altimeter topography. *Geology*, 2004. 32: p. 889.
- Schultz, R. and Fori, A. N., Fault-length statistics and implications of graben sets at Candor Mensa, Mars. *Journal of Structural Geology*, 1996. 18: p. 373-383.
- Shean, D.E., J.W. Head, and D.R. Marchant, Origin and evolution of a cold-based tropical mountain glacier on Mars: The Pavonis Mons fan-shaped deposit. *Journal of Geophysical Research (Planets)*, 2005. 110: p. 05001.
- Skilling, I.P., 1994. Evolution of an englacial volcano: Brown Bluff, Antarctica. *Bulletin of Volcanology*, 56(6): 573-591.
- Skilling, I. P., Subglacial to emergent basaltic volcanism at Höðufell, south-west Iceland: A history of ice-confinement. *Journal of Volcanology and Geothermal Research*, 2009.
- Skilling, I. P., White, J. D. L., and McPhie, J. Peperite: a review of magma-sediment mingling. *Journal of Volcanology and Geothermal Research*, 114, 2002, p. 1-17.

- Smellie, J.L. and Hole, M.J., 1997. Products and processes in Pliocene–Recent, subaqueous to emergent volcanism in the Antarctic Peninsula: examples of englacial Surtseyan volcano construction. *Bulletin of Volcanology*, 58(8): 628-646.
- Smellie, J.L., Hole, M.J. and Nell, P.A.R., 1993. Late Miocene valley-confined subglacial volcanism in northern Alexander Island, Antarctic Peninsula. *Bulletin of Volcanology*, 55(4): 273-288.
- Smellie, J.L., 2009. Terrestrial subice volcanism: Landform morphology, sequence characteristics, environmental influences, and implications for candidate Mars examples. *Geological Society of America Special Papers*, 453: 55-76.
- Smellie, J.L. and Skilling, I.P., 1994. Products of subglacial volcanic eruptions under different ice thicknesses: two examples from Antarctica. *Sedimentary Geology*, 91(1-4): 115-129.
- Smith, P.H. et al., 2009. H<sub>2</sub>O at the Phoenix Landing Site. *Science*, 325(5936): 58-61.
- Squire, R.J. and McPhie, J., 2002. Characteristics and origin of peperite involving coarse-grained host sediment. *Journal of Volcanology and Geothermal Research*, 114(1-2): 45-61.
- Stakes, D.S. et al., 2006. The Cleft revealed: Geologic, magnetic, and morphologic evidence for construction of upper oceanic crust along the southern Juan de Fuca Ridge. *Geochem. Geophys. Geosyst.*, 7(4): Q04003.
- Tuffen, H. and J.M. Castro, The emplacement of an obsidian dyke through thin ice: Hrafninnuhryggur, Krafla Iceland. *Journal of Volcanology and Geothermal Research*, 2009. 185(4): p. 352-366. 2009.
- Tuffen, H., Owen, J. and Denton, J., 2010. Magma degassing during subglacial eruptions and its use to reconstruct palaeo-ice thicknesses. *Earth-Science Reviews*, 99(1-2): 1-18.
- Warner, N. H., and Farmer, J. D., Sub-Glacial Hydrothermal Alteration Minerals in Sandur Deposits, Iceland: Implications for the Detection of Habitable Hydrous Environments on Mars. *Astrobiology Science Conference 2010*, LPI Contribution No. 1538, p.5602
- White, J.D.L. and Busby-Spera, C.J., 1987. Deep marine arc apron deposits and syndepositional magmatism in the Alisitos group at Punta Cono, Baja California, Mexico. *Sedimentology*, 34(5): 911-927.
- White, J. D. L., McPhie, J., and Skilling, I. Peperite: a useful genetic term. *Bulletin of Volcanology*, 2000, 62 , 65-66.
- Wilson, L., and Head, J. W., Heat Transfer in Volcano-ice Interactions on Earth. *Annals of Glaciology*, 2007, v. 45, p. 83-86.
- Wilson, L. and Head, J. Heat transfer and melting in subglacial basaltic volcanic eruptions: implications for volcanic deposit morphology and meltwater volumes. *Geological Society of London, Special Publications* 2002, 202, p 5-26, 2002.

- Wilson, L. and Head, J.W., 2002. Tharsis-radial graben systems as the surface manifestation of plume-related dike intrusion complexes: Models and implications. *Journal of Geophysical Research (Planets)*, 107: 5057.
- Wilson, L., and P.J. Mouginis-Mark (2003). "Phreato-magmatic dike-cryosphere interactions as the origin of small ridges north of Olympus Mons, Mars." *Icarus* 165: 242-252
- Winter, J.D.N., 2001. An introduction to igneous and metamorphic petrology. Prentice Hall., p. 59-74.
- Wörner, G. and Viereck, L., 1987. Subglacial to Emergent Volcanism at Shield Nunatak, Mt. Melbourne Volcanic Field, Antarctica. *Polarforschung*, 57 1/2: 27-41.
- Zimbelman, J.R. and Gregg, T.K.P., 2000. Environmental effects on volcanic eruptions: from deep oceans to deep space. Kluwer Academic/Plenum Publishers.